

ABSTRACT

Title of Document: DEVELOPMENT AND EVALUATION OF A
TOOL FOR EVA OR ROBOTIC PLANETARY
SAMPLING

David Wayne Gruntz, Master of Science, 2007

Directed By: Associate Professor David L. Akin
Department of Aerospace Engineering

NASA's current plans call for humans to return to the Moon by 2020 and eventually travel to Mars. The primary rationale for this undertaking is scientific exploration and discovery, especially in the area of geology. These missions will include both human and robotic explorers. In order to be successful, these human/robot teams will need specialized tools for geologic sampling and analysis. This thesis discusses a proposed multi-purpose tool for planetary sampling useful for researching surface exploration strategies for humans and human-robot teams. Previous planetary science missions were analyzed to define set of requirements for a sampling tool. From this, a concept was conceived and a prototype constructed. Various soil and rock samples were taken to verify the concept and requirements. The tool performance was tested against known soil models. The end result is a set of sampling requirements, a proven concept for a tool, and proposed future development and research.

DEVELOPMENT AND EVALUATION OF A TOOL FOR EVA OR ROBOTIC
PLANETARY SAMPLING

By

David Wayne Gruntz

Thesis submitted to the Faculty of the Graduate School of the
University of Maryland, College Park, in partial fulfillment
of the requirements for the degree of
Master of Science
2007

Advisory Committee:
Associate Professor David L. Akin, Chair
Assistant Professor J. Sean Humbert
Research Associate Dr. Craig R. Carignan

© Copyright by
David Wayne Gruntz
2007

Dedication

Mom and Dad,

I would not be who or where I am today if not for you.

Thank you.

Acknowledgments

This work was not a solo endeavor and I am grateful for all of the help I have received along the way. I fear these words may not adequately express my gratitude, but I'll try anyway...

I would like to thank Dr. Dave Akin for the opportunity to work at the SSL. The SSL is a great facility and Dave fosters an environment conducive to research by offering ideas, insight, and feedback as well as answering and, as is usually the case, asking questions. I would also like to thank the other members of my committee, Dr. Sean Humbert and Dr. Craig Carignan, for their input and suggestions.

The staff and students at the SSL are also deserving of thanks. Brian Roberts and Stephen Roderick were always available for help, whether related to my project or to the lab. The other grad students Agnieszka, Liz, Sharon, Emily, John, Joe, Tim, Martin, Ricco, Shane, and everyone else were always willing to offer ideas, support (moral and otherwise), sanity checks, and the occasional needed distraction. Thanks guys.

This research was conducted at the Space Systems Laboratory, part of the Aerospace Engineering Department of the A. James Clark School of Engineering at the University of Maryland, College Park. It was supported through the Institute for Dexterous Space Robotics.

Table of Contents

<i>Dedication</i>	<i>ii</i>
<i>Acknowledgments</i>	<i>iii</i>
<i>Table of Contents</i>	<i>iv</i>
<i>List of Tables</i>	<i>vii</i>
<i>List of Figures</i>	<i>viii</i>
<i>List of Abbreviations & Symbols</i>	<i>x</i>
CHAPTER 1 INTRODUCTION	1
1.1 Motivation	1
1.2 Thesis Goal	3
1.3 The Tool for EVA or Robotic Planetary Sampling	4
1.4 TERPS Applications	5
1.5 Thesis Organization	6
CHAPTER 2 BACKGROUND: PLANETARY SURFACE EXPLORATION & SAMPLING	7
2.1 Planetary Geology	7
2.2 Sampling Methods of Previous Missions	9
2.2.1 Manned Sampling	10
2.2.2 Drills	11
2.2.3 Scoops	13
2.2.4 Other Systems	17
2.3 Future Sampling Missions	19
2.4 Current Laboratory Research	21
2.5 Summary	26
CHAPTER 3 HUMAN/ROBOT GEOLOGY: REQUIREMENTS & LESSONS FROM APOLLO .	27
3.1 Apollo Era Sampling	27
3.1.1 Apollo 17	27
3.1.2 Apollo Sampling Tools and Usage	28
3.1.3 Problems with Apollo Tools	34
3.1.4 Areas for Improvement	36
3.2 Human/Robot Roles in Future EVA & Exploration	36
3.2.1 Astronaut-Rover Studies	36
3.2.2 EVA Robotic Assistant	38
3.3 Requirements for Sampling CAT/End-Effector	39
3.3.1 Geology/Sampling Requirements	39
3.3.2 Functional Requirements	40
CHAPTER 4 TERPS CONCEPT & PROTOTYPE	42
4.1 Design Methodology	42
4.2 Initial Concepts	43

4.3 Current Concept Overview	45
4.4 Scoops.....	47
4.5 Actuation.....	49
4.5.1 Gears vs. Linkage.....	50
4.5.2 Motor.....	52
4.5.3 Bearings	53
4.6 Drill.....	54
4.7 Electronics	55
CHAPTER 5 TERPS TESTING SET-UP.....	57
5.1 Lab Set-up.....	57
5.1.1 Physical Set-up.....	57
5.1.2 Data Collection	58
5.1.3 Data Processing.....	60
5.1.4 Power	60
5.1.5 Sand Box.....	60
5.2 Determination of Scoop Force	61
CHAPTER 6 SOIL MECHANICS & THEORY, TESTING, RESULTS, & DISCUSSION	64
6.1 Soil Mechanics Overview	64
6.2 Soil Cutting Model.....	65
6.3 Testing Approach.....	72
6.3.1 Statistical Analysis.....	72
6.4 Testing Results	73
6.4.1 Motor Characteristics.....	73
6.4.2 Soil to Soil Comparison.....	75
6.4.3 Soil to Model Comparison.....	76
6.5 Sensitivity Analysis	83
6.6 Discussion.....	85
CHAPTER 7 TERPS CONCEPT DEMONSTRATION & VALIDATION.....	87
7.1 Sample Collection Testing Approach.....	87
7.2 Sampling Testing Results	88
7.2.1 Soil and Chips Collection/Manipulation.....	88
7.2.2 Soil Coring.....	91
7.2.3 Rock Collection/Manipulation.....	93
7.2.4 Rock Coring/Abrading.....	94
7.2.5 Sandbox Tests	95
7.2.6 Summary	97
7.3 Discussion.....	97
7.3.1 Sampling Requirements.....	98
7.3.2 Mechanical Error/Issues.....	99
7.3.3 Sampling	100
CHAPTER 8 CONCLUSION & FUTURE WORK	101
8.1 Conclusions.....	101
8.2 Future Work.....	103

8.2.1 Design/Hardware Upgrades	104
8.2.2 Proposed Research & Experiments.....	106
<i>Appendix A Apollo Sampling Tools</i>	<i>107</i>
A.1 Apollo Tools Information	107
<i>Appendix B TERPS Hardware</i>	<i>108</i>
B.1 Materials List	108
B.2 CAD Drawings.....	109
B.3 Gear Specifications	128
B.4 Motor Specifications	130
<i>Appendix C Bearing Calculations</i>	<i>133</i>
<i>Appendix D McKyes/Ali Soil Model</i>	<i>139</i>
D.1 Soil Model.....	139
D.2 Soil Test Results	143
D.3 Sensitivity Analysis.....	149
<i>Appendix E MATLAB Code</i>	<i>152</i>
E.1 Scoop Soil Force Function	152
E.2 Parsing Function.....	156
<i>Appendix F Testing Supplemental</i>	<i>160</i>
F.1 Test Log.....	160
F.2 Photos	162
<i>References</i>	<i>164</i>

List of Tables

Table 2-1: Overview of Past/Current Successful Planetary Sampling Programs ([1, 7])... 9	9
Table 3-1: Summary of Apollo 17 Sampling Tools..... 34	34
Table 3-2: Human/Robotic Sampling Tool Requirements 41	41
Table 4-1: Initial Concept Comparison Matrix..... 44	44
Table 4-2: TERPS Bearing Loads for 7.5 kg-cm Max Input Torque and 144 rpm Speed 53	53
Table 5-1: Comparison of Lunar/Martian Soils to Sand [15, 44, 45, 45] 58	58
Table 6-1: P-values of t-tests on Soil to Soil Comparison Tests 75	75
Table 6-2: Soil Prosperities of Dry Sand [44] 77	77
Table 6-3: Results of Soil-Model Comparison t-Tests and Kolmogorov-Smirnov Tests 78	78
Table 7-1: TERPS Sample Collection Testing Tasks 87	87
Table 7-2: Masses of Soil Samples Collected..... 89	89
Table 7-3: Sampling Task Results 97	97
Table 7-4: Sampling Requirements Verification 98	98

List of Figures

Figure 1-1: Human/Robot Team Concept (image from [2]).....	2
Figure 1-2: Tool for EVA or Robotic Planetary Sampling.....	4
Figure 2-1: Apollo Lunar Surface Sampling Tools	10
Figure 2-2: Luna Sampler Arm and Drill (image from [12]).....	12
Figure 2-3: Venera/Vega Venus Surface Landers	13
Figure 2-4: Al Bean (Apollo 12) Standing at Surveyor III [1]	14
Figure 2-5: Viking Lander/ Sampling System	15
Figure 2-6: Mars Polar Lander/Phoenix Lander	16
Figure 2-7: Mars Exploration Rover “Sampling” System	17
Figure 2-8: Beagle 2 Sampling System	18
Figure 2-9: Hayabusa Projectile Sampling	19
Figure 2-10: MSL Sample Acquisition/Sample Processing and Handling System [23] ..	20
Figure 2-11: Honeybee Robotics Sampling Systems.....	21
Figure 2-12: Micro Robot for Scientific Applications (MRoSA2).....	22
Figure 2-13: Photograph and Sketch of USDC [24].....	23
Figure 2-14: Schematic of APL Pyrotechnic Rock Chipper [25]	24
Figure 2-15: Underwater Sampling Concepts.....	25
Figure 3-1: Small Adjustable Scoop (adapted from [9])	29
Figure 3-2: Jack Schmitt Using Scoop [29].....	30
Figure 3-3: Apollo Rake	31
Figure 3-4: Tongs (Apollo 12) [29]	31
Figure 3-5: Hammer Used to Break Rocks (Apollo 15).....	32
Figure 3-6: “Astronaut” and Marsokhod Rover in ASRO Study (photo from [39])	37
Figure 3-7: NASA/JSC EVA Robotic Assistant (photo from [42])	38
Figure 4-1: Initial TERPS Concepts	44
Figure 4-2: CAD Model of Overall System.....	46
Figure 4-3: Photograph of Current Prototype (without Drill Installed).....	46
Figure 4-4: Initial Overlapping Scoop Design.....	48
Figure 4-5: Current Scoop Design	48
Figure 4-6: TERPS Scoops	49
Figure 4-7: Scoop Actuation Drive.....	49
Figure 4-8: Initial Scooping Mechanism	50
Figure 4-9: Gear and Bearing Loading from Applied Torque	54
Figure 4-10: Drill, Bit, and Core Tube	55
Figure 4-11: Circuit.....	56
Figure 4-12: TERPS Switch Box.....	56
Figure 5-1: Lab Testing Setup	58
Figure 5-2: Scoop Angular Position	59
Figure 5-3: SSL Lunar Scaled Surface Simulation Facility.....	61
Figure 5-4: TERPS as a Crew Aid Tool	61
Figure 5-5: Grip Force Measurement	62
Figure 6-1: 3-D Sketch of McKyes/Ali Soil Failure Region (adapted from [44]).....	67
Figure 6-2: Side View of McKyes/Ali Soil Failure Region	67

Figure 6-3: Scoop Kinematics	68
Figure 6-4: High Rake Angle Soil Failure	70
Figure 6-5: TERPS No Load Motor Current Profile	74
Figure 6-6: Force Profile for 3 Soil Types at $h = 7$ cm and $h = 8$ cm.....	76
Figure 6-7: Scoop Force Measurements and Model for 6.2 cm	77
Figure 6-8: Soil Model Only Holds for 15-20° of Scoop Motion.....	78
Figure 6-9: Soil Rupture Zone Collision	79
Figure 6-10: Soil Rupture Zone Collision Scoop Angle vs. Scoop Height	79
Figure 6-11: The Angle Between Blade and Nut is 13°	80
Figure 6-12: Force/Velocity Profile for $h = 6.2$ cm.....	81
Figure 6-13: Force/Velocity Profile for $h = 5.5$ cm and $h = 7.7$	81
Figure 6-14: Theorized Soil Failure Pattern in Oscillating Region	83
Figure 6-15: Sensitivity Analysis of TERPS Soil Model	84
Figure 6-16: Force Requirements for Different Soil Types Based on Height	86
Figure 7-1: TERPS Collecting Pure Soil Sample	89
Figure 7-2: 210 g Sample of Soil Fines and Rock Fragments	90
Figure 7-3: TERPS Sifting Soil Sample	90
Figure 7-4: 113 g Sifted Rock Chip Sample.....	91
Figure 7-5: TERPS Collecting a Soil Core (<i>scoops not attached</i>).....	92
Figure 7-6: 4 cm Soil Core.....	92
Figure 7-7: TERPS Grasping and Holding a Small Rock (L) and Large Rock (R).....	93
Figure 7-8: TERPS Holding Other Tools (Hammer and Core Tube).....	93
Figure 7-9: Rock Coring/Abrading.....	94
Figure 7-10: Before and After Rock Abrading.....	95
Figure 7-11: Drill Demonstration on Foam	95
Figure 7-12: TERPS Sand Box Testing.....	96
Figure 8-1: Sketch of Next TERPS Prototype	104
Figure 8-2: TERPS as Crew Aid.....	105

List of Abbreviations & Symbols

ALSD	Apollo Lunar Surface Drill
APL	Applied Physics Laboratory
APXS	Alpha Proton X-ray Spectrometer
ASRO	Astronaut-Rover
CAT	Crew Aid Tool
DAQ	Data Acquisition
DOF	Degree of Freedom
ERA	EVA Robotic Assistant
ESA	European Space Agency
EVA	Extra-Vehicular Activity
IDD	Instrument Deployment Device
JPL	Jet Propulsion Laboratory
JSC	Johnson Space Center
KS	Kolmogorov-Smirnov test
MER	Mars Exploration Rover
MPL	Mars Polar Lander
MRoSA2	Micro Robots for Scientific Applications
MSL	Mars Science Laboratory
MSR	Mars Sample Return
NASA	National Aeronautics and Space Administration
RAT	Rock abrasion Tool
RP	Rapid Prototype
SA/SPaH	Sample Acquisition/Sample Processing and Handling
SAMURAI	Subsea Arctic Manipulator for Underwater Retrieval and Autonomous Intervention
SD2	Sampling Drilling and Distribution System (Rosetta)
SSL	Space Systems Laboratory
TERPS	Tool for EVA or Robotic Planetary Sampling
TGSS	Touch-and-Go Surface Sampler
UMD	University of Maryland
USA	United States of America
USDC	Ultrasonic/Sonic Driller/Corer
USSR	Union of Soviet Socialist Republics (currently Russian Federation)
VSE	Vision for Space Exploration

A	Ampere
c	Soil Cohesion
cm	Centimeter
d	Blade Depth
F	Force
g	Gram
in	Inch

kg	Kilogram
kPa	Kilopascal
m	Meter
mA	Milliamp
mm	Millimeter
PD	Gear Pitch Diameter
PR	Gear Pitch Radius
r	Soil Fracture Length
rpm	Rotations Per Minute
T	Torque
V	Volt
W	Watts
w	Blade Width
α	Rake Angle
β	Angle of Soil Fracture
γ	Scoop Angle
δ	Soil-Tool Friction Angle
θ	Secondary Soil Failure Angle
ρ	Soil Bulk Density
τ	Shear Stress
σ	Normal Stress
φ	Soil Internal Friction Angle
Ω	Ohms

Chapter 1

Introduction

The United States and Russia (as the Soviet Union) have been pursuing regular planetary exploration since the 1950s with the Europeans and Japanese becoming active in planetary exploration in the last 20 years [1]. Throughout this period, robots performed a majority of the work, taking pictures, collecting and analyzing samples, and transmitting data back to Earth for study. With the Apollo program came pairs of astronauts working to deploy science experiments and collect samples, again, to be analyzed and studied back on Earth. As the National Aeronautics and Space Administration (NASA) begins to implement its Vision for Space Exploration (VSE), robots will become more important in exploration of the solar system and will work in tandem with humans exploring the Moon and, eventually, Mars. In order for a human/robot team to be successful, numerous hardware, software, and behavioral issues need to be resolved. This thesis addresses one of the hardware issues, presenting a geologic sampling tool for human and/or robotic applications.

1.1 Motivation

Scientists study geology to learn the physical history of the earth and the processes involved in its formation. Comparable study of other planets can not only yield similar information for those planets, but can also offer insights into the history and

formation of the solar system. One of the most important aspects of geology is to create a spatial map of the structural features of a region or body. Another important aspect of geology, which is related to this spatial mapping, is sampling. Collecting and analyzing samples gives scientists a chemical profile that is useful for studying past atmospheric/weather conditions or looking for signs of water or life.

Most human experience with planetary exploration and sampling has been robotic. In these cases the spacecraft was only able, if at all, to collect a small sample (on the order of a few grams) for limited in-situ analysis. The Apollo astronauts were able to collect several hundred kilograms of lunar samples for wide ranging analysis on Earth, though there were limits to what they were able to accomplish. Concepts for future manned planetary expeditions (such as the one depicted in Figure 1-1 below) entail humans working together with robots to perform scientific surveys and deploy instruments and equipment. The human will provide high level intelligence and decision making lacked by the robot, and the robot will provide mobility and dexterity currently lacked by a suited astronaut.

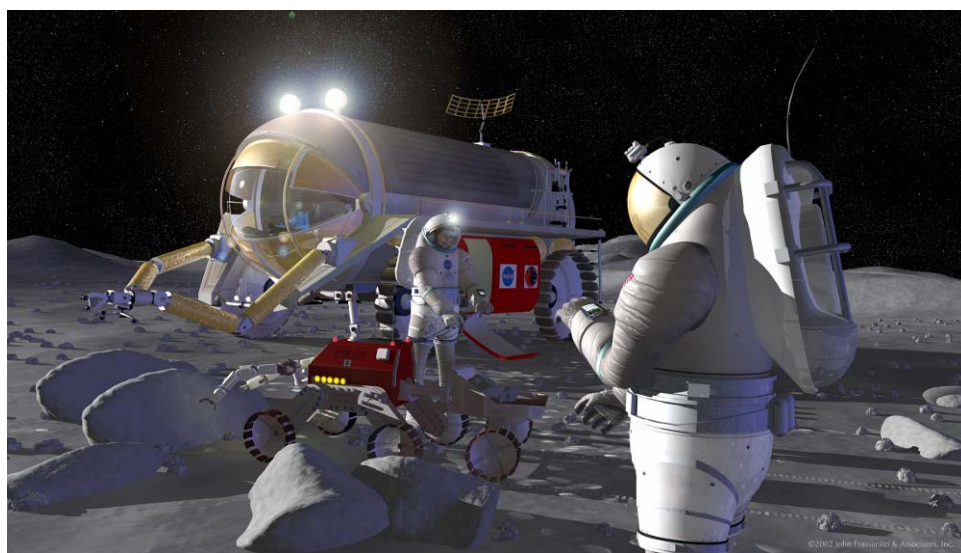


Figure 1-1: Human/Robot Team Concept (image from [2])

Humans and robots working together, especially in space, is an interesting and exciting idea, both technologically and ideologically. This is one of the primary areas of research at the University of Maryland Space Systems Laboratory (SSL) which studies space robotics, human factors, and human/robot interaction. The research at the SSL hopes to answer some of the questions regarding the astronaut/robot team that must be answered before they start exploring: What are the roles/task assignments for the astronaut and the robot? How does the robot know what to do? Is it autonomous or remotely operated? Will an astronaut/robot team be technologically practical? These are some of the general problems surrounding the astronaut/robot team. More specifically, what tools are required for astronauts and robots to work together, especially in the area of field geology? This is the question addressed in this thesis.

1.2 Thesis Goal

The goal for this project is to develop a tool that can be used as either a robotic end-effector or as a Crew Aid Tool (CAT) for geologic sampling and to use that tool for research in planetary surface systems and strategies. The goal for this thesis is to research and develop the requirements for a general sampling tool, produce an initial prototype(s), and evaluate its sample and data gathering abilities. The immediate goal is to define and evaluate the requirements associated with planetary sampling based on geology, lessons from previous planetary exploration, and soil/rock mechanics. The ultimate goal is to develop a tool that can be used in robotic, human factors, and/or human-robotic interaction research in support of future planetary exploration.

1.3 The Tool for EVA or Robotic Planetary Sampling

The result of this work is the Tool for EVA or Robotic Planetary Sampling (TERPS), pictured in Figure 1-2. TERPS consists of two clamshell scoops driven by a single motor and a drill. The scoop gear-motor drives a worm gear transmission, which can open and close the scoops up to 90° for the collection and manipulation of soil and small rocks. A small drill head protrudes from the “palm” allowing for cutting and coring both rocks and soil.



Figure 1-2: Tool for EVA or Robotic Planetary Sampling

TERPS was tested in a lab setting using bins of differing soil types as well as in a large sand box. The sand box testing confirmed TERPS’s ability to perform basic sampling tasks: scooping, digging, grasping, etc. In the lab testing, the electric current drawn by the motor was measured to estimate the torque produced, and therefore the forces exerted by the scoops on the soil. This was compared to a soil cutting model based

on soil parameters. Both sets of tests yielded positive results showing promise for future research using TERPS.

1.4 TERPS Applications

All of the research presented in this thesis was conducted at the Space Systems Laboratory (SSL) at the University of Maryland which is actively researching aspects of both manned and robotic space exploration. The SSL conducts research in EVA suit and tool technology, space related human factors, dexterous robotic manipulators for space/underwater applications, and human-robot interaction. With NASA planning to begin surface system development within the next five years for an expected 2020 lunar landing [2, 3], now is a good time for laboratories such as the SSL to begin addressing some of the issues associated with planetary exploration, especially human/robot exploration. One area not covered in depth is surface tools. TERPS is a sampling tool that provides a platform for investigating some of these exploration issues. For example, TERPS could be used to:

- Study the task assignments for an astronaut/rover team
- Study effectiveness of having identical or similar tools for both human and robot explorers
- Study remote/control methods and hardware for powered surface CATs (including both hand position/availability and glove/dexterity issues)
- Study the effects of dust on the mechanism and mitigation strategies

This is far from a comprehensive list of research possibilities. There are likely countless other problems for which TERPS would make an adequate research tool.

1.5 Thesis Organization

Chapter 2 gives an overview of planetary surface exploration, especially with regard to sampling missions and activities. Chapter 3 discusses a study of the Apollo surface activities, astronaut/rover studies in recent years, and how the two drive the requirements for a new sampling tool. The TERPS system and development is described in greater detail in Chapter 4. Chapter 5 discusses the laboratory set-up used to test the TERPS system. Chapters 6 and 7 discuss the testing and results. Finally, Chapter 8 presents conclusions and future work.

Chapter 2

Background: Planetary Surface Exploration & Sampling

Planetary exploration missions have ranged from orbital imaging and mapping to sample collection and return. The technological and financial constraints of spaceflight limit what hardware can be sent away from Earth, so the tools and instruments on these spacecraft tend to be limited and task specific. However, each new mission has more ambitious scientific objectives forcing improvements in technology and spacecraft capabilities, with the sampling and analysis systems building and improving on previous ones. This chapter discusses the goals of planetary geology, particularly with respect to robotic sampling technology and how that technology has evolved*.

2.1 Planetary Geology

The goals of planetary geology, as described by the Space Studies Board of the National Research Council, are to:

...‘understand how physical and chemical processes determine the main characteristics of the planets, thereby illuminating the workings of Earth.; (2) to ‘learn how planetary systems originate and evolve’; (3) to ‘determine how life developed in the solar system and in what ways life modifies planetary environments’; and (4) to ‘discover how the simple, basic laws of physics and chemistry can lead to the diverse phenomena observed in complex systems.’ [4]

* For the purposes of this review, sampling will be defined as collecting, manipulating, or destroying surface materials for analysis or imaging by another instrument. For example, impacting is not considered sampling because any data gathered is based on the impact itself. Grinding, on the other hand, is considered sampling because it exposes the subsurface to cameras or instruments.

These goals and the study of geology in general, are achieved by analyzing data gathered in the field. It is important to note that sampling is *not* the primary objective of geologic field work. The primary objective in field geology is to establish a “baseline of data” by mapping the spatial distribution of different rocks and features in an area and using that information to determine how they relate to each other and how geological events (fracturing, weathering, impacts, etc.) affect them [5]. This should not, however, diminish the importance of sampling. Collecting samples allows for in-depth analysis of the area’s physical/chemical composition adding detail to the observations made in the field. Sample analysis can help determine the chemical effects of catastrophic impacts, the thermal/chemical history of the region/body, the similarities or dissimilarities with Earth and other bodies, the potential for economic benefit, and the presence (past or current) of water or life [4, 6].

Chemically analyzing planetary samples allows scientists to classify and compare planetary bodies. Of particular importance, especially in studying asteroids and comets, is knowing the abundance of metals such as iron, magnesium, and aluminum, which classifies a body and, overall, identifies the mineral composition and distribution of the solar system. Geological histories can be observed by the abundances of rock forming elements (magnesium, silicon, calcium, titanium, chromium, iron, and nickel). Biologic studies look for water and other volatiles (chemical compounds containing carbon, hydrogen, oxygen, and/or nitrogen). There are several types of tests that can detect these elements. Alpha-Proton-X-ray Spectrometers (APXS), Gamma-ray spectrometers can detect most of these elements; the Mössbauer Spectrometers and X-ray Florescence devices can accurately detect iron and similar metals. All of these has spaceflight history

and can be deployed on a target – it is possible to use these devices without physically collecting a sample. Gas chromatographs and other mass spectrometers are useful for studying organics and volatiles. These instruments, which heat and vaporize the sample, do require sample collection and processing [4].

The types of analysis desired or required for any given planetary exploration mission drive the sampling system design. Many of the early missions were strictly observational, used mechanical measurements, or returned samples to earth for analysis, and the sampling system reflected that. Later missions, especially to Mars, performed more in-situ analysis and the sampling systems were based almost entirely on the capabilities of on-board scientific instrumentation.

2.2 Sampling Methods of Previous Missions

The first extraterrestrial planetary sample was taken in April of 1967 when Surveyor III began digging trenches on the moon with its scoop. Since then, 19 missions have collected samples of other planetary bodies [1]. This activity, outlined in Table 2-1, has included manned missions, stationary landers, mobile rovers, and several different sampling methods. By far, the most popular sampling methods are scooping and drilling, but other methods have been used or studied, including rakes, abraders, and projectiles.

Table 2-1: Overview of Past/Current Successful Planetary Sampling Programs ([1, 7])

Program (Country)	Planet	Time Frame	Sampling Method (Mission No.)	Sampling Activity
Luna (USSR)	Moon	1959-1976	Drill (16, 20 & 24)	330 g
Surveyor (USA)	Moon	1966-1968	Scoop (3 & 7)	49 tests
Apollo (USA)	Moon	1969-1972	Hand Tools (all)	382 kg
Venera/Vega (USSR)	Venus	1970-1984	Drill (13, 14, 1, 2)	Unknown
Viking (USA)	Mars	1975	Scoop (all)	81 activities
Hayabusa (Japan)	Asteroid	2003-	Projectile	Unknown
MER (USA)	Mars	2003-	Rock Abrasion	
Rosetta (ESA)	Comet	2004-	Drill	En-route

2.2.1 Manned Sampling

The most successful planetary sampling program in terms of quantity of samples was the Apollo Program. The six Apollo landings returned 380 kg of lunar regolith[†] and rock. On Earth, a geologist's field kit would typically include a hand lens, a hammer, a notebook, and a camera. He or she would observe, note/sketch, and photograph the area, using the hammer and hand lens to make note of rock types and composition. The loss of mobility and dexterity to the EVA suit, and the fact that only one of the 12 Apollo surface astronauts (Harrison "Jack" Schmitt, Apollo 17) was a trained geologist, precluded this type of typical field survey on the lunar surface. Instead, Apollo astronauts could only take pictures and relay observations to mission control vocally. Sampling required the use of several different tools, including a hammer, a rake, scoops, and tongs. Astronauts also made use of extension handles to avoid bending and kneeling. These tools, shown in Figure 2-1, and their usage will be discussed with greater detail in Chapter 3.

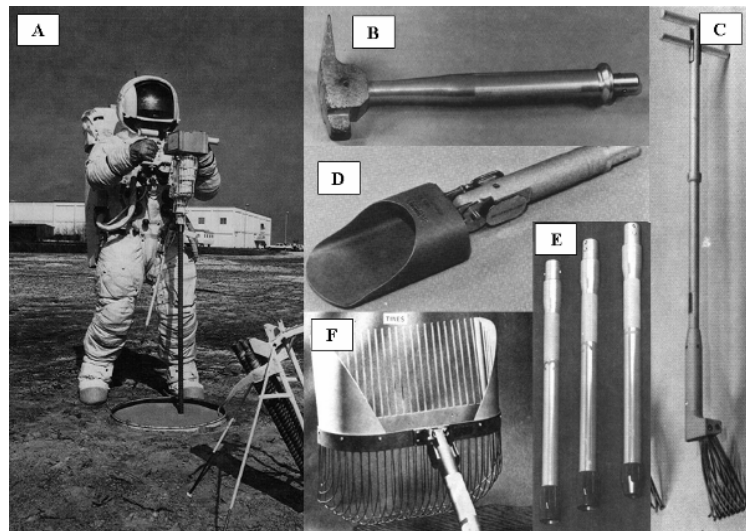


Figure 2-1: Apollo Lunar Surface Sampling Tools

(A) – Astronaut training with drill, (B) – Rock Hammer, (C)–Spring Actuated Tongs, (D)–Small Adjustable Scoop, (E) – Core tubes, (F) – Rake (images from [9])

^{††} Regolith is defined as, “The layer of rock and mineral fragments that rests on bedrock and is produced by the weathering of rocks. Regolith constitutes the surface of most land.”[8] While both loose rock and soil constitute the regolith on a planet, the term is used here and in literature interchangeably with “soil.”

2.2.2 Drills

The most common method for collecting surface samples is a drill, used on 19 of the 36 sampling missions [1]. The principle of drill is straight forward – rotary motion is used to cut, mill, or auger the sample from the surface or object. Mechanically, the drill is relatively simple, consisting of a motor, gear train, and drill bit. Collecting and transferring a sample typically only requires a one or two degree of freedom (DOF) mechanism. This mechanical/electrical simplicity makes drills ideal for planetary spacecraft. Drilling systems do, however, have limits. First, drills, at least the ones flown to date, can only collect a few grams of surface material, the bare minimum for most scientific instruments [10]. Second, as it moves across the rock/surface, the bit generates frictional heat which can chemically alter the sample or overheat the motor, neither of which is desirable. Third, drilling dulls the bit which limits the system's lifetime or requires changing bits. As long as these limitations are addressed, a drill system can successfully collect samples, as shown by the Luna, and Venera probes.

Luna

The Soviet Luna program consisted of three generations of lunar probes. The first and second generations were orbiters/impactors (Luna 1-3) and landers (Luna 4 – 14), respectively. The third generation spacecraft (Luna 15 – 24) were meant to advance exploration technology by either deploying a rover or collecting and returning samples to Earth (the first of this series was also likely mean to try and upstage the American Apollo 11 landing) [11]. Luna 16 (1970), 20 (1972), and 24 (1976) successfully returned about 330 g (total) of lunar regolith [1]. The samples were collected by a drill mounted to the

end of a 1 DOF boom (see Figure 2-2). After collecting the sample, the arm swung up to deposit the sample in the return vehicle.

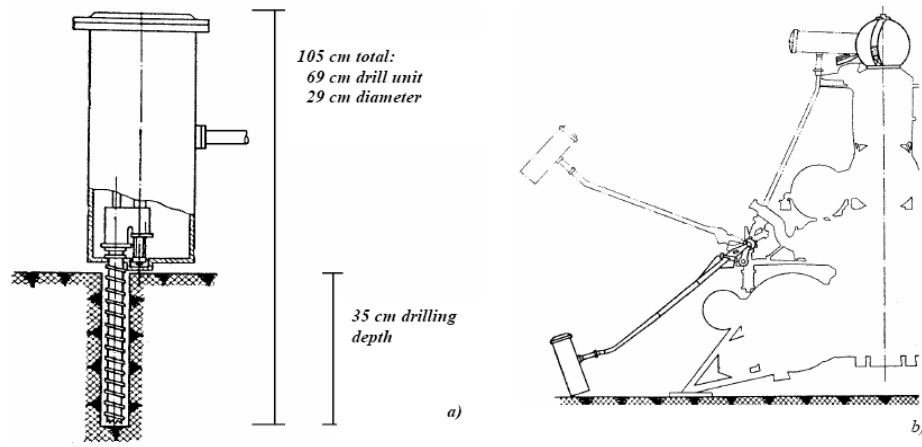


Figure 2-2: Luna Sampler Arm and Drill (image from [12])

Venera/Vega

The Soviet Venera and Vega probes were the only spacecraft to land on and sample Venus. Venera 13 and 14, launched in 1981, and Vega 1 and 2, launched in 1984, were all similar probes that had a small drill to collect a sample for on board spectrographic analysis [1]. The extraordinarily harsh surface environment on the Venusian surface made this an interesting engineering challenge, but all four of these probes were able to collect surface samples and return data to Earth for about an hour after landing.

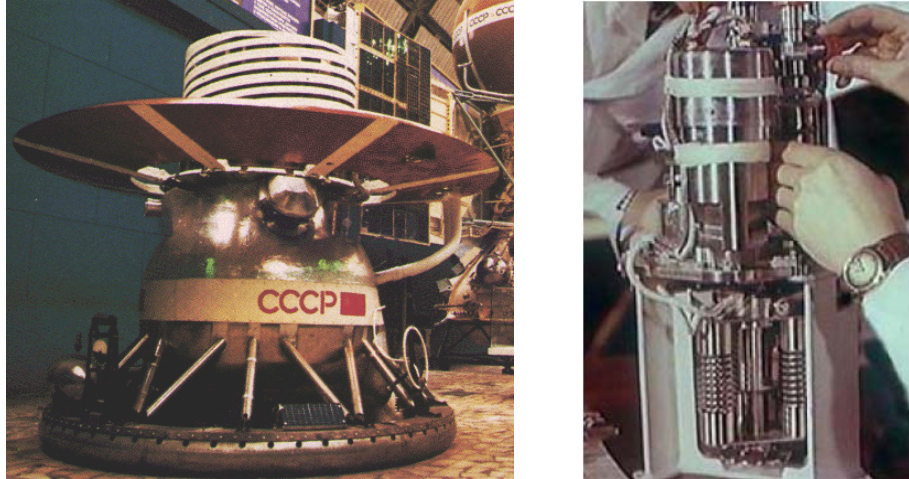


Figure 2-3: Venera/Vega Venus Surface Landers
(L) *Venera/Vega Lander* [1], (R) *Venus Surface Drill* [13]

Rosetta

A current example of a sampling drill system is the Sampling Drilling and Distribution (SD2) system aboard the European Space Agency's (ESA) Rosetta lander. Launched in 2004, this probe and lander is en-route to the comet 67P/Churyumov-Gerasimenko. After landing the SD2 will be able to collect up to 26 sample cores of up to 23 cm deep at different locations immediately surrounding the lander [14].

2.2.3 Scoops

A drill system may be a simple mechanical system, but the scoop is an easier method for collecting a sample – the sample is obtained by pushing or pulling a blade or container across the surface. This tends to require a multiple DOF arm, which makes it a generally more complex and power consuming system. It is, however, a very flexible system able to collect soil and rock chips (depending on size) with masses on the order of 10 – 100 g. Additionally, because it requires an arm, a scoop system can more easily manipulate the environment (dig trenches, move rocks, etc.). Scoops have been used on the Surveyor probes, Viking landers, and Mars Polar Lander type landers.

Surveyor

The Surveyor Program was a precursor to the Apollo Program with probes being sent to potential landing sites. In fact, the crew of Apollo 12, which landed near Surveyor III, retrieved hardware from the probe to return to Earth; see Figure 2-4. Two of the probes carried scoops (Surveyors III in 1967 and VII in 1968). The Surveyor scoops were designed to conduct soil mechanics tests on lunar regolith. The scoop was 12 cm long by 5 cm wide and mounted on a 3 DOF pantograph arm with a reach of 1.5 m [1]. Engineers measured electrical currents and temperatures in the arm's systems to determine the force exerted on the soil. This allowed them to estimate mechanical properties of the soil. Further inferences were made by examining images of soil piles and trench walls dug by the sampler [7].

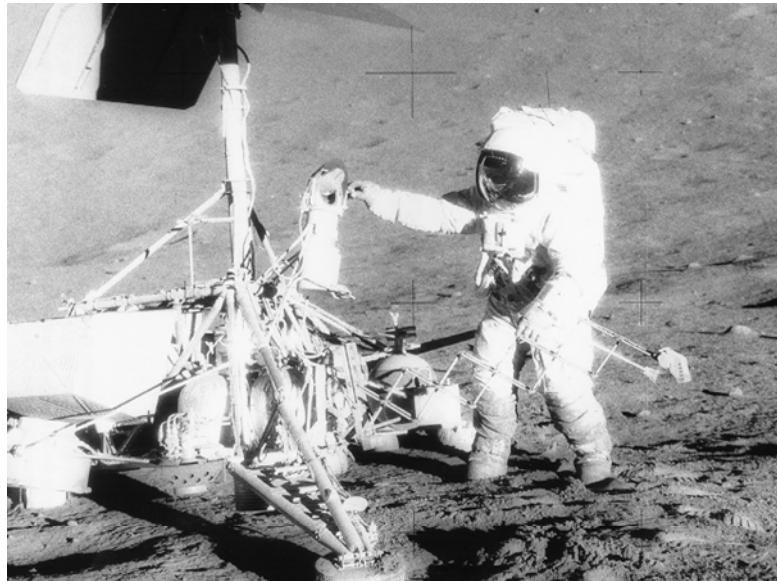


Figure 2-4: Al Bean (Apollo 12) Standing at Surveyor III [1]

Viking

The two Viking landers (1975) were the first to sample the Martian surface and were the first to carry a large suit of analytical equipment. The Viking landers carried meteorology sensors, cameras, spectrometers, and various other instruments to, “study the biology, chemical composition (organic and inorganic), meteorology, seismology, magnetic properties, appearance, and physical properties of the Martian surface and atmosphere” [1]. The samples were collected with a 4.8 cm wide surface sampler head (see Figure 2-5) attached to a 4 DOF extendable boom. The sampler head could either be pushed or pulled across the surface with surface properties estimated from the resulting motor currents. Collected samples were deposited into the onboard chromatograph and spectrometers for analysis [15].

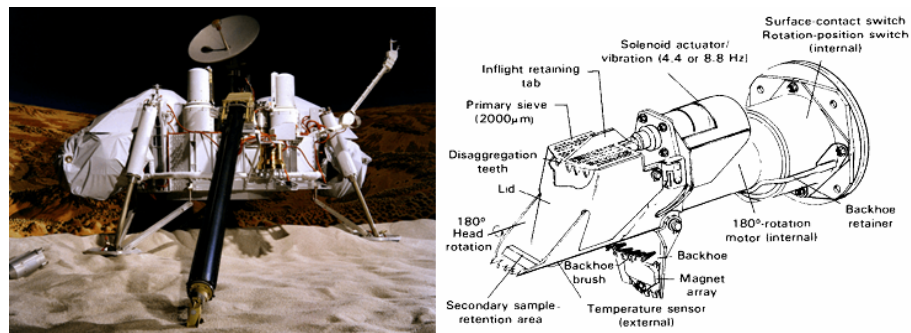


Figure 2-5: Viking Lander/ Sampling System
(L) Viking Lander Mockup with Sample Boom Extended [1], (R) Viking Sampler Head [15]

Mars Polar Lander / Mars Surveyor / Phoenix

After Viking, no Mars sample collection was attempted until the Mars Polar Lander (MPL) in 1999. The MPL was a stationary lander designed to collect samples with a 2.2 m long, 4 DOF, back-hoe style arm with a 500 cc capacity scoop. The arm and scoop were to deposit samples into a series of on-board chemical and biological analysis

instruments [16]. Communication with the MPL was lost just before landing and it is assumed a software glitch cut the engines too early cause the lander to crash. However, the system architecture had already been used in the design of the 2001 Mars Surveyor Lander. The Mars Surveyor '01 was to collect samples using a scoop on a 2 m, 4 DOF, back-hoe style arm [17]. This mission, plagued by technical issues and cost overruns was canceled before launch. Not to be deterred, NASA is using design and hardware heritage from MPL and the '01 Surveyor on the Phoenix lander, set to launch in late 2007 (see Figure 2-6). Phoenix will collect soil and rock samples for in-situ analysis using a scoop on a 2.3 m, 4 DOF, back-hoe style arm [18].

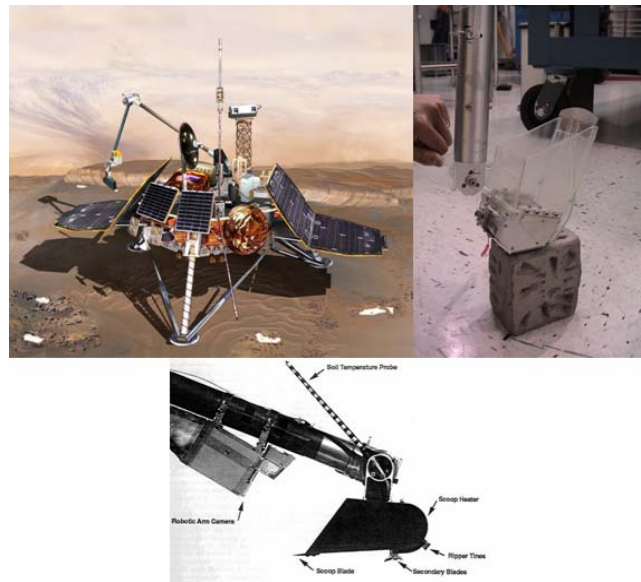


Figure 2-6: Mars Polar Lander/Phoenix Lander

(Top L) Mars Phoenix Lander/Polar Lander Artist's Concept (NASA used same image for both probes) [19], (Top R) Phoenix Test Scoop [19], (Bottom) Mars Polar Lander Scoop [16]

2.2.4 Other Systems

Scooping and drilling have not been the only sampling methods used in planetary research. In fact, the sampling missions in the past five years have made use of alternative sampling methods. The Mars Exploration Rovers use a grinder, the Mars lander Beagle 2 was to use a mole, and the asteroid probe Hayabusa used a projectile.

Mars Exploration Rovers (Abrasion)

The twin Mars Exploration Rovers (MERs), launched in 2003, are six wheeled rovers derived in part from the 1996 Pathfinder Rover, “Sojourner.” Unlike previous landers, Sojourner and the MERs were meant to drive to targets for analysis, as opposed to collecting samples and depositing them to on-board sensors. Sojourner carried only cameras and an Alpha-Proton-X-ray Spectrometer (APXS) [1]. The MERs each carry a microscopic imager, Mössbauer Spectrometer, APXS, and Rock Abrasion Tool (RAT). This instrument suite is mounted at the end of a 0.75 m, 5 DOF robotic arm called the Instrument Deployment Device (IDD), shown in Figure 2-7 [20].

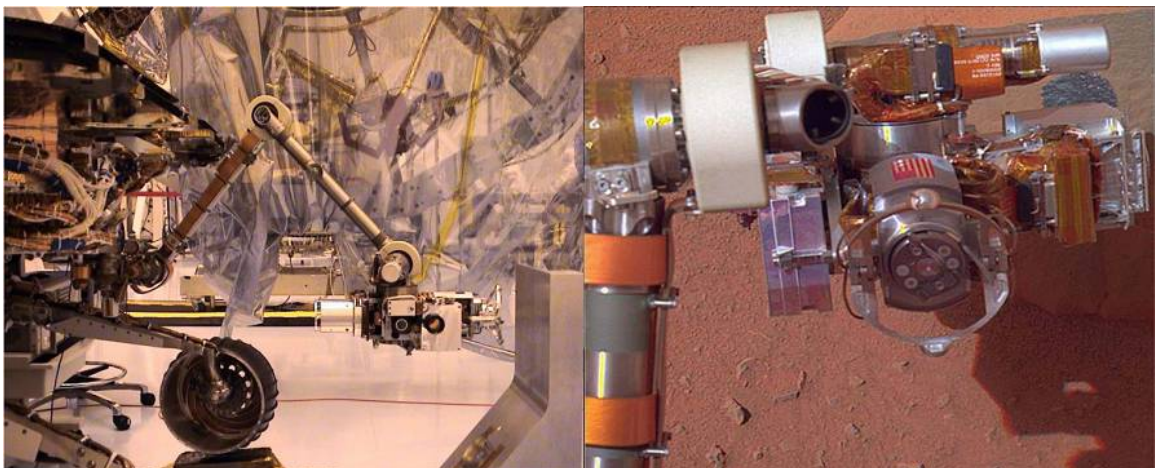


Figure 2-7: Mars Exploration Rover “Sampling” System
(L) MER Instrument Deployment Device [20], (R) RAT on MER Arm [21]

The sampling system on each MER is the RAT. The MER approaches a target of interest (a rock) and the IDD places the RAT near its surface. The RAT then grinds away a 45 mm diameter patch up to 9 mm deep [21]. This exposes the rock interior for analysis by the other instruments. With this system, the MER can conduct sampling without ever collecting a sample.

Beagle 2 (Grinder/Mole)

Beagle 2 was the lander part of the ESA's 2003 Mars Express mission. It included a robotic arm with a sensor suite similar to that of the MERs, containing a mole, stereo camera, grinder/corer, Mössbauer spectrometer, and optical microscope. Sampling was to be conducted with the mole and grinder. The mole contained a spring mechanism that would allow it to move across the surface or burrow beneath it. A cavity in the tip would collect and hold soil samples. The corer/grinder would function similarly to the RAT and would also collect small core samples of rocks within reach. Neither of these systems was ever used on Mars; ground controllers lost contact with the spacecraft after it entered the Martian atmosphere [1].

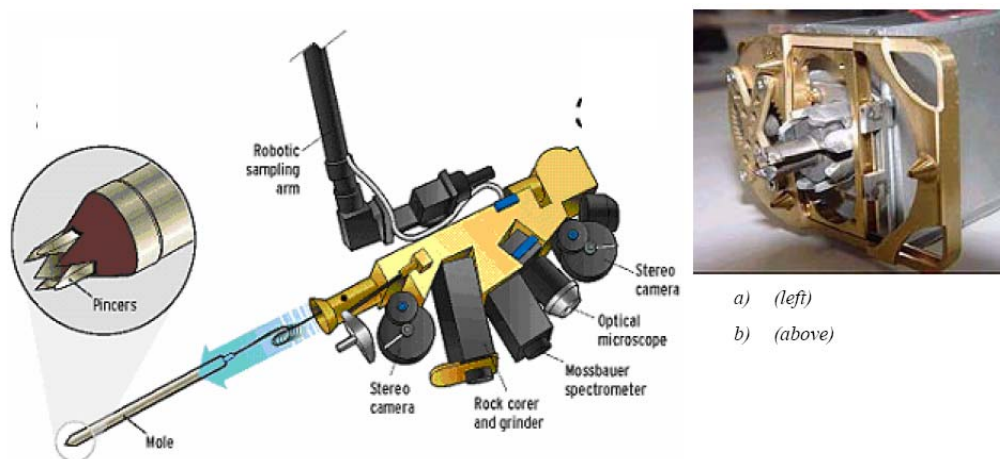


Figure 2-8: Beagle 2 Sampling System
(L) Sampling Suite on Beagle 2, (R) Corer/Grinder (image from [12])

Hayabusa (Projectile)

Hayabusa is a Japanese sample return probe to asteroid 25143, Itokawa. Launched in 2003, it arrived at Itokawa in 2005. The “lander” approached the asteroid surface (see Figure 2-9) and was to release a small projectile. The ejecta kicked up by the impact was to be funneled into a sampler horn and collected. It is unknown whether this maneuver was successful, but scientists are hopeful that at least some dust or small particles floated into the sampler horn. Hayabusa is scheduled to return to Earth in 2010 [1].

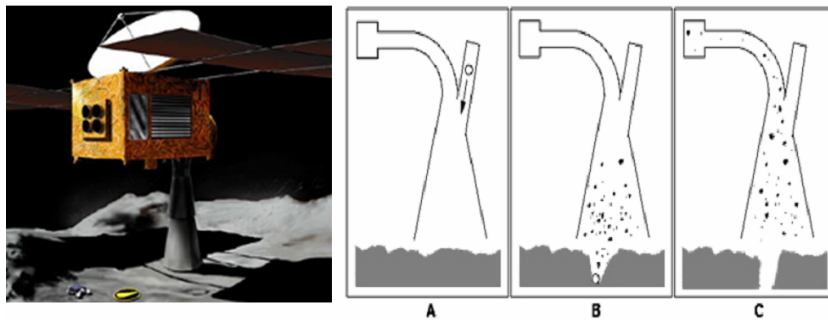


Figure 2-9: Hayabusa Projectile Sampling
(L) Artist's Rendering of Hayabusa, (R) Projectile Sampling Sketch [12]

2.3 Future Sampling Missions

The next five to ten years will see a slew of Mars exploration/sample collection missions. Phoenix is scheduled to launch later this year (2007), NASA's Mars Science Laboratory (MSL) and Russia's Phobos-Grunt missions are scheduled to launch in 2009, and the ESA is planning on launching its ExoMars Rover in 2011. Further on, NASA is planning more Mars landers and a sample return mission.

Mars Science Laboratory

NASA's next generation rover is the Mars Science Laboratory (MSL) set to launch in 2009. MSL is comparable in size, weight, and scientific payload to the Viking landers, but is wheeled like the MERs [1]. Samples will be collected using the Sample Acquisition/Sample Processing and Handling (SA/SPaH) system under development at NASA's Jet Propulsion Laboratory (JPL). The SA/SPaH system (see Figure 2-10) includes a 5 DOF manipulator and an end effector which includes an abrader similar to the RAT, a corer and scoop [22]. It will be able to collect both regolith and rock cores of up to 5 cm, grind them down to particles as small as 150 μm for the on-board chemical and spectrographic analyzers [23].

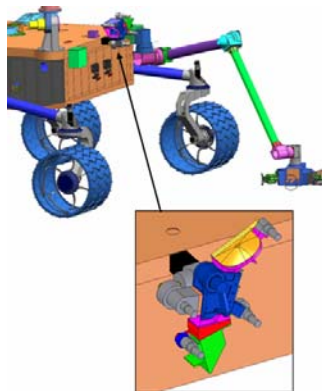


Figure 2-10: MSL Sample Acquisition/Sample Processing and Handling System [23]

Future Sampling

The other planned sampling missions are early enough in development that many of their systems have not been fully designed. The trend in these missions is mobility, which is scientifically useful as a mobile robot can examine or collect more diverse samples. These systems have limited equipment and few sampling requirements (only a few grams), so the sampling systems for these rovers continues to be small corers or

grinders, and will probably remain so until collecting larger samples become the main goal.

2.4 Current Laboratory Research

All of the systems discussed thus far have been mission specific and tailored to the requirements for that particular spacecraft. Several organizations are conducting or have recently conducted research into similar types of sampling systems. The goal for these projects has been to expand the technology by finding better ways of sampling (i.e. using less power, accessing deeper soil, etc.).

Honeybee Robotics Sampling Systems

The Honeybee Robotics Spacecraft Mechanisms Corporation (New York) has been active in sampling research. Honeybee is the designer/developer of the MER RAT as well as the MSL corer/abrader tool. They specialize in drilling systems but have done work on several interesting sampling platforms. They have designed and tested drillers for 1 m and 10 m depths (see Figure 2-11) as well as tried to integrate sensors directly into the drill stem for direct measurements during cutting.



Figure 2-11: Honeybee Robotics Sampling Systems
(L) Mars Deep Drill (10 m), (R) Touch and Go Sampler [21]

Another of Honeybee's interesting systems is the Touch-and-Go Surface Sampler (TGSS). This system, also shown in Figure 2-11, was designed for a balloon-based or hover-type craft. The TGSS hangs below the craft from a flexible shaft. The rotating sample head and counter rotating sample bits kick up debris into chutes on the system or on the base of the craft [21].

Micro Robot for Scientific Applications

The Helsinki University of Technology Laboratory of Space Technology developed a Micro Robot for Scientific Applications (MRoSA2) as part of an ESA grant. The goal was to design a 5 kg 11 X 11 X 35 cm sampling drill capable of collecting a core sample of up to 2 m of regolith. The sampling system, pictured in Figure 2-12, houses a carousel ten 20 cm core pipes that automatically attach or detach to the drill motor. Testing showed this type of sampling to be feasible with great promise for future development [12].

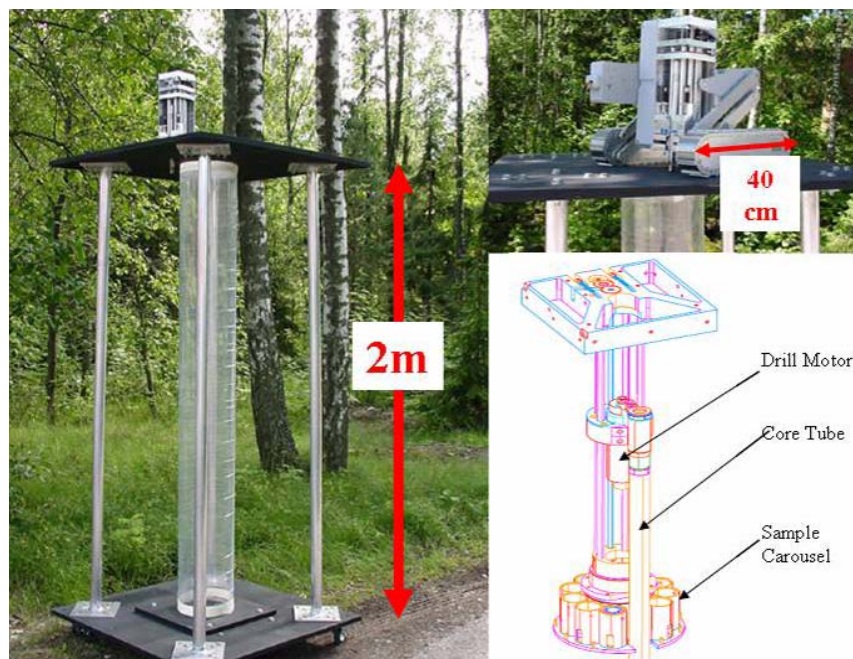


Figure 2-12: Micro Robot for Scientific Applications (MRoSA2)
(L/Top R) MRoSA2 Drill on 2m Test Stand, (R) MroSA2 Sampling System Model (adapted from [12])

Ultrasonic/Sonic Driller/Corer (JPL)

JPL has developed an interesting, unconventional sampling device. The Ultrasonic/Sonic Driller/Corer (USDC) uses high frequency vibration to “bounce” a free floating mass off the drill bit to fracture the target rock (see Figure 2-13). The USDC unit has been successful in drilling 5 mm holes in several types of rock, doing so with 10 times less axial force and power draw than a conventional drill. It also works as a “lab-on-drill” showing promise in determining rock properties based on power draw and sample rate [24]. It can “drill” holes, collect cores, abrade, or mole depending on the bit used.



Figure 2-13: Photograph and Sketch of USDC [24]

Pyrotechnic Rock Chipper (APL) – 2004

Another interesting, unconventional sampler was developed at John Hopkins’s Applied Physics Laboratory (APL). APL designed a pyrotechnic rock chipper that uses a projectile to collect a sample (similar to the Hyabusa sampling discussed in Section 2.2.4). The pyrotechnic chipper consists of a small explosive charge, a steel penetrator, and a catcher. The charge fires the penetrator into the rock/surface (see Figure 2-14) which kicks up 3 – 16-g of chips and dust into the catcher [25]. This system has the benefit of being light weight and drawing very little power (only enough to ignite the

charge) making it an extremely efficient method of sampling. The drawback to this system is that it is not reusable; each sample requires a new charge.

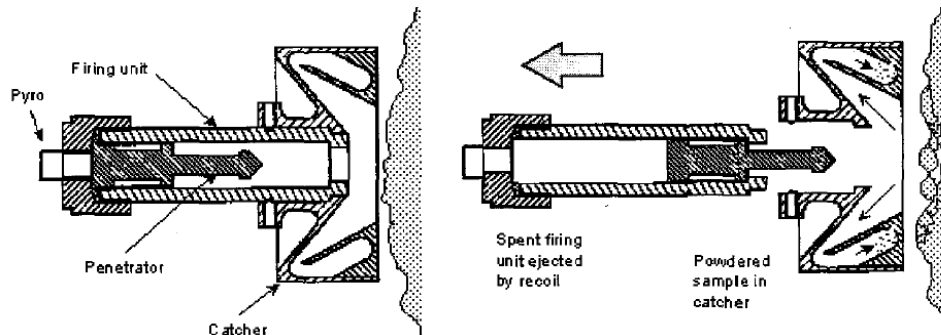


Figure 2-14: Schematic of APL Pyrotechnic Rock Chipper [25]

Underwater Sampling Methods (UMD SSL) - 2007

The University of Maryland SSL, in conjunction with the Woods Hole Oceanographic Institute, is developing a robotic manipulator called SAMURAI (Subsea Arctic Manipulator for Underwater Retrieval and Autonomous Intervention) to autonomously collect geological and biological samples around geothermal vents on the floor of the Arctic Ocean [26]. Several of the concepts for end-effectors for the SAMURAI arm show the similarities and differences between sampling in two harsh environments, deep underwater and extraterrestrial planetary surfaces.

Two concepts under review for the SAMURAI system are the Bushmaster basket device and the Mussel Pot device shown in see Figure 2-15. The Bushmaster device, developed at Pennsylvania State University, consists of a flexible cage that can close around the sample it is trying to collect. The Mussel Pot, developed at Pennsylvania State University and the College of William and Mary, is similar in function to the Bushmaster, but with a rigid sample container with the opening sealed either by an iris mechanism or drawstring cloth. These two devices are adequate for collecting geologic

samples, but are primarily intended to collect biologics (tubeworms, mussel and clams, etc.). The considered geologic samplers are somewhat more traditional. The claw design and the Pacman scoop, both also shown in Figure 2-15, look more like what one would expect to find at the end of a sampling manipulator. The claw is a basic gripper design that can grasp tubeworms and other biologics as well as rocks. The Pacman scoop consists of two hollow semi-cylinders that open and close like a clam [27].

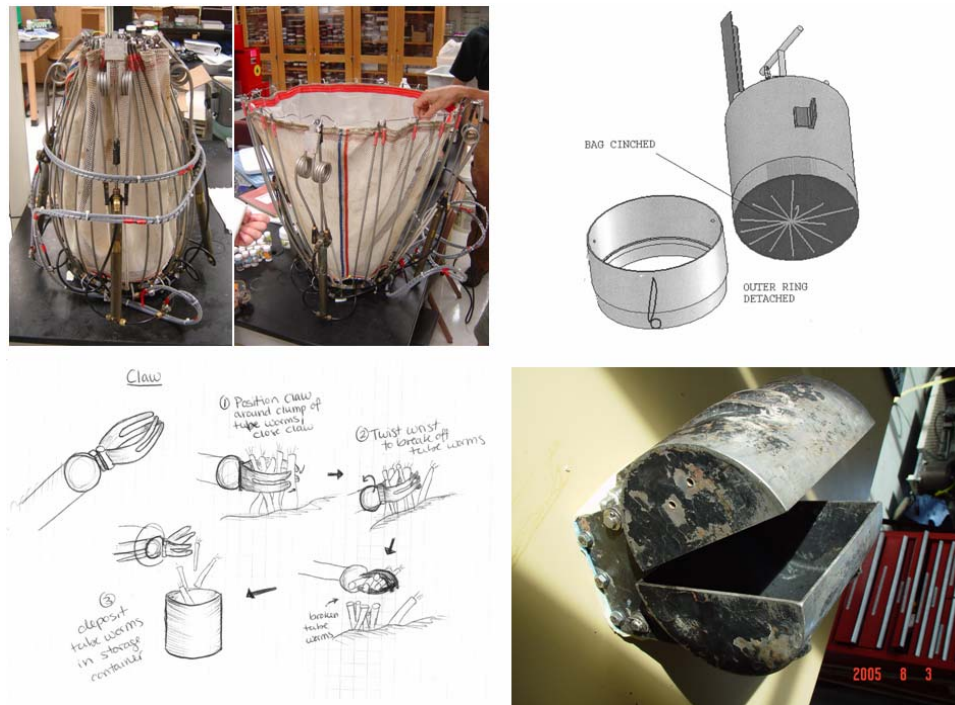


Figure 2-15: Underwater Sampling Concepts
 (Top L) Bushmaster netting device closed and open, (Top R) Mussel Pot / Sample Collection Can,
 (Bot L) Claw concept sketch, (Bot R) Pacman Scooping Device—All images from [27]

The SAMURAI project faces many similar design issues as this project, specifically how to collect various, diverse sample types in a harsh, inaccessible environment. Certainly, some of the elements of planetary surface sampling can be applicable to sub sea sampling and vice versa – note the similarities between the Pacman scoop and the TERPS concept – but the differences in the two environments are important to remember. This is especially true for rock and soil samples (geologic

samples). Water drastically affects the physical properties and behavior of soil, making the collection and/or manipulation of soils from the sea floor very different from collecting and/or manipulating dry planetary regolith.

2.5 Summary

There have been a few different means of collecting planetary surface samples. The most common forms are drills and scoops. Each offers its own advantages and disadvantages for robotic exploration—drills are simple and well suited, mechanically, for robots but are limited in what they can collect, and scoops can be better at collecting and manipulating samples, but are more complex and power consuming. This chapter has concentrated mostly on these robotic sampling systems. When humans enter the loop, the sampling methods will, obviously, depend more heavily on the human capabilities.

Chapter 3

Human/Robot Geology: Requirements & Lessons from Apollo

The previous chapter mainly discussed robotic sampling technology. It is self evident that sampling technology will differ for human sampling and again for human/robot sampling. This chapter will analyze astronaut EVA sampling tools, review human/robot interaction in field geology, and define the requirements for a human/robot sampling tool.

3.1 Apollo Era Sampling

Since the Apollo program is the only instance of manned planetary exploration, it serves as a baseline for designing future manned surface systems. For this thesis, Apollo 17 was used as a case study in EVA geology tools and their usage. Audio and video downlinks from the mission were studied to determine how astronauts used their tools and what problems arose during the mission [28, 29]. The *Catalog of Apollo Lunar Surface Geological Sampling Tools and Containers* [9] and astronaut post flight comments [30] were also examined for broader look at Apollo sampling technology.

3.1.1 Apollo 17

Launch in December of 1972, Apollo 17 was the last of the Apollo flights and is considered one of the most interesting scientifically. Commander Gene Cernan and

Lunar Module Pilot Harrison “Jack” Schmitt performed the most EVA (22 hours total), covered the most distance (30km), and collected the most samples (111 kg) of any mission in the Apollo program [31]. The crew explored the Taurus-Littrow Valley along the rim of Mare Serenitatis, one of the more geologically interesting landing sites of the program. This was also the first and only mission to have a geologist, Jack Schmitt, as part of the crew. These factors make it an ideal mission for studying for surface systems and tools.

3.1.2 Apollo Sampling Tools and Usage

The Apollo tools were designed to allow the suited astronauts to collect samples. EVA suits are bulky and stiff making mobility, bending, and grasping difficult and tiring. Additionally, the tools had to be designed to minimize weight and sample contamination. Many of the earlier tools were deemed inadequate on the first few flights – Al Bean on Apollo 12 noted, “...the lunar equipment we have is generally too flimsy” [32] – and were redesigned. By Apollo 17, the tools were proven and the astronauts knew what worked and what did not in terms of collecting samples.

The tool catalog [9] in conjunction with the Apollo 17 video downlink [28] provided valuable insight into the tools, their usage, and their pros and cons[‡]. The tool catalog contains information (size, weight, material, sample capacity, etc.) and photos of each of the surface tools used in the Apollo program. The Apollo 17 video downlink consists of the videos recorded from the lunar rover camera – so it only shows those portions of the EVA when the camera was on, which does not include preparation/closeout activities or driving. It does, for most of the time, show at least one

[‡] Any mention of tool specifications or usage, unless otherwise noted, is attributed to [9] and [28].

of the astronauts performing tasks – there are times when they are separated or out of sight. It also shows at least one example of each tool being used.

Scoops

The scoops used on Apollo 16 and 17 were large, adjustable scoops based on previous flight models (see Appendix A). Each had an overall length of 35 cm with an 11 cm wide, 15 cm long, 5 cm high pan, and a 76 cm long extension handle – at no point was either astronaut visible using the scoop without the extension handle. The scoop had a joint to adjust the angle between the scoop pan and handle (see Figure 3-1). Schmitt, whom the camera usually followed, used the scoop most of the time. He used it for collecting soils and rocks, and trenching, usually to a depth of about 5 cm.

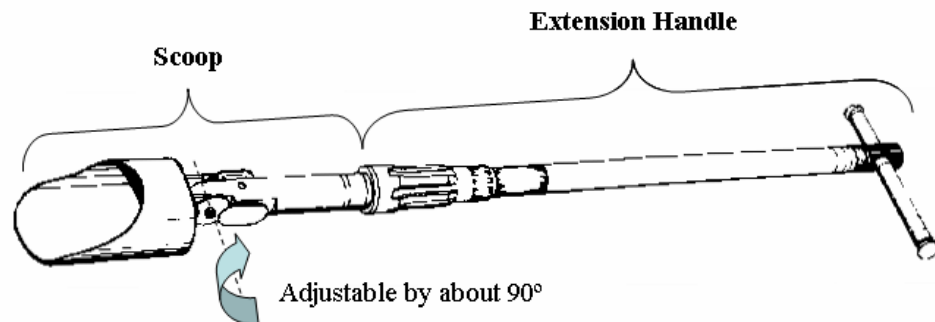


Figure 3-1: Small Adjustable Scoop (adapted from [9])

The astronauts (Cernan and Schmitt) had a few different ways collecting a sample with the scoop, all of which were one handed. In one method, he would hold the scoop to the ground in front of him and push, sometimes leaning into it, then lift it out. Similarly the astronaut would hold the scoop out to his side and push it into the soil. This method, however, required him to bend one knee and lean to that side. Using the same position, he could swing his arm forward and collect a sample at his side.



Figure 3-2: Jack Schmitt Using Scoop [29]

Sample collection with the scoop was usually a two-man job. One would collect the sample while the other held the bag. It was possible, however, to scoop alone by adjusting the scoop to be perpendicular to the handle. In either case, it often appeared awkward for the astronaut taking the sample to hold the scoop steady while trying to pour the sample into the bag.

Rake

The rake was used for collecting bulk chip and rock samples. It consisted of a 29 x 29 x 10 cm open ended basket on a 22cm handle with an attachment for the extension. The rake was also always observed being used with the extension handle. The rake tines were 1 cm apart to allow for sifting out fines from larger rocks. Samples were collected by moving the rake across the surface (Figure 3-3). For this task, the astronaut either held the rake out to his side then side stepped, dragging the rake along, or swung the rake in front of him as if sweeping with a broom. Because the rake was so large, collecting the bulk sample always required both astronauts (one to rake and the other to hold the sample bag).

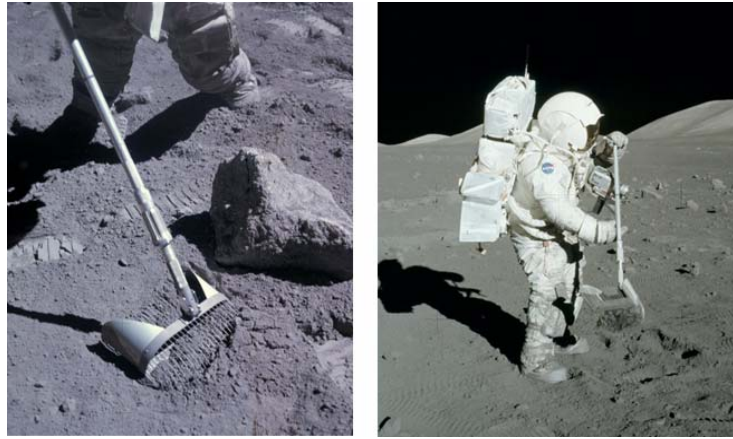


Figure 3-3: Apollo Rake
(L) Rake in Lunar Soil (Apollo 16), (R) Jack Schmitt Using Rake [29]

Tongs

The tongs were designed as grasp augmenters/extenders, capable of picking up single rocks and other objects up to 10 cm wide. The tongs were 80 cm long (76 cm on earlier missions) with spring loaded tines (Figure 3-4). The tines were held shut by the springs; the astronaut would squeeze a t-bar on the handle to open them. Gene Cernan mainly used the tongs, and since he spend much time out of camera view, it is hard to accurately determine its usage. It does appear, though, that it is a useful tool, especially for picking up other tools, but it also appears that it is tiring to use because it requires a firm grasp.



Figure 3-4: Tongs (Apollo 12) [29]

Hammer

The hammer was an important yet problematic tool. It was meant to break chips off large rocks and boulders, and drive core tubes. It could also be used as a hoe or pickax when attached to the extension handle, though this use was not observed during any of the Apollo 17 EVA. Thirty-nine centimeters long and weighing 1.3 kg, the hammer was used the same way a hammer would be used on Earth. This, however, is where the problems lie. Hammering requires a tight grip and large, quick motions, both of which are difficult in a pressurized space suit.



Figure 3-5: Hammer Used to Break Rocks (Apollo 15)

Core Tubes & Drill

The drill and core tubes were designed to collect subsurface samples while preserving the soil structure and layering. There were two versions of the core tubes: the 2 cm diameter core tubes were used on the early missions and the 4 cm diameter drive tubes used on the later ones, including Apollo 17. The 4 cm drive tubes were 42 cm long and could hold a 35 cm soil column. A single core could be taken or two tubes could be attached together to collect a single, 70 cm “double core.” The astronaut collecting the core attached the “top” of the tube to the extension handle and pushed the bit into the

surface. He would then pound the tube to depth by hitting the extension handle with the hammer after which he would use the handle to pull out the core.

The Apollo Lunar Surface Drill (ALSD) had a similar function, but was able to take a 3 m core using 8 2.5 cm diameter, 43 cm long (40 cm soil column) drill stems. The 4 kg rotary-percussive drill head, containing a 0.4 horsepower, Black & Decker motor, drove the stems into the ground at 2270 blows per minute and 280 rotations per minute. A 3.5 kg, 16 cell, silver-oxide/zinc battery powered the system. The astronaut would assemble the drill head, battery, 2 or 3 stems, and then drill down. When the drill reached the ground, he would detach the head, attach more stems, reattach the drill, and repeat the process until he collected the full core. He would then have to jack the complete core out of the ground.

Sample Sizes

The consensus among geologists is that astronauts and/or rovers should collect a small amount of a large number of different samples [4, 10, 33]. This was the case for the later, so called J-type Apollo missions (Apollo 15-17). These missions collected 1,842 samples weighing a total of 284 kg for an overall average sample size of 154 g. The samples collected can be categorized by type: rocks, rakes, soils and chips, and cores. Rocks are the individual rocks collected by either the scoop or tongs and, for the J-type missions, had an average mass of 400 g. The rake samples were the rocks and chips larger than 1 cm that were collected in bulk, but which averaged only about 5 g each. The average mass of the regolith samples (collected with the scoops), which also included small rock chips, was about 200 g [33].

Table 3-1: Summary of Apollo 17 Sampling Tools

Tool	Sample Type	Sample Capacity	Sample Mass	Note
4 cm Drive Tube (single)	C	470 cm ³	450 g	
Drill (3 m core)	C	940 cm ³	1400 g ⁺	
Heavy Weight Hammer	R	N/A	400 g	
LRV Soil Sampler	SCh, R	650 cm ³	500 g ⁺	1
Rake	Ch	> 1 cm	5 g	2
Large, Adjustable-Angle Scoop	SCh, R	825 cm ³	200 g	
32 Inch Tongs	R	6-10 cm	400 g	

Sample Type: C – Core, R – Rock, SCh – Soil & Chips, Ch – Chips

Sample Mass: Averages based on [33], + - Approximate based on capacity and soil density

Note: 1 – See Appendix A, 2 – 5 g average mass per chip, rake could collect up to 1 kg of chips [28]

3.1.3 Problems with Apollo Tools

The Apollo tools, especially the modified and redesigned tools used on the later missions, were adequate for their task. David Scott and James Irwin of Apollo 15 agreed that, “...the geology tools and concept and the manner of sampling were just fine.” [34] There are, however, issues that must be addressed for any long term missions to the moon, whether those missions are just human or human and robotic. Suit mobility and glove dexterity will be a major factor not only in suit design, but also in tool design. Stability will also play a large role in tool development. A third, major issue to consider is dust, which will affect the design of any and every human or robotic system on the Lunar and Martian surface.

Dexterity

The biggest problem for the Apollo astronauts was the gloves. At least once during each of the three of the Apollo 17 EVAs, one of the crew can be heard commenting that his hands were tired. They complained in their debriefing that the glove exerts a constant pressure on the top of the hand and fingers that was particularly bad in

highly dexterous activities and caused fatigue and bruising [35]. Interviews with eight of the Apollo surface astronauts in 1994 (which ones is unknown) also show that the gloves were a problem during EVA [30].

Mobility/Stability

Mobility and stability are related when it comes to lunar EVA. Pressurizing the suit makes it stiff and makes any motion or bending difficult – this is what makes the gloves so problematic. Adding to the pressure related difficulties, the mass of the suit and the backpack affected balance. The Apollo astronauts had to conduct their sampling activities while carrying a total 30 kgf [36]. This makes any bending, whether for scooping, raking, drilling, or hammering, difficult. Every time either Schmitt or Cernan (while on camera) had to bend over, kneel, reach for the ground, or try to get back up, they had to try more than once before succeeding. This was clearly due to the suit.

A good example of this occurred during the second EVA at mission elapsed time 144:50:52 [29]. Schmitt was trying to collect a sample by himself using the scoop, and was having trouble. He eventually dropped both the scoop and the sample bag *and* fell over. He stood up, dropped the bag again, fell over again, trying to pick it up, and tried twice to get back on his feet. He had to try twice to get the sample back off the ground and had to have Cernan pick up the other equipment he dropped with the tongs.

Dust

Lunar dust particles are very fine, very sharp, and very corrosive. As Gene Cernan put it, “Everything is just full of dust. There's got to be a point where the dust just overtakes you, and everything mechanical quits moving” (mission elapsed time

167:21:05, [29]). He said this as he was trying to adjust his scoop which was stuck. At this point in the mission, both Cernan and Schmitt were completely covered in dust and were having trouble with the scoop, the tongs, and the extension handle. In general, the dust was a major problem for tools, fasteners, connectors, zippers, and suit bearings [30].

3.1.4 Areas for Improvement

Obviously, the biggest area for improvement is in the suit and the gloves, which need to be more flexible. This, however, is out of the scope of this thesis, which focuses on sampling tools. In general, EVA tool designs should reduce the amount of dexterity required to hold and operate. The scoops, especially the improved, larger ones on Apollo 16 and 17, appeared to work adequately but did require bending and stooping, which is undesirable. The tongs were useful as a tool but required a squeezing grasp to actuate, something that future tool designs should avoid. Other tools, like the drill, were so taxing, that many of the Apollo astronauts thought they should be automated or performed robotically [30].

3.2 Human/Robot Roles in Future EVA & Exploration

The idea of using robots as assistants has long been a theme in science fiction. Astronauts have been using a robotic assistant on-orbit for more than 20 years (the Shuttle Remote Manipulator System). In 1999 NASA began field testing human robot interaction in planetary surface exploration [37].

3.2.1 Astronaut-Rover Studies

NASA Ames Research Center conducted Astronaut-Rover (ASRO) experiments to study how robots could help astronauts in the field, develop operational roles and

procedures for members of a human/robot team, and identify requirements for future rover and suit system designs [37]. The ASRO team members for these experiments were an “astronaut” and the Marsokhod rover (Figure 3-6). The “astronaut” was a subject in an EVA I-1 prototype suit with a rock hammer, hand lens, and Apollo style tongs. The Marsokhod rover is a Russian built, six-wheeled, 120 kg rover used by Ames as a research platform; it includes a 1 m long, 5 DOF manipulator with a small sampling end-effector [37, 38].



Figure 3-6: “Astronaut” and Marsokhod Rover in ASRO Study (photo from [39])

The ASRO team studied four mission scenarios. In the first, the rover acted as a scout, performing a preliminary survey of an area to determine its interest for human EVA. In the second, the rover acted as a videographer, following the suit subject and documenting his work. The third scenario had the rover acting as a science assistant; the suit subject would place color-coded flags on targets of interest and the rover would follow, photographing or sampling based on the flag color. Finally, the fourth scenario had the rover acted as a field cart, carrying tools and supplies.

These experiments provided positive results that a human-robot team can improve EVA performance. The ASRO experiments also identified several areas for further

research and development. Specifically, with regards to this thesis, they found that, “The astronaut tools are currently not adapted to provide an efficient science field work. They generate delays in task completion and over-exhaustion of the of the EVA test subjects,” and that, “It is critical to provide proper investigation tools. It is necessary to develop a ‘science tools box’ for EVA-Rover planetary surface exploration.” [37]

3.2.2 EVA Robotic Assistant

In 2000 and 2002, NASA Johnson Space Center (JSC) conducted field studies with the EVA Robotic Assistant, based on the ASRO studies. The 2000 field trials dealt mainly with autonomy and interaction issues. The rover, “Boudreaux,” performed passive tasks, such as laying cable and carrying tools, autonomously and in response to commands from the suit subject. These experiments yielded a desire for Boudreaux to be able to manipulate its environment, so a 7 DOF arm with a Barrett Hand was added for future trials [40]. The 2002 field trials explored more active interaction between the rover and the suit subject (Figure 3-7) [41]. These trials were considered successful by those involved and are evidence of a continuing and serious study into using robots in the field with astronauts on EVA.



Figure 3-7: NASA/JSC EVA Robotic Assistant (photo from [42])

3.3 Requirements for Sampling CAT/End-Effector

Everything discussed to this point provides the basis for the development of a human-robot sampling tool (TERPS). The requirements driving its design can be divided into two main categories: geologic and functional.

3.3.1 Geology/Sampling Requirements

The baseline for future, manned planetary sampling is the later Apollo missions, so it makes sense for TERPS to be at least able to replicate the sampling capacity of the Apollo tools, with priority going to the most scientifically useful sample types. The most studied sample types from the later Apollo missions were individual rocks, soil cores, and soils, in that order [33]. In terms of soil and rock collection, the baseline requirement, based on average samples from Apollo, is that TERPS should be able to collect up to 200 g of regolith fines, and a rock up to a 400 g in mass. This equates to an approximate soil volume of 100 cm³ and a rock diameter of 6-10 cm. These sizes are adequate for allowing the division of the sample for several different tests or experiments. The tool should also be capable of, at a minimum, interfacing with a 30 cm long, 3-4 cm wide core tube.

There was some interest in rock fragments collected by the rake and extracted from the soil (about 1,600 allocations of Apollo samples compared to 13,000 for the rocks and 6,000 for the soils, [33]). So while soil and rock collection is the priority, TERPS should be capable of collecting and sifting bulk samples containing soil fines as well as chips (larger than 1 cm). It should also be able to break rocks – expose at least a few square centimeters of rock interior and collect at least a 5 g sample.

Manipulation was also important in the Apollo missions. The astronauts routinely used their tools to manipulate large rocks as well as pick up other tools and deploy scientific instruments. It is a fair assumption that this will also be the case in future manned exploration, TERPS should be able to grasp and manipulate large rocks – up to 2-kg – and other surface tools and equipment.

3.3.2 Functional Requirements

Other requirements, not directly related to sampling, also came out of the study of previous sampling missions and the objectives of this research. Since TERPS is meant to be used as either a crew aid or a robotic end-effector, nothing about its sample collection method should preclude its use for either function. This is not to say that the tool should be interchangeable as a CAT or end-effector, but differing human and robotic versions of the tools would still need to meet the same requirements.

In general, the only functional requirements identified thus far have to deal with dust. Long term Lunar and Martian missions will have to deal with prolonged exposure to dust and tool design, whether it be for research hardware or flight hardware, needs to take this into account. This means that TERPS should be designed to protect, as much as possible, all moving parts against dust intrusion. Additionally, all parts of the mechanism should be accessible, either by access panels or by disassembly/reassembly, for cleaning and study.

Table 3-2: Human/Robotic Sampling Tool Requirements

No.	Requirement Statement
<i>Sampling Requirements: TERPS should be capable of:</i>	
S-1	Collecting 200 g of regolith fines
S-2	Collecting multiple rock chips greater in size than 1 cm diameter
S-3	Sifting rock chips larger than 1 cm from regolith fines
S-4	Collecting single rocks up to 10 cm in diameter
S-5	Grasping and manipulating rocks larger than 10 cm, up to 20 cm in diameter and up to 2 kg of mass
S-6	Abrading away a 4 5cm ² area of rock surface
S-7	Collecting a sample of up to 5 g from large rocks and/or boulders
S-8	Collecting a soil core of at least 30 cm
S-9	Grasping and manipulating ordinary hand tools*
<i>Functional Requirements:</i>	
F-1	No aspect of the mechanical design or function of the sampling system should preclude its use as either a crew aid tool or a robotic end-effector
F-2	Differing mechanisms for human and robotic use shall both meet this list of requirements
F-3	All moving components should be protected as much as possible from exposure to dust
F-4	Any and all components must be physically accessible

* - This does not include ability to operate or use tools

The next chapter discusses the development of TERPS as per these requirements. It is important to note that while all these requirements were considered in developing the tool concept, the prototype focused mainly on meeting and evaluating the sampling requirements.

Chapter 4

TERPS Concept & Prototype

TERPS is a tool designed based on the requirements defined in the previous chapter, particularly the sampling requirements. As it stands, TERPS represents several design iterations and three prototypes. This chapter discusses the current prototype and its development.

4.1 Design Methodology

The goal in this thesis was to develop a multipurpose sampling tool within a limited budget. The approach taken was to first design around the sampling task requirements, prove concepts, then use this experience to optimize the mechanical design. As a result, many design choices were made based almost entirely on financial considerations, available materials, relative ease of manufacture and modification, etc.

The first step in any design is to identify and define the requirements for the system. This was discussed in the previous chapter. For this work, the next step was to identify possible concepts, one to study further. Having chosen a concept to pursue, a prototype was designed and constructed based on the sampling requirements, and then against those requirements. This process involved quickly producing inexpensive, low fidelity prototypes. Thus, as any issues or problems that arose during testing could be

addressed relatively quickly and easily. Once the sampling requirements were met satisfactorily, emphasis was added on more detailed requirements and mechanical design.

4.2 Initial Concepts

Given the task of designing a sampling tool, even with the requirements previously discussed, there are a countless number of design possibilities. Initially, several different methods for sample collection were considered. The driving requirement in concept generation was the ability to cut rock chips and soil cores. This, intuitively, meant that it should include a drill mechanism, so one of the first concepts was a drill and auger system where all samples are carried up a rotating shaft (see Figure 4-1). Another design was idea was to combine the scoop and tongs into a single tool where the sample is collected by a rigid scoop and secured with an actuated “finger.” Another design type was a grasping scoop, where the sample is collected with multiple actuated scoops. Both of the latter two concepts would also include drills.

The decision of which concept to pursue in depth ended up being only a matter of the requirements – a qualitative analysis outlined in Table 4-1 showed that multiple scoops met all the sampling requirements in the simplest fashion. Looking at each of the concepts, it was clear that some requirements could definitely or probably be easily met. For example, all three concepts would clearly be able to collect soil – ensuring that it collects the required 200 g would be a matter of sizing the scoop or auger blade accordingly. Likewise, it was clear that an auger, whose function is to lift regolith, would not be able to grasp any regular or irregular shaped objects or tools. Other requirements were no as easy to evaluate. An auger, for example, may be able to catch and pinch small

or medium sized rock fragments. Determining whether or not these requirements could be met would involve more design detail, analysis, and perhaps testing.

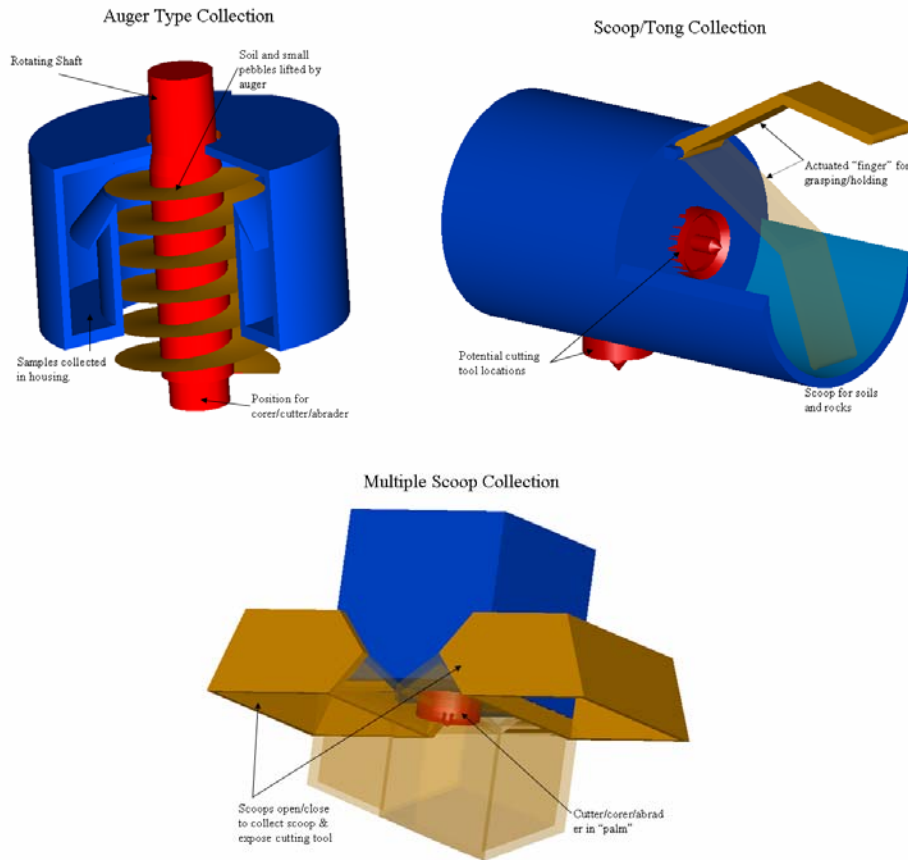


Figure 4-1: Initial TERPS Concepts

Table 4-1: Initial Concept Comparison Matrix

Sampling Requirements	Auger	Scoop/Finger	Multi-scoop
200 g Soil	Yes	Yes	Yes
1 cm Chips w/ Soil	Yes	Yes	Yes
1 cm Chips w/o Soil	FSR	Yes	Yes
Fist-sized Rocks	FSR	Yes	Yes
Football-sized Rocks	No	FSR	Yes
5 g Boulder Chip	Yes	FSR	Yes
Soil Core	Yes	Yes	Yes
Grasp/Hold Tool	No	Yes	Yes

Yes – Highly likely, if not certain, to meet requirement. Any issues/problems relating to requirement are trivial or depend on specifications.

FSR – Further Study Required. More detailed development required to determine if requirement can be met.

No – Highly unlikely, if not impossible, to meet requirement.

The auger would have been simplest mechanically, requiring only one DOF. Unfortunately, it would be unable to grasp or manipulate tools or large objects. The rigid scoop, in theory, would have met all of the sampling requirements, but would have introduced unnecessary complexity in getting the sample collection device to the sample. Positioning a drill in the center area, the “palm,” would require an additional, translational degree of freedom to get the bit to the rock; placing it elsewhere on the system would add potentially, over-complex orientation requirements on the positioning system/device. Multiple scoops give the flexibility to grasp tools and collect samples of different sizes. In this concept, rock cutting involves opening the scoops wide enough to expose a drill. This system also has an advantage of clearly meeting, or has clear potential for meeting, all of the sampling requirements. This was the concept chosen for development and evaluation.

4.3 Current Concept Overview

TERPS, at present, consists of two scoops and a drill. The scoops are driven by a single motor with planetary gear head and a worm-gear drive system. They can open and close in a clam-shell fashion. An off-the-shelf cordless drill motor and transmission serve as the drill. The scoops and housing are made from 3 in (7.6 cm) wide, 0.125 in (0.3 cm) thick, square aluminum structural tubing[§]. Other components were machined from aluminum, with the exception of shafts and gears, which are steel and brass. All components were designed, modeled, sized, and fit using UGS I-DEAS CAD software (example of CAD models is shown in Figure 4-2, materials and drawings are shown in Appendix B).

[§] Note on units. Because of available stock and machining tools, all mechanical design uses the Imperial System (English units). All analysis uses SI (metric units).

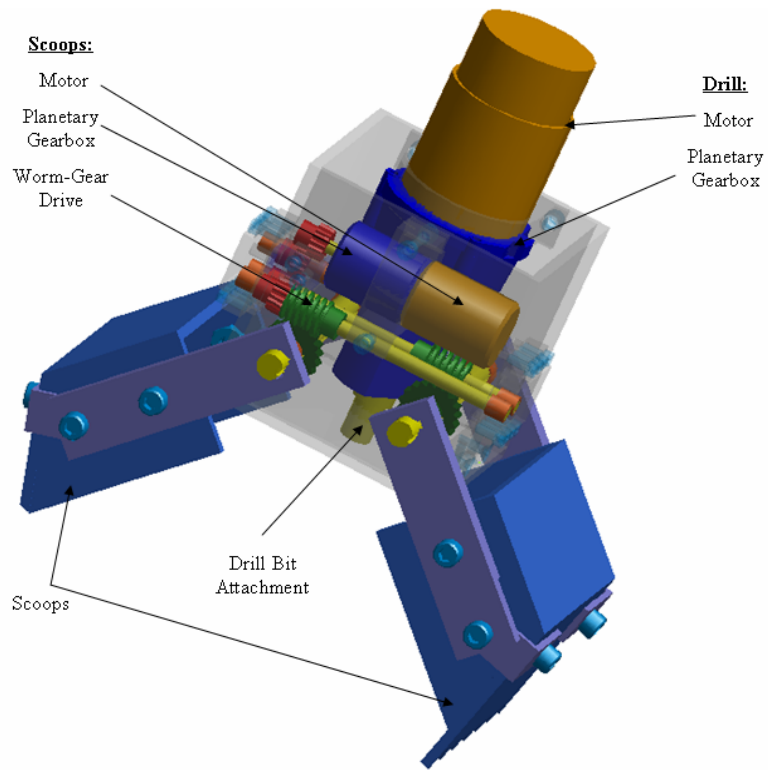


Figure 4-2: CAD Model of Overall System

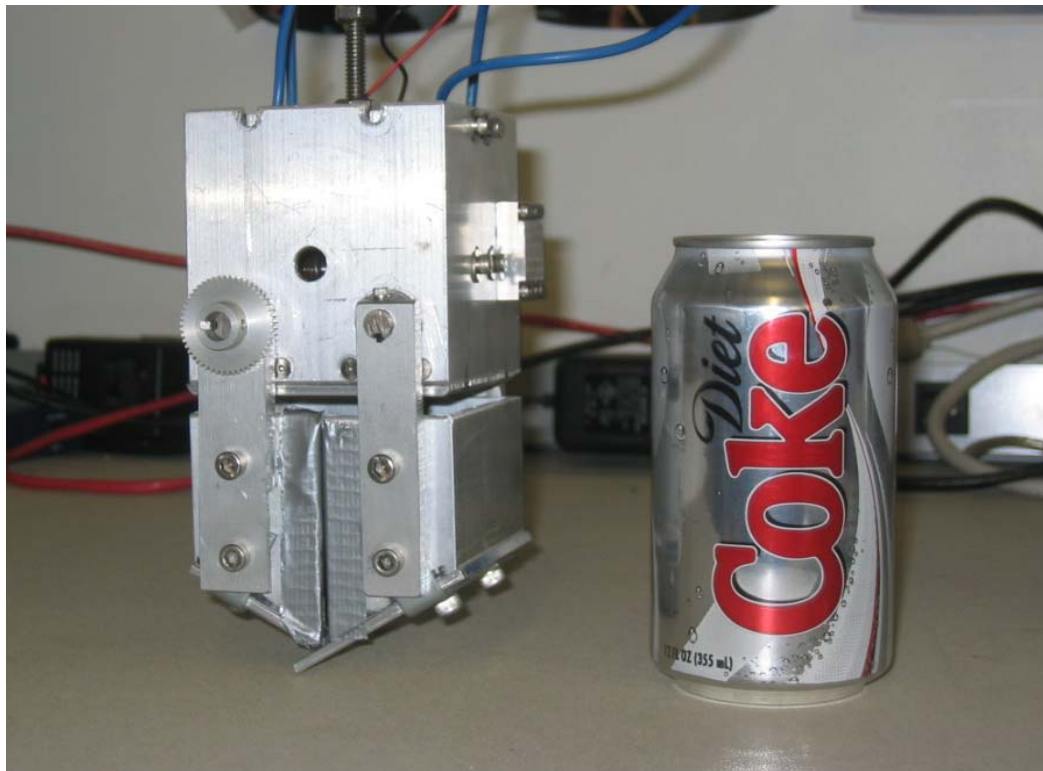


Figure 4-3: Photograph of Current Prototype (without Drill Installed)

4.4 Scoops

The scoops are the main component of TERPS, responsible for most of the sampling functions. The most obvious of these functions is soil collection. The scoops, which rotate in a clam-shell style motion, can open to an angle of 90° (parallel to the palm) and close completely to hold up to 305 cm³ of sample material – this includes completely encompassing a rock with up to a 7 cm diameter/width. With an open span of 22 cm, the scoops can grasp objects as wide as 15 cm.

This combination scoop/gripper design is ideal for several reasons. Mainly, it meets all sampling requirements and does so without requiring a change in orientation – whether collecting soil fines, chips, or rock/soil cores, the palm is only required to be placed roughly parallel to the surface. This, potentially, reduced the dexterity requirements any manipulator design. This also makes it relatively easy for a human to use. As discussed in Chapter 3, many of the Apollo sampling tools required the astronaut to bend forward or to the side while pushing or pulling against the soil. With this design, an astronaut would only have to hold the tool over the sample to collect it. Additionally, as a CAT, this configuration is intuitive and simple to use and handle.

Initially, the scoops were designed such that the sides overlapped as they closed (see Figure 4-4). This was the preferred design because it would prevent any sample loss out of the sides and would allow for greater control over sample release and sifting. These scoops would have been fabricated using a rapid prototyping (RP) machine which would automatically form plastic into each part directly from the virtual CAD model. Using RP scoops also had the advantage of being easy to redesign/re-fabricate as needed. Unfortunately, persistent malfunctions in the RP machine prevented this approach.

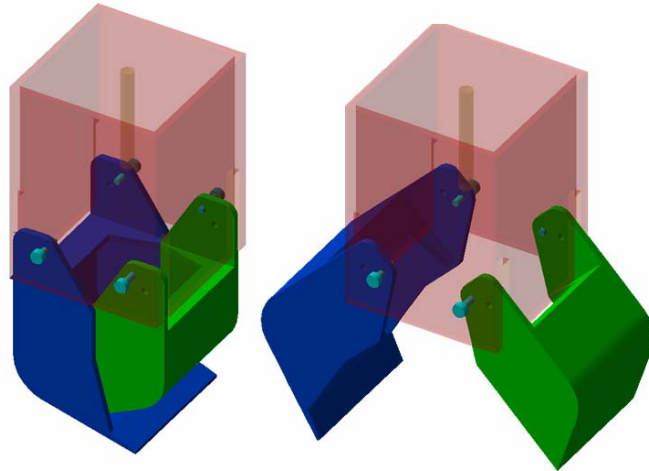


Figure 4-4: Initial Overlapping Scoop Design

Instead, the scoops were fabricated from the same aluminum tubing used for the housing. Each scoop consists of half of a 2.5 in (6.4 cm) length of the 3 in (7.6 cm) aluminum square stock with one end cut at an angle of 30° (see Figure 4-5). The bottom, blade, is a 0.125 in (0.3 cm) thick aluminum plate held in place by two corner brackets. One blade was serrated to allow for scrapping and scratching. The other was smooth so that the two could close together (Figure 4-6). Two aluminum strips bolted to the side attach the scoop to its drive shaft.

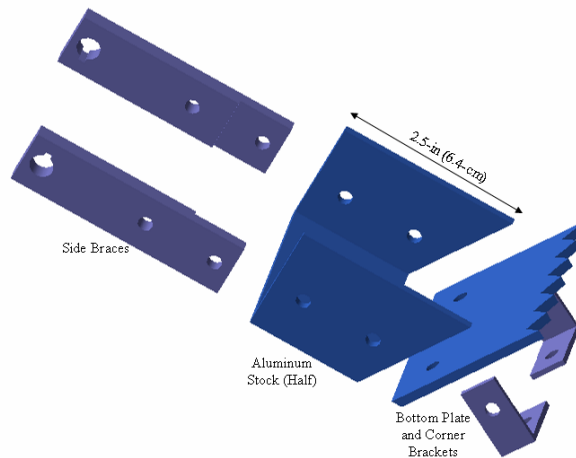


Figure 4-5: Current Scoop Design

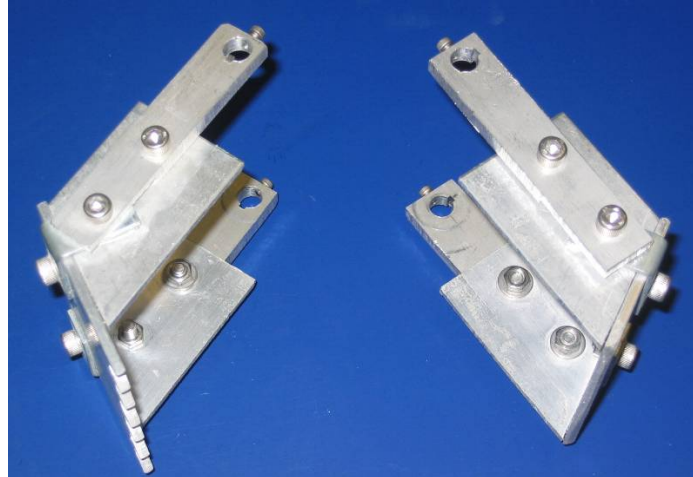


Figure 4-6: TERPS Scoops

4.5 Actuation

A single motor drives the scoops through a single planetary gearbox and a pair of parallel worm gear sets (Figure 4-7). The gear-motor spins a series of spur gears which spin two worms in opposite directions. This, in turn, spins two more shafts, each rigidly attached to one of the scoops. The single motor configuration minimizes the required space in the mechanism and ensures that the scoops stay synchronized.

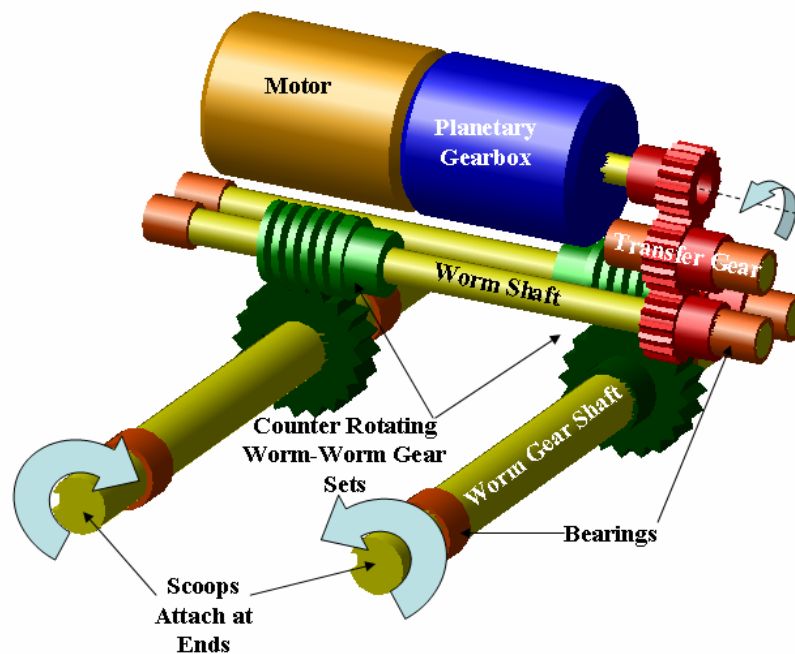


Figure 4-7: Scoop Actuation Drive

4.5.1 Gears vs. Linkage

Design of the actuation system centered around the desire to be able to grasp and hold a sample without continuously running the motor, which draws more power and wears out the motor. So the options were a brake, which tend to be heavy and bulky; a mechanism that is biased closed, which would require the motor to run to keep the scoops open; or a self locking mechanism, which remains stationary in any position once power to the motor is cut.

Lead Screw Driven Linkage

Initial actuator design involved a lead screw driven slider-crank mechanism (see Figure 4-8). The rotating lead screw applies linear motion and force to the slider element of the mechanism. This, in turn, drives the crank, which is the scoop. A lead screw and crank mechanism have great potential for mechanical advantage and lead screws resist backward motion, that is, a force applied to the slider element will not cause the lead screw to back rotate.

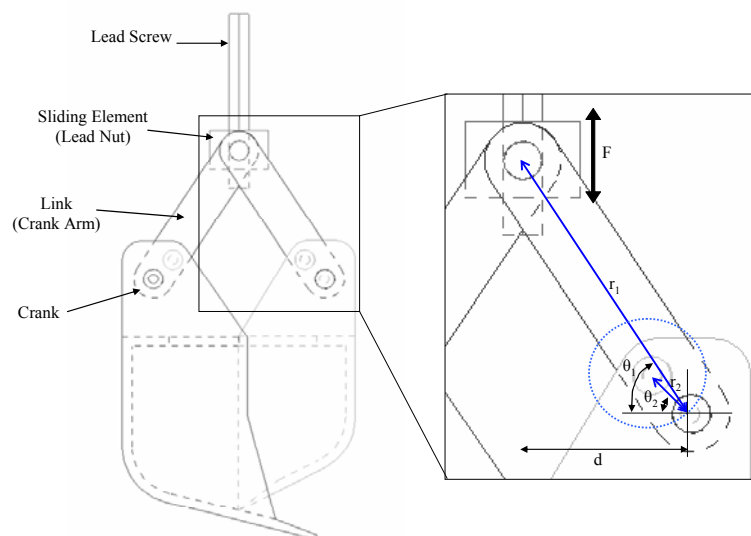


Figure 4-8: Initial Scooping Mechanism

A force analysis was performed to identify the mechanical advantage of the system, the ratio of the output torque (on the scoop) to the input torque (from the motor). Assuming no friction, the force resulting from a supplied torque to a lead screw is given in equation 4-1, where F, T, and L are force, torque, and screw lead, respectively [43]. The torque output to the scoop can be calculated from summation of forces and moments in static equilibrium and is given by equation 4-2 where r is the length of the link. Combining these two equations equation 4-3 shows that mechanical advantage is a function of the angle between the two links.

$$F = 2\pi \frac{T_{in}}{L} \quad (4-1)$$

$$T_{out} = F r_2 \sin(\theta_1 - \theta_2) \quad (4-2)$$

$$\frac{T_{out}}{T_{in}} = 2\pi L r_2 \sin(\theta_1 - \theta_2) \quad (4-3)$$

The mechanism shown in Figure 4-8 has a mechanical advantage of 13, which can be increased to between 22 and 45 depending on the position of crank arm (θ_2). Avoiding the two limit positions, where both links are collinear, is desirable as these are the points with little or no mechanical advantage. For a full scooping motion, this means the extreme positions (fully opened and fully closed) will have the lowest mechanical advantage. A hand operated prototype was constructed to test this system. The scoops performed well and the mechanical advantage issues were, at worst, inconvenient. There was, however, a great deal of error in fabricating the system – ± 0.01 in (0.025 cm) at each pin – which caused problems. Errors in holes drilled for pins in the links and small misalignments in the parts often lead to asymmetrical motion and/or forces in the system. This usually cause the mechanism to stick and made the system unusable. This led to the

use of a gear train, where such high tolerances (which accompany quick prototyping) do not drastically affect functionality.

Gears

The gear train developed for TERPS, shown in Figure 4-7, make use of worm gears, which as with lead screws, tend to resist back-drivability. Worm gears also tend to have high gear ratios in relatively compact packaging. Gear sizing depended on the available space within the body, so 20:1 worm gears, which had pitch diameters less than 1 in (2.54 cm), were chosen. Spur gears, 1:1 gear ratio, were used to transfer and split motion from the motor to the worms.

4.5.2 Motor

Motor selection was based mostly on size and cost. The intention was to test system using a small, inexpensive motor to evaluate its performance and clarify requirements before investing in a high quality (high priced) motor. The motor used for scoop actuation is a Hennkwell PK22G2150-104** Micro DC Planetary Gear Motor (specifications in Appendix B). This is a small motor (140 g, 5.4 cm long, 2.2 cm diameter) that operates at 12 V with an operational range of 6 V – 18 V. Attached to the motor is a two stage planetary gearbox with a gear ration of 104:1. The combined system has a no-load speed of 144 rpm drawing 0.2 A, and is rated to output 2.5 kg-cm of torque continuously (0.8 A) and 7.5 kg-cm momentarily (1.9 A). This motor turned out to be quite capable. The overall gear ratio of 1700:1 gave an estimated/calculated pinch force of 150 N (discussed in the next section and in Appendix C) and performed well in testing.

** Broken motor replaced with PK22G650-016 motor in April 2007

4.5.3 Bearings

For the purposes of this work, the prototype had to be easy to modify and reconfigure. In the interests of simplicity, bronze Oilite® plain bearings (also called bushings) were used on the shafts. These bearings only support radial loads. Worm gears, however, induce axial loads (thrust loads) as well as radial loads. The current prototype supports these axial loads directly through the structure, which adds friction to the system. While this is not ideal, it does not prevent motion and still allows for sampling experiments. Obviously, each shaft should be supported by a bearing(s) appropriate to the loading condition. The loading condition for TERPS in its current configuration is outlined in Table 4-2. This was based on a static analysis of all of the forces on the gears applied due to torque from the motor. The forces on the gears are shown in Figure 4-9, the complete analysis and calculation of the loads is shown in Appendix C.

Table 4-2: TERPS Bearing Loads for 7.5 kg-cm Max Input Torque and 144 rpm Speed

Bearing	Radial Load (N)	Axial Load (N)	Velocity (rpm)
Transfer Gear Shaft	200	0	144
Worm Shaft	235	450	144
Worm Gear Shaft	800	35	7

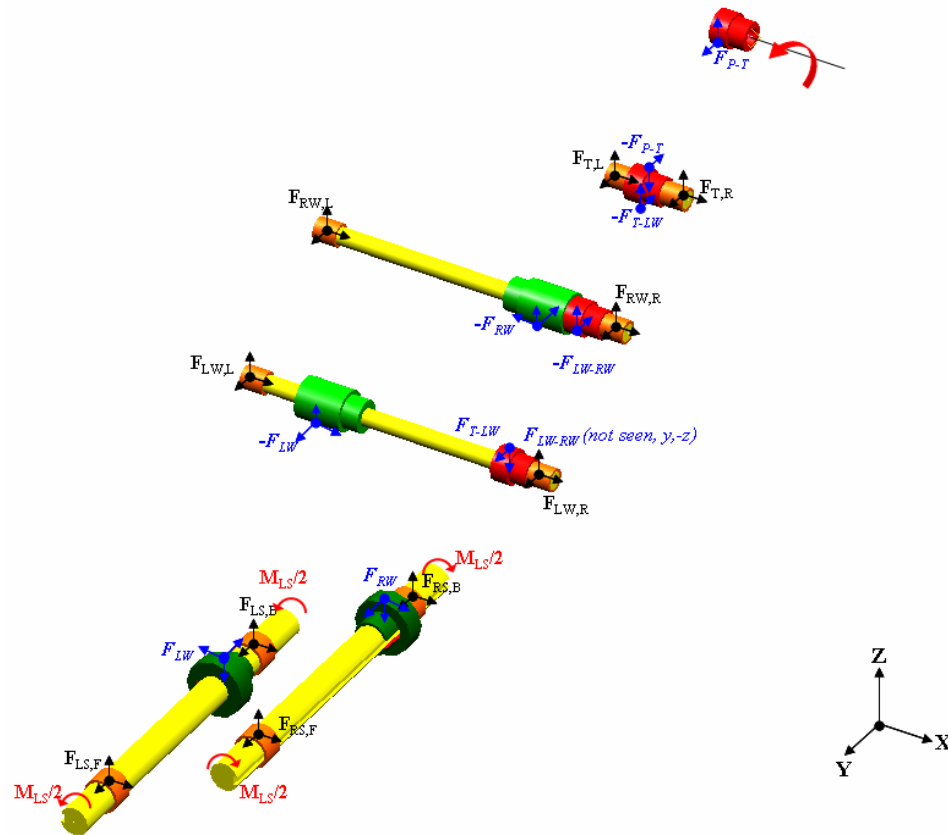


Figure 4-9: Gear and Bearing Loading from Applied Torque

4.6 Drill

The drill is meant for sampling from large rocks, coring, abrading, and cutting. The TERPS drill was cannibalized from a Skil® 12 V Cordless Drill/Driver Model 2466-02 (see Figure 4-10). The motor is a LESHI LS-550PX with a no-load speed of 24,000 rpm and current of 2 A (see Appendix B). The gearbox is a two-stage planetary gear train with a gear ration of 36:1. A 3/4 in (1.9 cm) hole-saw serves as the bit for abrading and rock cutting. A 3.5 cm diameter, 30 cm long aluminum tube serves as a core tube for soil cores.



Figure 4-10: Drill, Bit, and Core Tube

4.7 Electronics

All work done to-date has only required manual switching, so the electronics are fairly simple (see Figure 4-11). The scoop motor was operated using a double-pole-double-throw (DPDT) toggle switch, allowing for the motor to run in both directions. Two limit switches were included to protect the motor from running against itself while fully open or fully closed. A cam on each scoop shaft engages the switch, breaking the circuit, when the scoops reach either their open or closed limit. The drill is operated with a simple, on-off, push button switch. The electrical leads from these switches as well as the two motors connected to cables leading to a small box containing a toggle switch for the motor, a push button switch for the drill, and wiring for the switches (Figure 4-12). This box is also where power is applied.

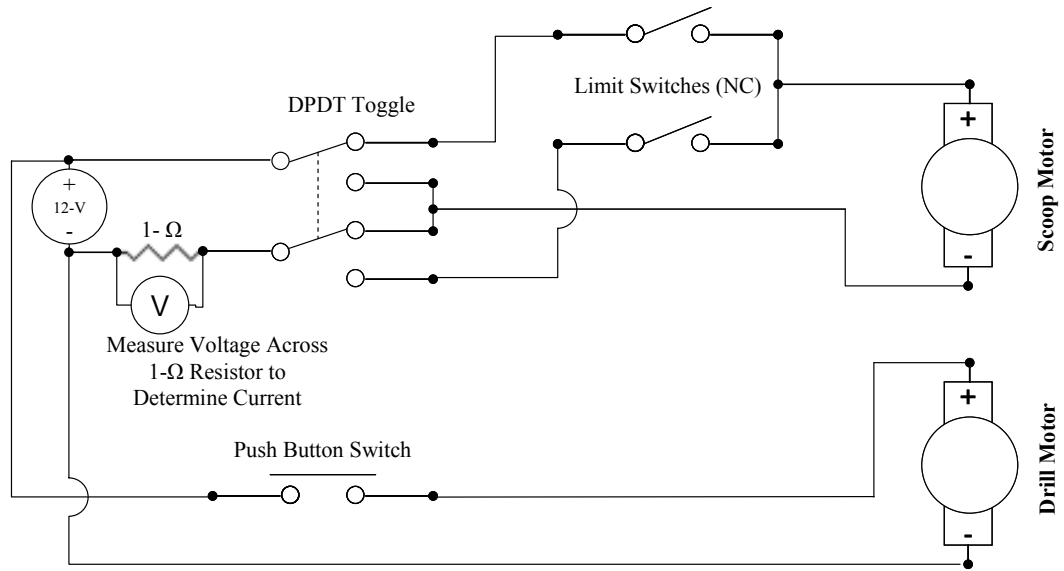


Figure 4-11: Circuit

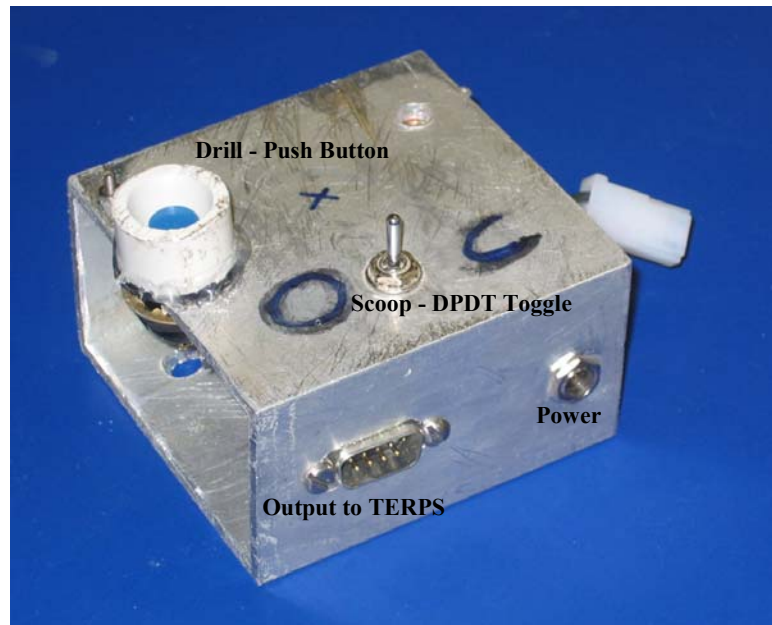


Figure 4-12: TERPS Switch Box

Chapter 5

TERPS Testing Set-up

Two types of testing were performed on TERPS. One set of tests was to verify the motor performance based on a soil failure model described in the Chapter 6. The other set of tests were to verify the requirements defined in Chapter 3. These tests were performed both in a lab setting, using bins of soil, and in the “field,” using a large sand box. This chapter discusses the overall set-up for this testing and evaluation. Chapter 6 and Chapter 7 discuss the specific approach and results of the soil theory testing and sampling evaluation, respectively.

5.1 Lab Set-up

5.1.1 Physical Set-up

Sample collection testing was conducted using bins of several different soil types easily available. TERPS could be mounted to a frame over the soil bin (Figure 5-1) or operated hand-held. TERPS was mounted to the frame with a threaded rod; it could move freely vertically in either direction or be rigidly attached with a nut to maintain a constant position. Dry playground sand, purchased from Home Depot, was the main soil type tested. Dry sand shares similar properties to Lunar and Martian regolith, making it an ideal analog for basic testing. The similarities in properties between sand [44] and

lunar regolith, JSC lunar stimulant [45], Martian soil [15], and JSC Mars soil stimulant [45] are outlined in Table 5-1. The soils are similar in density and friction angle, but sand is less cohesive (i.e. less “sticky”). To compensate, TERPS was also tested in increasingly more cohesive soils, specifically: moist sand, clay-like loam, and sandy gravel.



Figure 5-1: Lab Testing Setup

Table 5-1: Comparison of Lunar/Martian Soils to Sand [15, 44, 45, 45]

Soil	Bulk Density (g/cm³)	Cohesion (g/cm²)	Friction Angle (°)
Dry Sand	1.5	2.0	35
Lunar Soil	0.0 – 2.3	3.0 – 18.4	25 – 50
MSL-1 (JSC)	1.9	9.2	37
Martian Soil (Viking1)	1.2	6.1 – 18.4	39
Mars-1 (JSC)	1.9	9.2	41

5.1.2 Data Collection

Scoop performance data, namely motor current and scoop angular position, was collected with a National Instruments USB-6008 Multifunction Data Acquisition (DAQ) Board and software running at a rate of 500 samples per second. The NI-6008 cannot

measure electric current, so the motor's power draw were measured through the voltage drop across a 1 Ω shunt resistor placed in series between the motor and ground (see Figure 4-11) – according to Kirchoff's current law, the current through this resistor is the same as the current through the motor. Using Ohm's law, which states that the current through a resistor is equal to the voltage drop divided by the resistance, the motor current can be calculated.

The scoop angle, defined as the angle between the scoop arm and the local vertical (see Figure 5-2), was measured with a potentiometer attached to one of the scoop axils via a 1:1 spur gear set. The voltage source for the potentiometer was a 9 V battery. Prior to any tests measuring position, the voltage across the potentiometer was measured with the scoops closed and opened. At this point, the scoop angle, γ , can be found from the measured voltage, V , as shown in equation 5-1.

$$\gamma = \gamma_{\text{open}} \left(\frac{V_{\text{closed}} - V}{V_{\text{closed}} - V_{\text{open}}} \right) \quad (5-1)$$

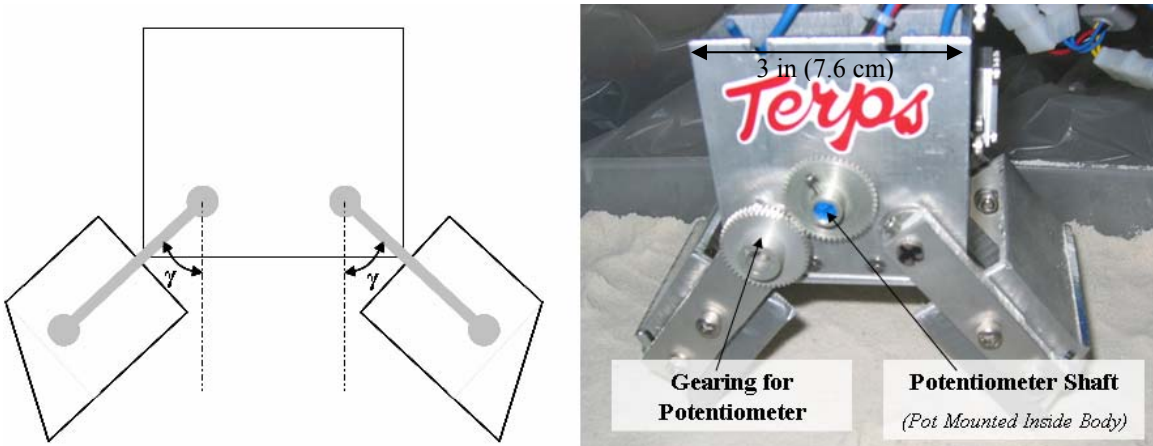


Figure 5-2: Scoop Angular Position
 (L) Scoop Angular Position Convention, (R) Potentiometer

5.1.3 Data Processing

All data collected was parsed, processed, and analyzed using MathWorks MATLAB. The data collected by the DAQ board was recorded with the accompanying software and stored as a tabulated text file. MATLAB code was written to extract and analyze that data. A copy of the MATLAB code is available in Appendix E.

5.1.4 Power

The scoop motor operated at 12 V and 2 A and the drill motor operated at 12 V and 10 A. To accommodate this, power was supplied through a Hewlett Packard 6674A System DC Power supply. This system was capable of providing up to 60 V at up to 35 A. Testing away from the power supply was accomplished with a Makita 9000 9.6 V, 1.3 A-hour cordless drill battery.

5.1.5 Sand Box

In addition to hand-held operation at a workbench, TERPS was also evaluated at the SSL “Lunar Surface Scaled Simulation Facility,” a 2.4 m by 3.7 m sandbox with about 15 cm of playground sand (Figure 5-3). This sandbox, intended for rover research, makes an excellent “lunar landscape” for research in small planetary surface systems. Here, TERPS was mounted to a 1.2 m wood staff for study as a CAT and mobility aid. Sampling tasks were performed to demonstrate TERPS’s use as a CAT and identify any issues associated with that use.



Figure 5-3: SSL Lunar Scaled Surface Simulation Facility

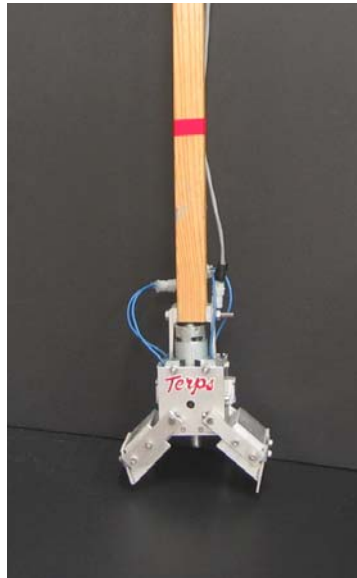


Figure 5-4: TERPS as a Crew Aid Tool

5.2 Determination of Scoop Force

There was no requirement defined for the amount of force the scoops must exert. The force exerted by the scoop is related to the torque output by the motor, which is proportional to the electric current flowing through the motor. Knowing this relationship is useful for selecting a motor for a known task, or conversely, determining limitations of a given motor for unknown tasks. Additionally, as will be discussed in Chapter 6, the

motor torque/current relationship can also be used to monitor or measure reaction forces in the environment and use this data to infer information about the environment – in this case, soil properties.

For this work, the relationship between the scoop force and the motor current was measured directly. To do this, the scoops were closed around one end of a scissor device (see Figure 5-5). The resulting force, f , was measured on the other end with a Shimpo FGV-50A Digital Force Gauge. With this setup, a force, F , applied to the small end is five times the force, f , measured by the force gauge. The scoop applies the force by torque through the scoop arm, which in this setup is at a 10.4° angle, so the scoop force acting perpendicular to the moment arm is actually 5.1 times the measured force. Comparing this force to the measured current during the grip yields a linear relationship shown in equation 5-2.

$$F = 12.5I - 2.7 \quad (5-2)$$



Figure 5-5: Grip Force Measurement

Section 4.5.3 and Appendix C describe the calculation of bearing loads based on an input torque. These calculations also yield the torque on each scoop axel, which can

be translated into a force at the blade. Comparing this calculation with measured values yields the mechanical efficiency of the gear train. The maximum measured current during strength testing was 2.1 A which, according to the derived model, means a scoop force of 23.6 N. According the motor manufacturer's specifications, 2.1 A results in a motor output of 8.2 kg-cm and a calculated pinch force of 156 N – a mechanical efficiency of only 15%.

The drastic losses are a result of the nature of the study and the prototype. Since this work is primarily “proof-of-concept,” less than optimal performance in the system is acceptable. As mentioned previously, the plain bearings were used instead of the nominal bearings for financial reasons. In manufacturing the prototype, ease of modification was more important than precision, so tolerances and errors were high. For this study, cost-effective functionality was the top priority, so performance was sacrificed. Future models should aim to optimize the system for both task functionality and mechanical performance.

Chapter 6

Soil Mechanics & Theory, Testing, Results, & Discussion

The overall objective of this work is to develop a research tool for planetary sampling. The primary component of the concept developed in Chapter 4 is the scoops. As discussed, this prototype's function is to evaluate its ability to meet the sampling requirements defined in Chapter 3 as well as explore and define other requirements, functional or mechanical, in order to improve and refine the design. Of particular interest are the performance requirements for the two motors. Since the drill motor was added late in the process and the mechanics of drilling are known and understood [12], this thesis emphasizes the mechanics of scooping. As an object cuts, breaks, or moves through soil, the soil imparts resistive on that object. In the case of TERPS, the soil imparts forces on each scoop as it closes. This chapter briefly discusses soil mechanics in general before going on to describe the derivation of a model to predict the forces on the scoops.

6.1 Soil Mechanics Overview

Since most of this work involves scooping or manipulating regolith, it is important to understand its classification and mechanics. Regolith is classified by particle size. Cobbles and boulders, rocks, are particles larger than 60 mm. Gravel is regolith particles between 2 and 60 mm in size – for the purposes of this work, these are

rock chips. Sands have particles ranging from 0.06 mm to 2 mm, silts sizes range between 0.002 mm and 0.06 mm, and any smaller particles are called clays [46].

Soils, like any solid material, have mechanical properties and respond somewhat predictably to stress and strain. Of particular interest, as with other materials, is how soils fail. Soil failure is dependant on two properties, cohesion and internal friction. Cohesion, c , is the tendency of soil particles to stick to each other. The internal friction angle, ϕ , is the internal resistance angle between shear (τ) and normal (σ) stress. The critical values of shear and normal stress are related to cohesion and friction by Coulomb's equation (6-1). These parameters are important in determining the load bearing capacity of soil, necessary for construction and mobility.

$$\tau = c + \sigma \tan(\phi) \quad (6-1)$$

In addition to determining loading capacity, cohesion and internal friction angle are two parameters often used to describe soils, especially when dealing with excavation and failure [44, 45, 45]. These are two parameters that are affected by soil particle size, particle shape, moisture content, etc., so different soils behave differently under similar loads. Knowing and understanding these differences can be of use geologically when studying an unknown region. Pertinent to this work, the cohesion and friction angle of a soil will determine how well the current prototype can perform in that soil.

6.2 Soil Cutting Model

Determining soil properties is important for geological reasons as well as logistical reasons (traversability, bearing capacity, etc). Previous planetary surface probes have sought to estimate soil properties by using motor currents to determine the resistance force of the soil and comparing that to tested soil cutting models. The last

probe to do this through manipulation was Viking 1 and Viking 2 (Pathfinder and the MERs used wheel/soil interaction for similar analysis).

Any probe that used or uses a scoop for soil, bases its analysis on soil cutting models. These models were developed to optimize the design of Earth-moving, excavation, and farming equipment. Planetary surface probes have used models based on the fundamental earth moving equation:

$$F = (\rho d^2 N_p + c d N_c + q d N_q)w \quad (6-2)$$

The force, F , is related to the density, ρ , blade depth and width, d and w , cohesion, c , surcharge, q , and dimensionless coefficients, N . Several soil/tool models have used 6-2 or a variant as a base. The Godwin and Spoor, McKyes and Ali, and Perumpral models all use this base with differing methods for determining the coefficients [45].

The Viking probes used a soil/tool interaction model proposed by E. McKyes and O. S. Ali at McGill University [44]. This model assumes that soil in front of a blade fractures away from the blade forming a prism of failed soil in front of the blade and fanning out to the side (Figure 6-1, Figure 6-2). According to this model, a force, F , applied to the soil by the blade will face a resistive force, R , based on cohesion, soil-soil friction, and pressure from the weight of the soil within the failure region, ρ , as well as any soil above the failure region (called surcharge), q . This will also be influenced by the blade width, depth, and angle from the surface (called rake angle), α .

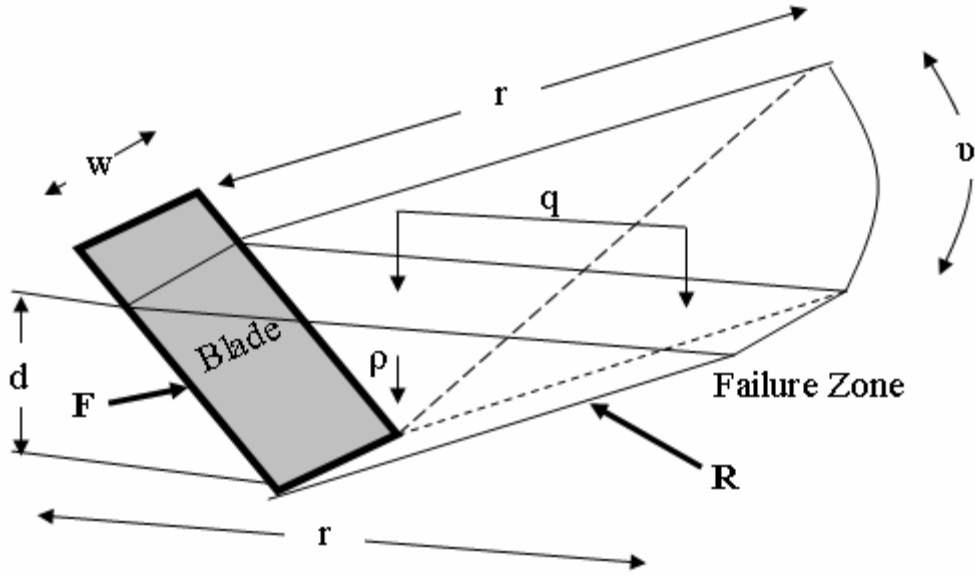


Figure 6-1: 3-D Sketch of McKyes/Ali Soil Failure Region (adapted from [44])

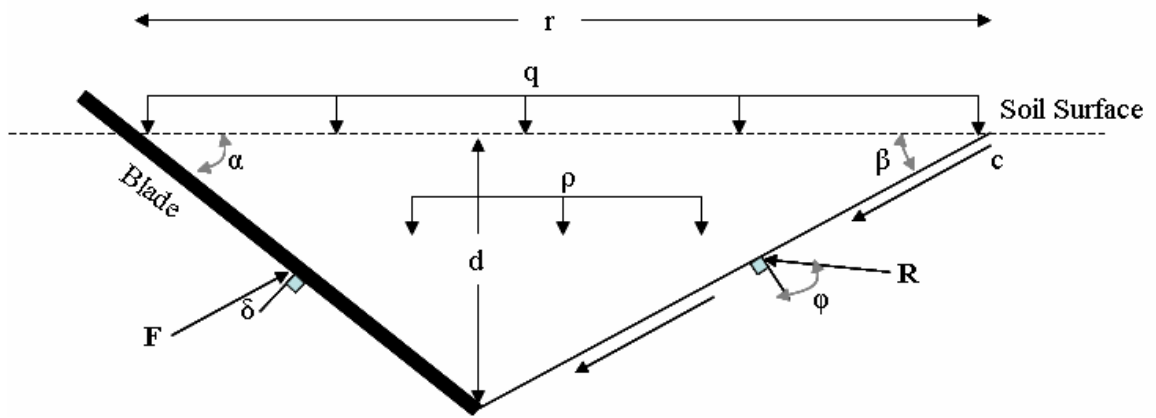


Figure 6-2: Side View of McKyes/Ali Soil Failure Region

The two forces, F and R , are each the sum of forces on failure prism (F_1 and R_1) and the side wings (F_2 and R_2). For both sections, summing the forces and solving for F_1 and F_2 results in the following (complete derivation is shown in Appendix D):

$$F_1 = \frac{\left(\rho d^2 \frac{r}{2d} + c d [1 + \cot(\beta) \cot(\beta + \varphi)] + q d \frac{r}{d} \right) w}{\cos(\alpha + \delta) + \sin(\alpha + \delta) \cot(\beta + \varphi)} \quad (6-3)$$

$$F_2 = \frac{\left(\frac{1}{6} \rho d r^2 + \frac{1}{2} c r d [1 + \cot(\beta) \cot(\beta + \varphi)] + \frac{1}{2} q r^2 \right) \sin(\nu)}{\cos(\alpha + \delta) + \sin(\alpha + \delta) \cot(\beta + \varphi)} \quad (6-4)$$

Where, from geometry:

$$\frac{r}{d} = \cot(\alpha) + \cot(\beta) \quad (6-5)$$

$$\cos(\nu) = \frac{d}{r} \cot(\alpha) \quad (6-6)$$

The total force on the blade, F, is given by:

$$F = F_1 + 2(F_2) \quad (6-7)$$

This equation (6-7), when expanded, results in an equation of the same form as equation 6-2. Here, all terms are known except β which is chosen to minimize the N_p term.

In any particular soil, the independent variables are rake angle, α , and depth, d . This model, originally developed for narrow bladed agricultural tools, assumes linear motion through the soil with a constant depth and rake angle. The TERPS scooping motion, however, is an arc, meaning a variable depth and rake angle based on the scoop angle, γ . The relationship between depth, scoop angle, and rake angle is depicted in Figure 6-3.

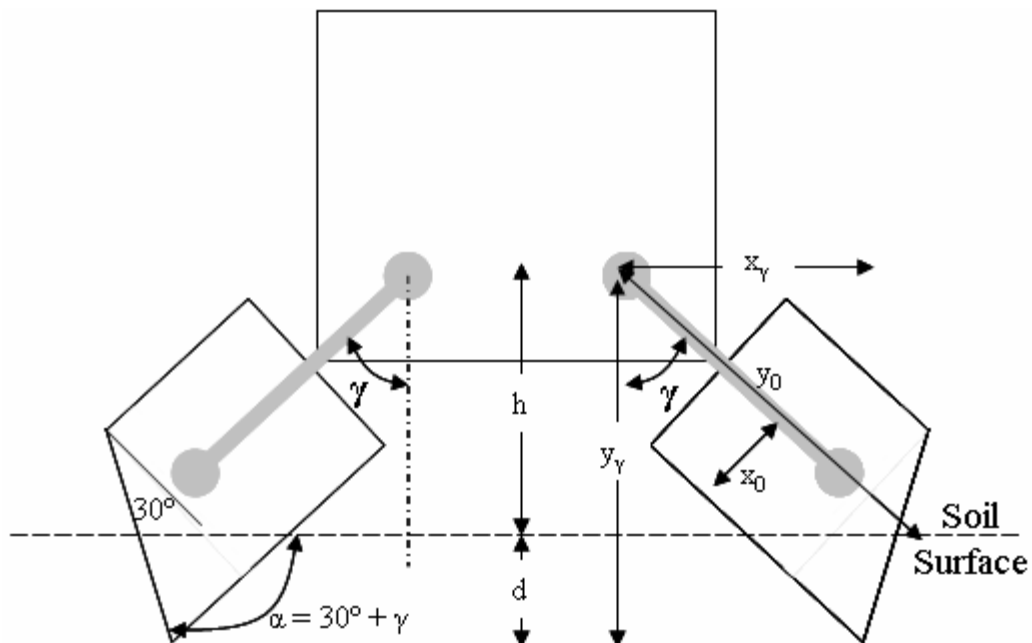


Figure 6-3: Scoop Kinematics

The rake angle, at any time in the scoop swing, depends only on the scoop angle. The rake angle is simply the sum of the scoop angle and the natural angle of the blade, 30° (equation 6-8). The blade depth, on the other hand, actually depends on two parameters, the scoop angle (γ) and the height of the scoop axel above the surface (h). Any point on the scoop cross section – in this case the tip of the blade – can be described as a set of x-y coordinates with respect to the scoop and centered at the axel. At any time during the scoop swing, that point can then be represented with respect to the stationary TERPS body though a simple rotation (see equation 6-9). The blade depth is then the difference between $y(\gamma)$ and h (equation 6-10) – a negative depth represents the scoop being above the surface.

$$\alpha(\gamma) = 30^\circ + \gamma \quad (6-8)$$

$$\begin{bmatrix} x(\gamma) \\ y(\gamma) \end{bmatrix} = \begin{bmatrix} \cos(\gamma) & -\sin(\gamma) \\ \sin(\gamma) & \cos(\gamma) \end{bmatrix} \begin{bmatrix} x_0 \\ y_0 \end{bmatrix} \quad (6-9)$$

$$d(\gamma) = y(\gamma) - h \quad (6-10)$$

Substituting equations 6-8 and 6-10 into equations 6-3, 6-4 yields an expression for the scoop force as a function of scoop angle:

$$F(\gamma) = (\rho d^2 N_p(\gamma) + c d N_c(\gamma) + q d N_q(\gamma)) w \quad (6-11)$$

Where:

$$N_p(\gamma) = \frac{\frac{1}{2} \frac{r}{d(\gamma)} \left[1 + \frac{2}{3} \left(\frac{r}{w} \right) \sin(\nu) \right]}{\cos(30^\circ + \gamma + \delta) + \sin(30^\circ + \gamma + \delta) \cot(\beta + \varphi)} \quad (6-12)$$

$$N_c(\gamma) = \frac{[1 + \cot(\beta) \cot(\beta + \varphi)] \left[1 + \frac{2}{3} \left(\frac{r}{w} \right) \sin(\nu) \right]}{\cos(30^\circ + \gamma + \delta) + \sin(30^\circ + \gamma + \delta) \cot(\beta + \varphi)} \quad (6-13)$$

$$N_c(\gamma) = \frac{1 - 2 \frac{d'}{d(\gamma)} - \left[2 \frac{d'}{d(\gamma)} \tan(\varphi) - \cot(30^\circ + \gamma) \right] \cot(\theta + \varphi) + \frac{d'}{d(\gamma)} N_{c,H}^* \cot(\theta + \varphi)}{\cos(30^\circ + \gamma + \delta) + \sin(30^\circ + \gamma + \delta) \cot(\beta + \varphi)} \quad (6-18)$$

$$N_q(\gamma) = \frac{\frac{d'}{d(\gamma)} N_{q,H}^* \cot(\theta + \varphi)}{\cos(30^\circ + \gamma + \delta) + \sin(30^\circ + \gamma + \delta) \cot(\beta + \varphi)} \quad (6-19)$$

Where:

$$\frac{d'}{d(\gamma)} = \frac{\cos(\varphi)}{\sin(30^\circ + \gamma)} \left[\sin(30^\circ + \gamma + \varphi) + \cos(30^\circ + \gamma + \varphi) \tan\left(105^\circ - \frac{5}{2}\varphi - \gamma\right) \right] \quad (6-20)$$

$$\theta = 105^\circ - \frac{3}{2}\varphi - \gamma \quad (6-21)$$

The N*-terms in equations 6-17, 6-18, 6-19 are simply equations 6-12, 6-13, 6-14 evaluated with a rake angle of $90^\circ - \varphi$ (which is equivalent to $\gamma = 60^\circ - \varphi$), $\delta = \varphi$, and $d = d'$. In either case, the component of the force perpendicular to the scoop arm, the component sensed by the motor is:

$$F_{\text{motor}}(\gamma) = F(\gamma) \cos(2\gamma + \delta - 60^\circ) \quad (6-22)$$

There now exists a model relating the force on one scoop to the scoop's position and the soil properties. It is assumed that the force exerted by/on each scoop is the same, so doubling the calculated force yields the total force on both scoops (which would be the force that corresponds to the power draw of the motor – see section 5.2). Thus, it is possible to compare the current readings from the motor to the forces predicted by this model.

6.3 Testing Approach

To test the soil model, TERPS was mounted to a frame (see Figure 5-1 on p. 58) at a set height over a soil bin. The scoop position and motor current were measured as described in Section 5.1.2. The first step was to ensure that the current measurements would differentiate between dissimilar soil types. Motor current were measured on dry sand, moist sand, and clayey loam and compared to each other.

The next step was to compare the current measurements against the soil model using a soil of known properties. Sand was used for these tests since it has well known and documented properties. Several scoops were made at differing heights and the measured force compared to forces predicted by the model. Student-t tests and Kolmogorov-Smirnov tests were used to quantify the statistical significance of the difference between the two.

6.3.1 Statistical Analysis

The Student-t test is a statistical hypothesis test that can tell whether or not two samples come from the same population based on their variance. The null hypothesis is that the means of the two samples are equal. The Kolmogorov-Smirnov (KS) test is a test used to measure the so called “Goodness-of Fit” between predicted or modeled values and actual measured ones, based on the maximum difference between a measured value and the model. Again, the null hypothesis is that the measured sample has the same continuous distribution as the model (that it fits). Both of these tests were conducted using built-in MATLAB functions – the “ttest2” and “kstest2” functions for the t-test and KS-test, respectively.

The key value in each of these tests is the p-value. This is the probability, given the null hypothesis is true, of the observed sample being as unfavorable or more unfavorable to the test statistic. For example, a null hypothesis that the means are equal and a p-value of 0.1 means there is a 10 percent chance, based on the sample, that hypothesis is true. So p-values close to zero imply that the null hypothesis is not true. Typically, the decision to reject the null hypothesis is made when the p-value is less than 0.01 – 0.05. The p-value itself, however, is a useful value for judging the validity of a test or comparison and is the basis for inferences made in this work [47].

6.4 Testing Results

6.4.1 Motor Characteristics

The motor specifications (see Appendix B) given by the manufacturer, Hennkwell, show the scoop gear motor to have a no load current of 246 mA – meaning the motor running by itself at 12 V should draw 3 W. The motor was run by itself and the current measured as described in Section 5.1.2 to verify this. The results actually showed the motor to draw only 125 mA, about half of what it should be – this is most likely a characteristic of the individual motor compared to the one(s) used by Hennkwell in their tests. Regardless of the difference between this motor and the published specifications, knowing the no load current provides a baseline of data for evaluating the mechanical performance of TERPS.

The scoops were closed in open air (not in any soil) to establish the general motor behavior in a single scoop motion and estimate friction in the system by comparing the difference between the measured current and that of the no load case. The resulting profile is shown in Figure 6-5. The profile shows the amount of friction in the system.

When the motor is first powered, it must overcome static friction in the gear train so there is a spike in current – and therefore torque – to set the gears and scoops in motion. After this spike, the motor encounters dynamic friction in the gears. This is evidenced by the increase in measured current. The average current draw for motor with the scoops is 172 mA. Based on the published torque curve for this motor, the 47 mA difference between the scoop load and the no load case indicates that the motor sees approximately 0.2 kg-cm of torque due to friction within the system.

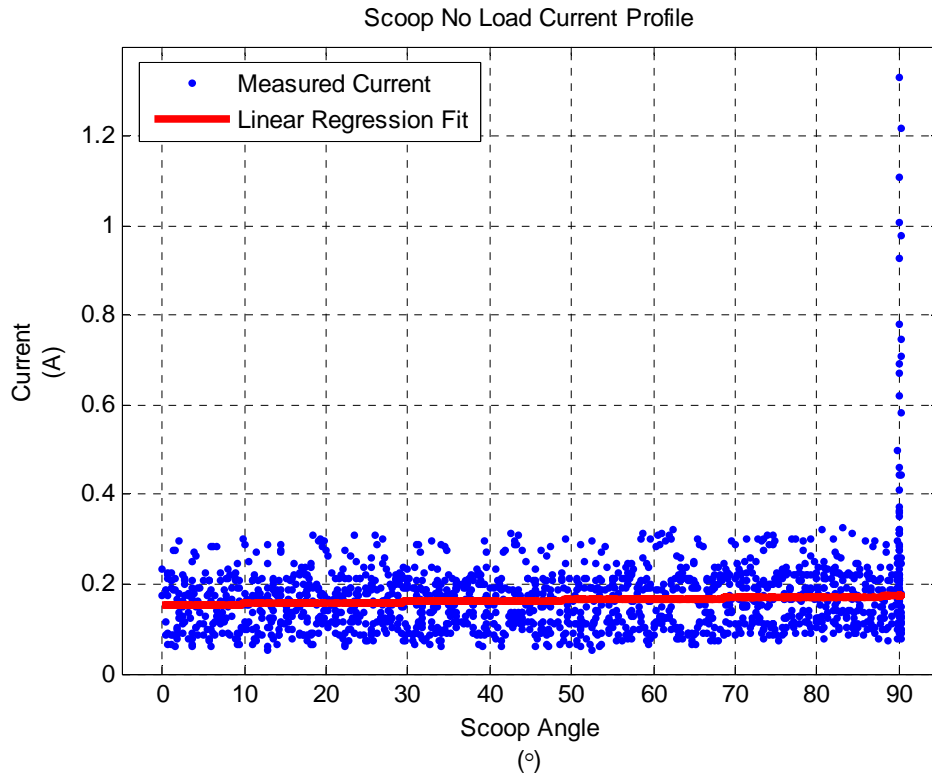


Figure 6-5: TERPS No Load Motor Current Profile

Gravity also plays a role in the motor profile. The linear regression of the measured current (neglecting the initial spike) has a slope of 0.215 mA/° or a 19 mA difference between when the scoop is near open and when the scoop is near closed. This makes sense because the scoops have mass so when they are open the gravity acting on

them causes a closing torque. As the scoops close, the center of mass of the scoop moves laterally towards the TERPS body. This reduces the moment arm, thus reducing the magnitude of this closing torque. When applied to soil, one would expect the motor current to increase once the blades make contact with the soil with the motor current profile matching the soil model shown above. This comparison is discussed in the succeeding sections.

6.4.2 Soil to Soil Comparison

Tests were run on the three soils, dry sand, moist sand, and clayey loam, from heights of 9 cm, 8 cm, and 7 cm. The results from the three comparisons from all three heights are summarized in Table 6-1 and the force profiles during a scoop are shown in Figure 6-6. At a height of 9 cm, the scoop blades barely penetrate the surface. This scenario represents the skimming force, the force required to scrape the surface. Here, there is no statistical (or visual) difference between the dry sand and the clay. As the depth is increased, this similarity disappears. In all three cases, there were highly significant statistical differences between the clayey soil and the moist sand. However, at 8 cm there is an unexpected and as yet unexplained similarity between the two sands.

These tests also demonstrate how TERPS responds to each soil type at different depths. As expected, decreasing the height above the surface increases the resistance on the scoop.

Table 6-1: P-values of t-tests on Soil to Soil Comparison Tests

		Comparison		
		Dry Sand/Clay	Dry Sand/Moist Sand	Moist Sand/Clay
Height (cm)	9	0.7401	0.0000	0.0000
	8	0.0000	0.2502	0.0000
	7	0.0000	0.0000	0.0024

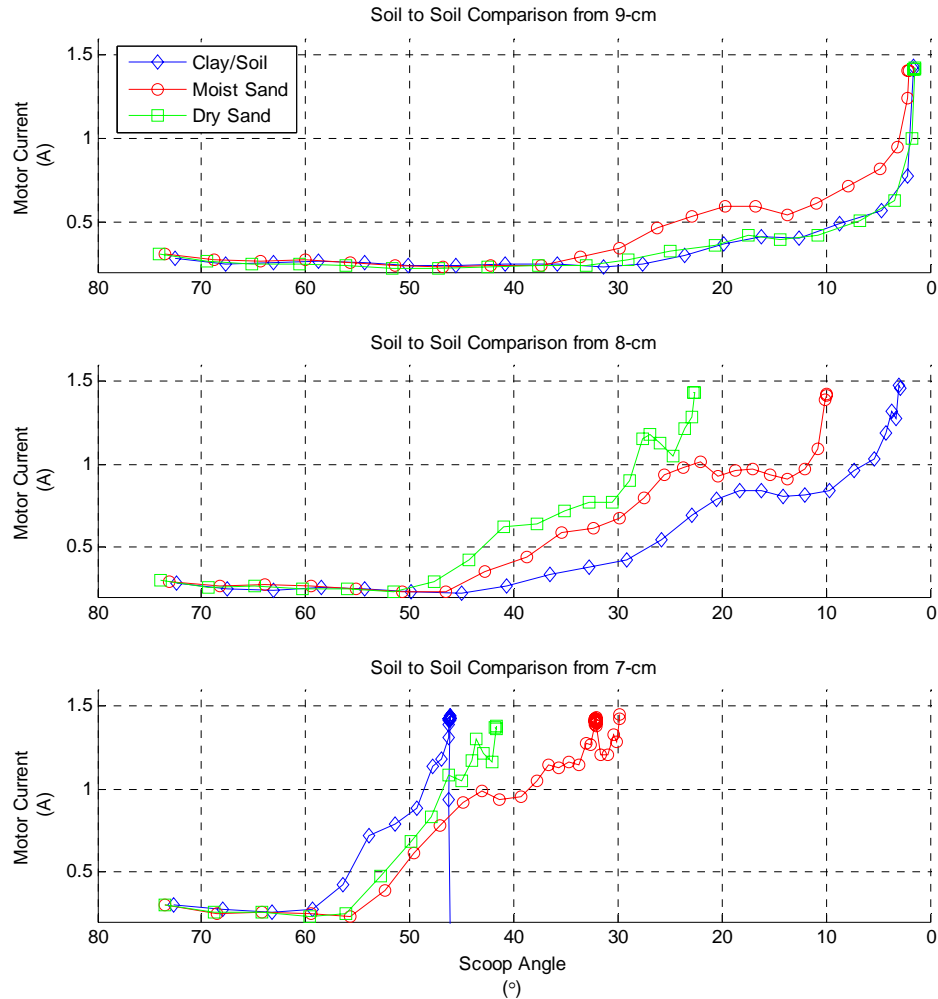


Figure 6-6: Force Profile for 3 Soil Types at h = 7 cm and h = 8 cm

6.4.3 Soil to Model Comparison

Dry sand was used to test the soil model because it has well known and well documented properties (outlined in Table 6-2). Tests were run with TERPS at heights of 8.8, 8.2, 7.7, 6.6, 6.2 and 5.7 cm. The measured and predicted force profiles for the 6.2 cm test are shown in Figure 6-7. The run starts with the scoop fully open (90°). At 60° the scoops break the surface, which starts adding resistance to the motor. This resistance builds steadily until about 45° where fluctuations begin to occur in the power draw. The motor stalls with the scoops at 22°.

Table 6-2: Soil Prosperities of Dry Sand [44]

Parameter	Dry Sand
Density – ρ (g/cm ³)	1.53
Cohesion – c (g/cm ²)	2.32
Internal Friction – ϕ (°)	35
Soil-Tool Friction – δ (°)	23

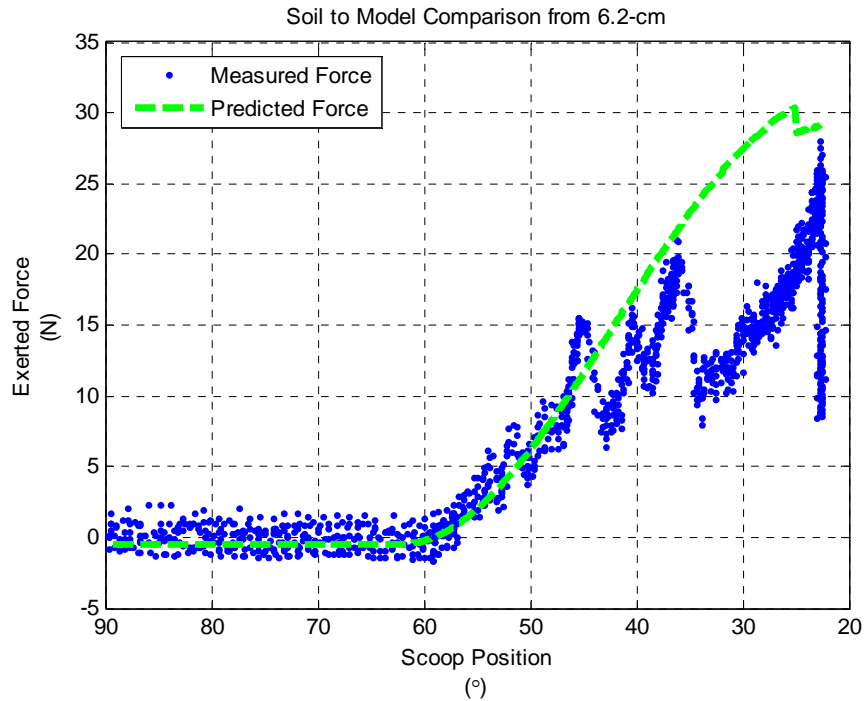


Figure 6-7: Scoop Force Measurements and Model for 6.2 cm

Comparison to Model

Looking at the model prediction, it appears, visually, to be accurate for about the first 15° of the swing through the soil. After this point, the measured data diverges from the model. Testing the model and the data over the whole swing yielded negative results. The KS-test yielded a p-value of 1.5×10^{-100} and the t-test a p-value of 1.1×10^{-40} , meaning there is effectively a zero probability of this data set representing the model. However, in the initial 15° the KS-test and t-test yield p-values of 0.18 and 0.21, respectively, meaning this portion of the measurements fit the model reasonably well.

The other samples, at other heights, show similar behavior (see Figure 6-8 for two more examples of this). In every run, the overall comparison yielded p-values of zero in both statistical tests. However, when only the first 15-20° of the swing is considered, the data matches the model accurately. The statistical test results of all runs are shown in Table 6-3 (force profiles from all of the runs can be found in Appendix F).

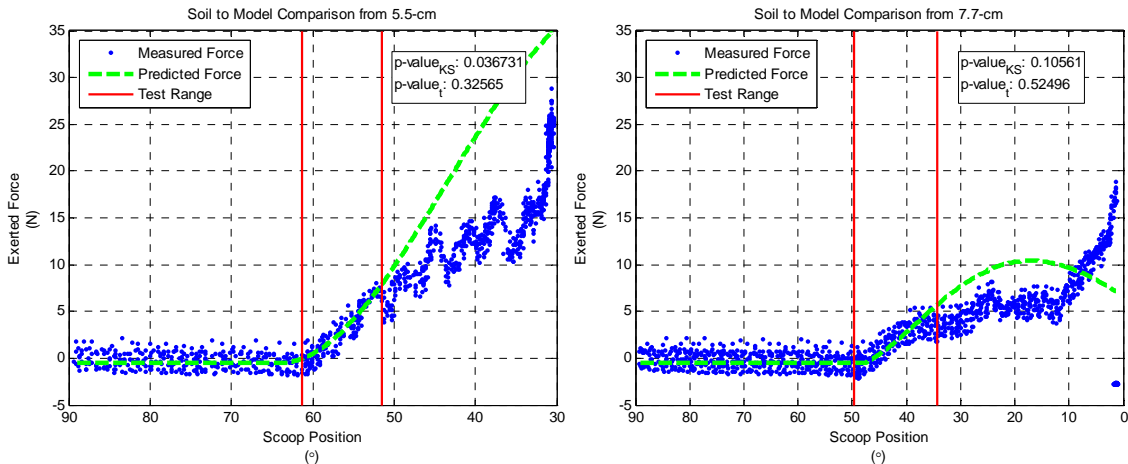


Figure 6-8: Soil Model Only Holds for 15-20° of Scoop Motion

Table 6-3: Results of Soil-Model Comparison t-Tests and Kolmogorov-Smirnov Tests

Height (cm)	Predicted Avg. Force (N)	Measured Avg. Force (N)	Percent Difference	Test Range (°)	KS-test p-value	t-test p-value
8.8	0.5870	0.1952	200	26	0.0000	0.9306
8.2	1.4236	2.2976	38	14	0.0013	0.5542
7.7	2.5450	4.6487	45	15	0.1056	0.5250
6.6	10.3749	13.8570	25	18	0.1209	0.8459
6.2	11.0783	16.3400	32	13	0.1816	0.2091
5.7	10.6353	17.1774	38	10	0.0367	0.3256

Discussion of Theory/Model Divergence

According to the model described in this chapter, the length of the soil rupture region (r in Figure 6-2 and Figure 6-4) grows as the scoop angle decreases, i.e. the depth

increases. Therefore, at a certain scoop angle, the two opposing rupture zones will collide (this point, γ_{rc} , is shown in Figure 6-10 as a function of the initial scoop height). At this point, the geometric basis for the model would no longer exist, thus the model would no longer hold. Here, the scoops are pushing against themselves and the soil within them. This is where one would expect the measured data to diverge from the model. However, this critical scoop angle does not match when compared to the angles at which the data diverges from the model.

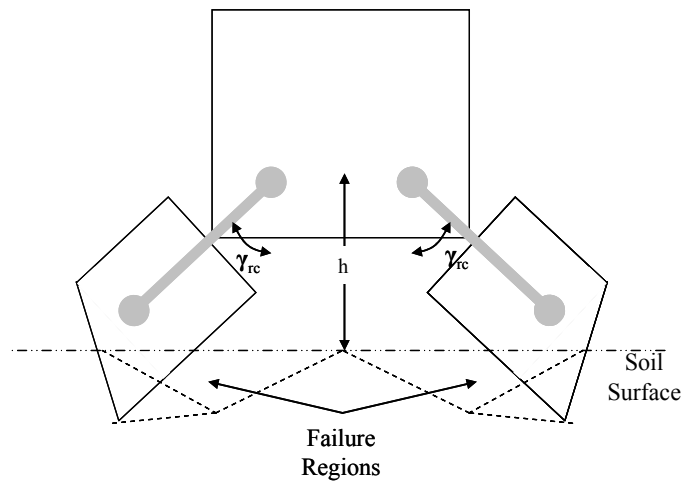


Figure 6-9: Soil Rupture Zone Collision

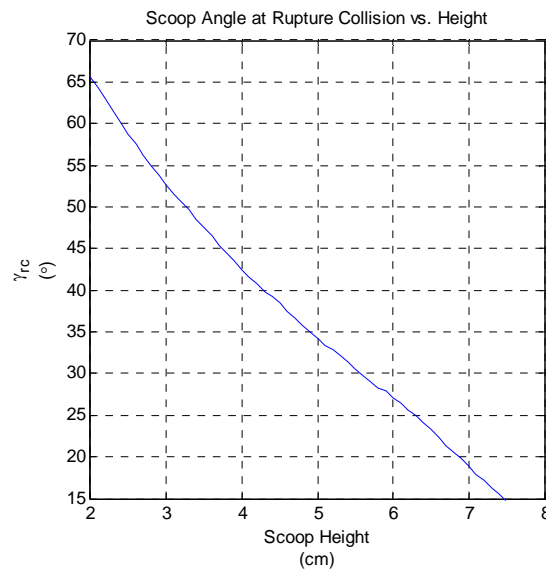


Figure 6-10: Soil Rupture Zone Collision Scoop Angle vs. Scoop Height

The fact that the soil model and the measurements diverge at approximately the same point, 15-20° after contacting the surface, indicates there is something about the scoops themselves that disrupts the soil in a way not expected by the McKyes model. The angular separation between the tip of the blade and the bolt that holds the scoop blade in place is 13° (see Figure 6-11). After 13° of scooping motion, the soil begins to pass over the two nuts, which, based on Figure 6-7 and Figure 6-8, apparently reduces the soil resistance, but in an unpredictable way (there is no consistency between runs in how the soil behaves after this point). Currently, this appears to be the most likely cause for the model divergence.

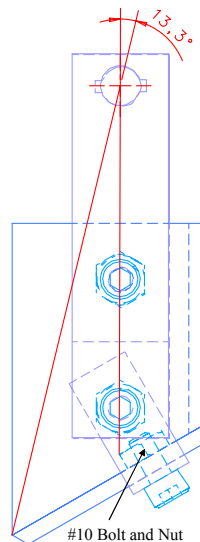


Figure 6-11: The Angle Between Blade and Nut is 13°

Looking at Figure 6-7 and Figure 6-8 it is clear there is some oscillation occurring in the power draw during the scoop. This occurs both before and after the measured data diverges from the model, but the amplitude of this oscillation increases dramatically after

the divergence point. Figure 6-12 shows the same force profile shown in Figure 6-7 with the velocity profile for the same run. Figure 6-13 shows a similar profile for Figure 6-8. The velocity was found by numerically differentiating the scoop angle.

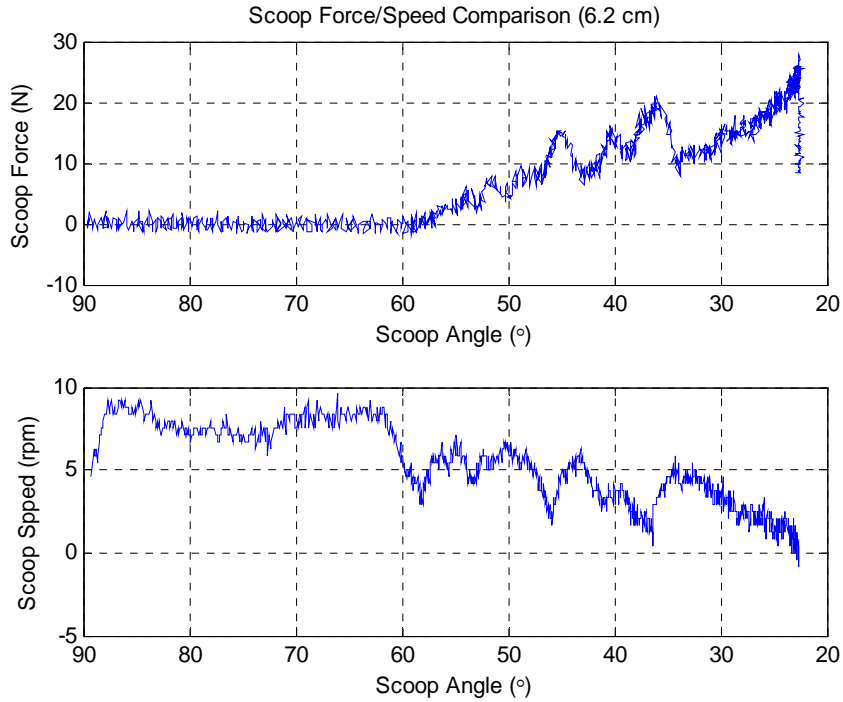


Figure 6-12: Force/Velocit Profile for $h = 6.2$ cm

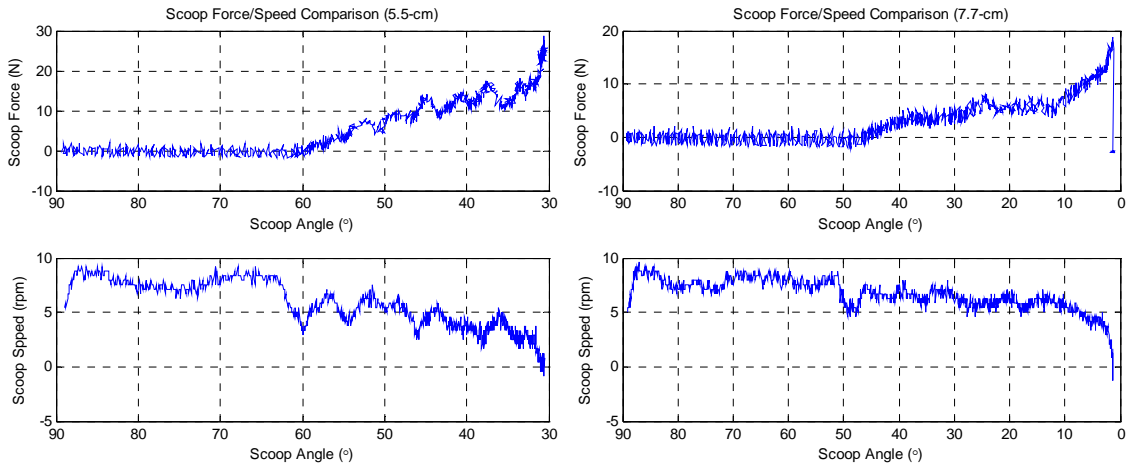


Figure 6-13: Force/Velocit Profile for $h = 5.5$ cm and $h = 7.7$

The velocity profile (bottom plot) and the force profile (top plot) show the relationship between the two. The expected profile would be similar to that in Figure 6-13 (right) where the rotational velocity is relatively steady before the scoops reach the soil. Once the scoop reached the soil surface it sees a sudden, but slight, increase in resistance causing a sudden slowing in speed without much change in current. As the scoop cuts through the soil, the velocity slowly decreases until the scoops close in on themselves and the velocity goes to zero as the motor stalls.

In the other cases, the cases where there is the oscillation in the motor current, the velocity profile matches the force profile. The velocity remains fairly constant until the scoops reach the soil surface and there is the drop in speed and recovery. The velocity then slowly decreases with occasional sudden drops that then recover to the original deceleration trend line. These valleys match the sudden peaks in the force profile meaning there is a certain amount of “stiction” in the soil. Following the force/velocity profile in Figure 6-12 it is clear that the blade reaches the soil surface at about 59° -- the force profile begins to increase and there is a drop in angular velocity. At about 45° , 40° , and 37° there are sudden jumps in scoop force with corresponding sudden decelerations in scoop speed.

This means that the motor is sensing increasing resistance and slowing down as the torque grows and the motor stalls. Before it can stall, however, the soil gives way, suddenly releasing the resistance and allowing the motor current and scoop velocity to return to previous states. This pattern, especially in the deeper test runs (see Appendix F), indicates that the soil is failing discontinuously. In other words, instead of a clean cut all of the way through, resistance builds up and is released, multiple times, through out

the swing, creating several layers of failures (see Figure 6-14). As before, it is unclear whether this is a result of inadequacy of the soil model or disturbances from the scoop structure.

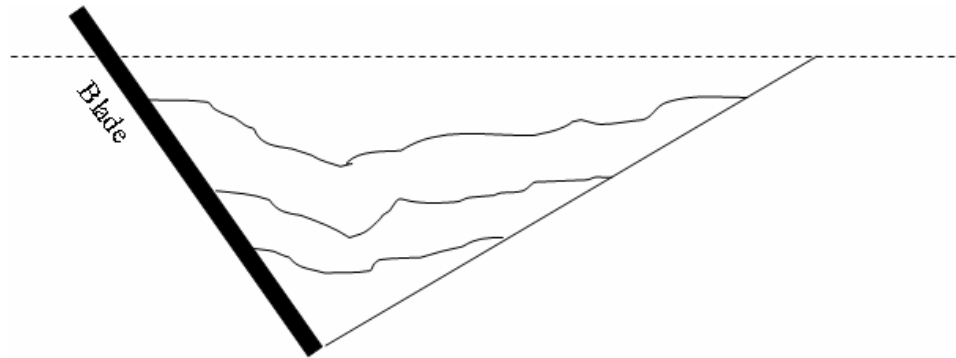


Figure 6-14: Theorized Soil Failure Pattern in Oscillating Region

Summary

The comparison of the modified McKyes soil model and the measured data showed similarities for the first 10-15° of the scooping motion. Analysis of the current and velocity profiles indicated that discrepancies in the measured data are likely not a result of the motor itself. The differences between the measured data and the model are most likely a result of disturbances caused by the actual structure of the scoop, though more work is required to confirm this hypothesis.

6.5 Sensitivity Analysis

A sensitivity analysis was performed to determine the effect of varying the four soil parameters on the force outcome. This allowed for estimating the accuracy of the model given noisy data. The soil internal friction angle and the soil-tool friction angle were each varied by $\pm 5^\circ$, the cohesion by $\pm 5 \text{ g/cm}^2$, and the density by $\pm 5 \text{ g/cm}^3$ and percentage change of the average output force calculated. The results are shown in

Figure 6-15. Clearly, the model is most sensitive to changes in density with 60% change in average force for a small variation ($\pm 1 \text{ g/cm}^3$) and over 100% change for larger variations. This is not surprising; as shown in equation 6-2, the density is amplified by the square of the blade depth.

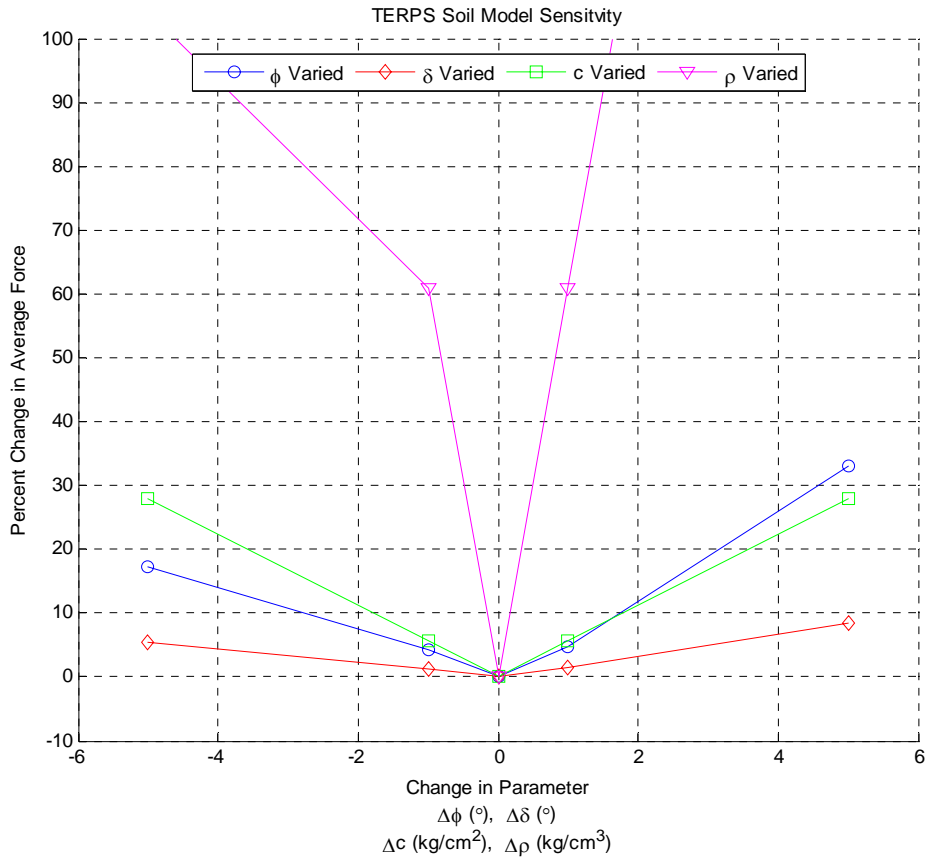


Figure 6-15: Sensitivity Analysis of TERPS Soil Model

Varying cohesion and internal friction angle are relatively insensitive to small variations, but not to larger variations. Again, this is not surprising as cohesion, c , is a coefficient in the fundamental equation and internal friction angle, ϕ , is in a cotangent term, which is not bound. Soil-tool friction, δ , which is only part of sine and cosine terms, has a limited effect on the output.

This analysis also shows the accuracy of the model parameters when evaluating noisy data. The parameters used for sand in the previous section are not exact. They were determined empirically and confirmed experimentally of the past few decades, so there is error. Varying these parameters and reapplying the tests, as before, yields a range of parameters which would result in a similar profile. Given the data in Figure 6-15, it is no surprise that the density prediction is accurate. A statistically similar result would only be achieved with a density of $1.43 \pm 0.25 \text{ g/cm}^3$. Similar profiles would also result from internal friction angles of $33.5 \pm 4.5^\circ$, tool friction angles of $23 \pm 9^\circ$, and cohesions of $2.32 \pm 3 \text{ g/cm}^2$.

6.6 Discussion

Chapter 5 discussed the validation of TERPS as a sampling tool concept. This chapter sought to delve deeper into the theory of soil cutting and sampling. A classic soil cutting model was introduced and its application to TERPS derived. This model was tested against a known soil and confirmed.

This testing also revealed information useful to the mechanical design of the system. With the soil model confirmed, motor requirements can be defined based on expected usage. Using the soil model described in the sections above can be used to find the maximum force required for a given soil. Figure 6-16 shows the relationship between the maximum force required to scoop the soils listed in Table 5-1 and the height above the soil. As discussed in Section 5.2, the theoretical maximum force TERPS can exert (with 100% mechanical efficiency in the transmission) is 156 N. At this limit, TERPS would be able to completely close on a highly resistive soil, like JSC Mars stimulant,

from about 5 cm – a reasonably sized sample. This suggests that the current motor is adequate for future testing.

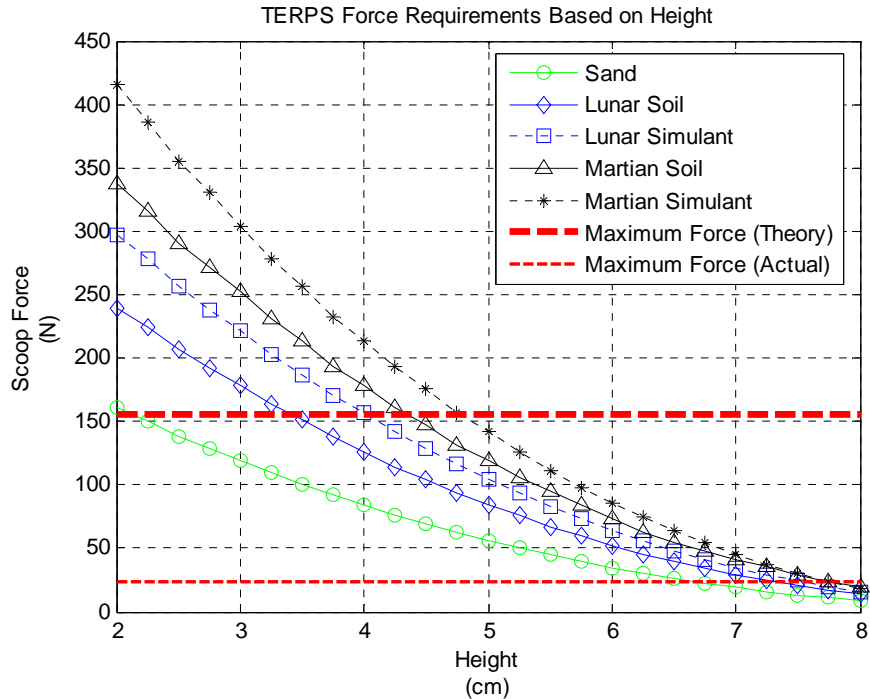


Figure 6-16: Force Requirements for Different Soil Types Based on Height

The ability to collect soils, as described here, also assumes perfect soil behavior as predicted by the model. The testing also showed that the resistance on the scoop tends to decrease after about 15° of the scoop motion. If this is, as hypothesized, a result of the nuts holding the blade in place, then there may be a way to partially control the resistive force on the blade. This could be useful in further clarifying the force, and thus, motor requirements. Therefore, it is worth investigating the cause of the resistance drop and the effect of removing, changing, or controlling it.

Chapter 7

TERPS Concept Demonstration & Validation

One of the objectives of this research is to evaluate TERPS described in Chapter 4. The scoops were tested by collecting samples of different soil types as well as grasping small and large rocks and other objects. The drill was tested on hardened concrete. This chapter discusses this evaluation.

7.1 Sample Collection Testing Approach

The easiest and most obvious way to test a sample collection tool is to collect samples. A series of sampling activities, corresponding to the requirements defined in Section 3.3, was devised and performed, both in soil bins and in the large sandbox. The masses of the samples were used to compare TERPS performance to its requirements as well as to Apollo. Specifically, the sampling tasks are given in Table 7-1.

Table 7-1: TERPS Sample Collection Testing Tasks

Task No.	Task	TERPS Component
1	Collect plain soil sample and deposit in a container	Scoops
2	Collect multiple rock chips with soil	Scoops
3	Collect single small to medium sized rock with soil	Scoops
4	Sift soil from chips and small rock	Scoops
5	Grasp, hold, manipulate, and/or lift large objects	Scoops
6	Grasp, hold, and lift tools and “surface equipment” (hammer, core tube, wire bundle, etc.)	Scoops
7	Abrade the surface of a rock	Drill
8	Drill into a rock ^{††}	Drill
9	Drill into and collect soil core	Drill

^{††} The ultimate goal would be to collect a core. The current bit, however, is unable to break and extract a sample. This is an area for future development.

With TERPS in its current configuration, sampling is either a two-handed operation. When testing in the soil bins, like in Figure 5-1, one hand was used to hold TERPS in place, whether it be to hold/adjust the height when attached to the frame or to just hold when free. The other hand operated the switch. When working in the sandbox with TERPS on the staff (Figure 5-4), holding the staff required one hand and holding and operating the switch required the other.

7.2 Sampling Testing Results

TERPS was successful in 9 of the 10 sampling tasks listed above. All of the tasks requiring the scoop were successful. This section describes the evaluation and results for each of these tasks.

7.2.1 Soil and Chips Collection/Manipulation

Collecting and manipulating fines, soils and small rock chips, is one of the primary goals for this tool. This is represented by tasks one through four. These tasks were tested by performing them repeatedly all four soil types and in the sand box.

Soil Collection

This is the most basic of the sampling tasks, and is also the easiest. The scoops were opened, held over the soil, and then closed. For the dry sand, this was enough to collect a sample. In the other cases, the soil had to be worked free, which usually meant lifting TERPS during the scoop. TERPS was able to collect full scoopfuls of dry sand (Figure 7-1). For the moist sand and clay loam, TERPS was able to collect between 2/3

and 3/4 scoopfuls. TERPS was only able to collect about half scoopfuls of the gravel. The masses of the collected soil samples are shown in Table 7-2.



Figure 7-1: TERPS Collecting Pure Soil Sample

Table 7-2: Masses of Soil Samples Collected

Sample Number	Dry Sand (g)	Moist Sand (g)	Clay Loam (g)	Gravel (g)
1	350	281	176	210
2	356	166	149	143
3	114	262	221	113
4	333	289	136	165
5	245	275	191	173
6	277	243	169	154
7	130	191	193	145
8	341	150	168	214
9	201	181	121	236
10	335	250	178	113
Avg	268	229	170	167

Small Rock Collection and Sifting

There are two ways of collecting small rock samples with TERPS, both of which were successfully demonstrated in these tests. One way is to collect a bulk sample of soils and rock fragments. One such sample is shown in Figure 7-2; this sample (gravel)

contained sand as well as chips ranging from 0.5 cm to 4 cm with masses ranging from 1 g to 18 g. If soils are not desired, TERPS can sift out the fines leaving only the chips (see Figure 7-3) by opening the scoops by a few degrees and allowing smaller particles to fall out of the opening. One such sample, shown in Figure 7-4, was similar to the one shown in Figure 7-2. It has a mass of 113 g and consists of mostly 0.5 cm or larger fragments (a few grams of sand remained).



Figure 7-2: 210 g Sample of Soil Fines and Rock Fragments



Figure 7-3: TERPS Sifting Soil Sample



Figure 7-4: 113 g Sifted Rock Chip Sample

7.2.2 Soil Coring

Soil cores were collected using the drill motor. The core tube consisted of a 3 cm diameter, 30 cm long aluminum tube capped with a tapped fixture to attach to the drill. This particular task, because of the depth required, could only be accomplished out doors where the soil was extremely dense, compacted and wet. TERPS, with the core tube attached, was pushed into the surface – about 1 cm before stopping (Figure 7-5). The drill was engaged and the tube pushed further into the ground. The first core achieved a depth of 7 cm and the second a depth of 4 cm before stalling the motor.

Despite the inability to reach depth in the wet, clayey soil outside, this system does show promise. The core tube was able to be pushed, without drilling, to the bottom of the 15 cm deep sandbox. The dense, wet, clay and dry sand represent the extremes of soil types, so the meager performance in one and the “perfect” performance in the other indicate that further work on this part of the system would be beneficial.



Figure 7-5: TERPS Collecting a Soil Core (scoops not attached)



Figure 7-6: 4 cm Soil Core

7.2.3 Rock Collection/Manipulation

Three of the sampling tasks required using TERPS to grasp and hold objects. TERPS was able to pinch a 6 x 3 x 3 cm, 60 g rock; a 9 x 6 x 3 cm, 160 g rock; and a 13 x 9 x 9 cm, 1.3 kg rock (see Figure 7-7). TERPS was also able to grasp and hold several objects that an astronaut may use on EVA, including a hammer, core tube, and tool box (see Figure 7-8).

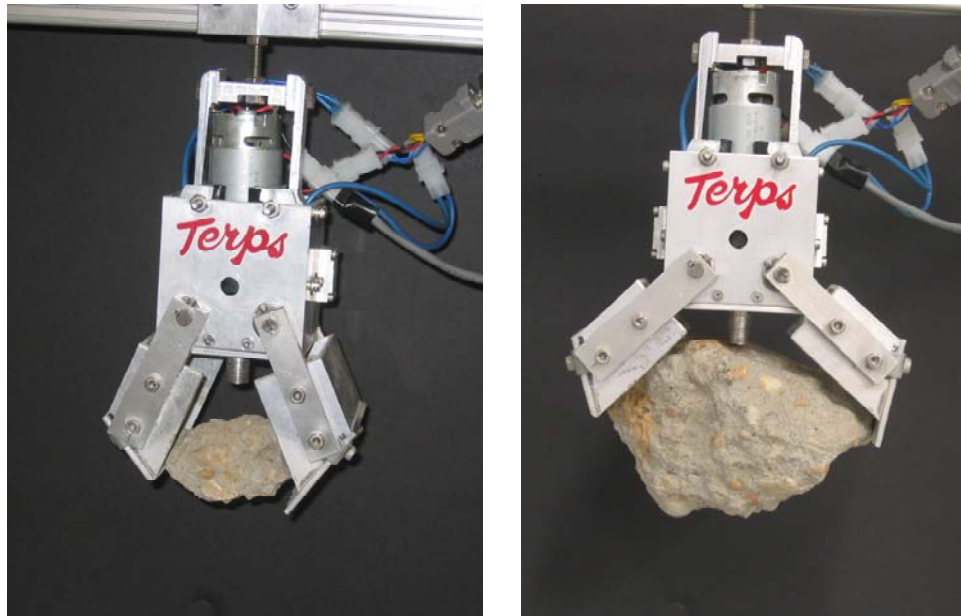


Figure 7-7: TERPS Grasping and Holding a Small Rock (L) and Large Rock (R)

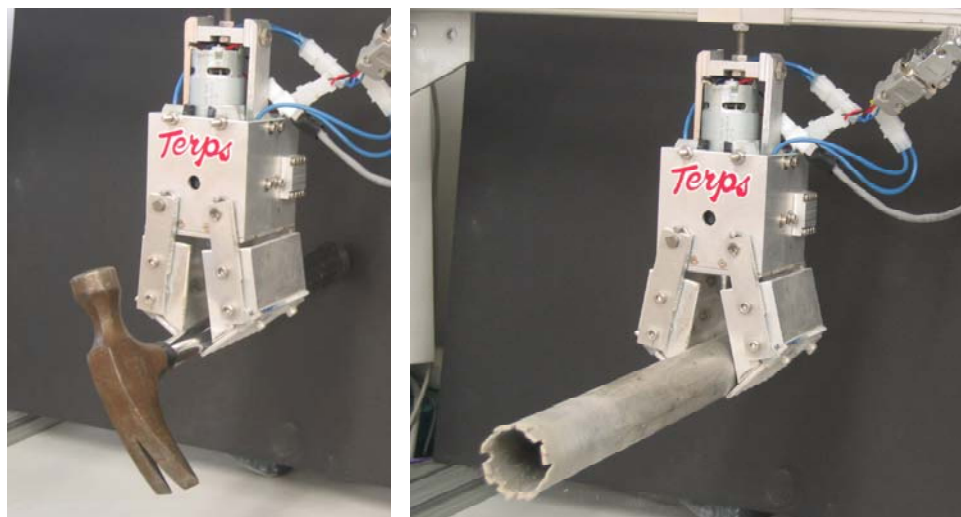


Figure 7-8: TERPS Holding Other Tools (Hammer and Core Tube)

7.2.4 Rock Coring/Abrading

The two remaining sampling tasks to be evaluated are rock drilling and abrading. Here, the “rock” is a 1.3 kg piece of hardened concrete. The corer/abrader is a $\frac{3}{4}$ in hole-saw attached to the drill (Figure 7-9). When placed on the rock, the bit acts as an abrader, grinding away the uppermost surface of the rock and exposing the interior. This was done successfully with TERPS as shown in Figure 7-10. Drilling or coring into the rock proved problematic. Available resources prevented the use of a dedicated rock cutting bit, so an ordinary hole-saw (available in any hardware store) was used. This hole-saw would normally have a guide bit. Without it, the hole-saw could not catch on the rock surface enough to start cutting into it. Instead, the motor torque would kick the bit away from the rock. After applying enough force to keep the bit in place on the rock surface, it did start to grind a core (a single circle of scratches is visible on the rock) but by this point the teeth had dulled to a point where any penetration was impossible^{**}. The rock coring concept was demonstrated, though less impressively, on a piece of foam (Figure 7-11).



Figure 7-9: Rock Coring/Abrading

^{**} Using a bit dedicated to cutting/coring rock and/or metal (a diamond blade for example) would solve this problem. It is important to note, however, that any bit will eventually dull.



Figure 7-10: Before and After Rock Abrading

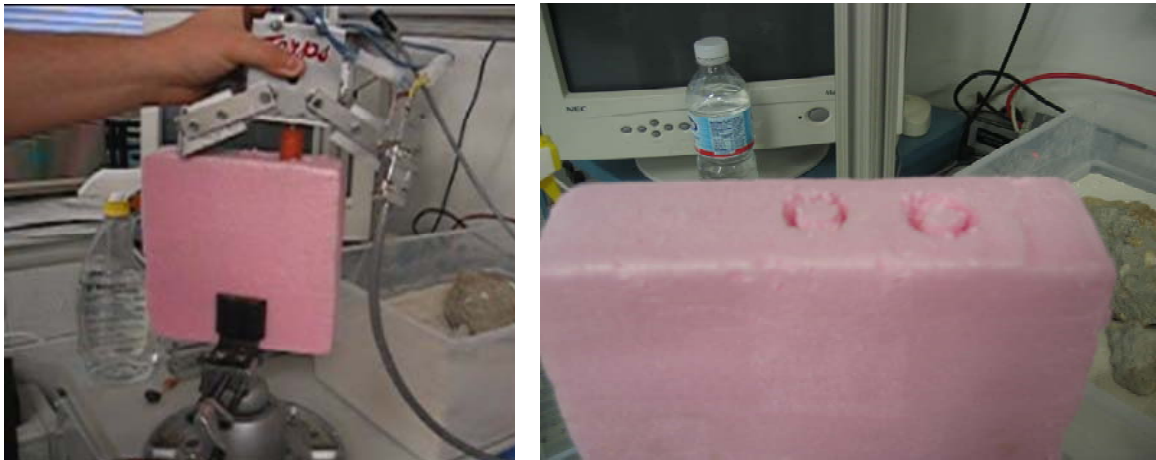


Figure 7-11: Drill Demonstration on Foam

7.2.5 Sandbox Tests

TERPS was demonstrated as a crew aid tool in the large sand box. TERPS was attached to the 1.2 m staff, which was held in one hand. The battery and switch were held in the other (Figure 7-12). Because of the problems associated with drilling discussed above, only scooping tasks were shown in the sand box.



Figure 7-12: TERPS Sand Box Testing

Several of the sampling tasks were attempted with TERPS on the staff, including soil collection, soil/rock collection and sifting, and grasping/holding large objects. Soil collection was relatively simple. TERPS was placed over the soil and the scoops closed. This only required significant motion in the arm and did not require any bending or stooping. The same was true of grasping objects. However, in this case, it required a little more effort get to the right angle or orientation to take hold of the object.

Two areas of concern that should be addressed before proceeding along this line of research (TERPS as a CAT) are mass and control. TERPS has a mass of 1.75 kg (2.35 kg with the staff), which is neither heavy nor unmanageable. However, at the end of a 1.2 m staff this produces a large moment and can be difficult to handle one handed. This relates into the other area of concern. Holding TERPS in one hand and the switch in the

other is fine for preliminary evaluations such as these, but as a practical matter the control switch(es) should be on the staff so as to free the second hand.

7.2.6 Summary

The testing described above was to demonstrate and evaluate TERPS's sample collecting abilities. Of the nine sampling activities laid out, TERPS was able to perform all but one, rock coring. The sampling activities and their results are summarized in Table 7-3.

Table 7-3: Sampling Task Results

Task No.	Task	Results
1	Collect plain soil sample	Collected an average of 220 g of pure soil per sample
2	Collect rock chips w/ soil	Collected an average of 170 g per sample of sand and chips
3	Collect single small to medium sized rock with soil	Collect 60 g rock with 150 g of soil
4	Sift soil from chips/small rock	Sifted approximately 50 g sand from 113 g bulk chip sample and approximately 150 g from single rock scoop
5	Grasp, hold, manipulate, and/or lift a rock(s) bigger than scoops	Lifted and held 15 cm wide, 1.3 kg rock
6	Grasp, hold, and lift tools and "surface equipment"	Held hammer, core tube, tool box, etc.
7	Abrade the surface of a rock	Abraded about 4 cm ² of rock surface
8	Drill into a rock	Unsuccessful
9	Drill into and collect soil core	2 cores, 7 cm and 4 cm

7.3 Discussion

The testing described above shows that the current TERPS concept and configuration is sound. It met all but one of the sampling requirements and shows promise for future development.

7.3.1 Sampling Requirements

The sampling tasks identified above and the testing described above all sought to verify that TERPS met the sampling requirements defined in Chapter 3 (summarized again in Table 7-4). TERPS was successful in meeting all but one of the defined requirements, the drilling. In soil collection, the collected masses ranged from 113 g to 356 g with an average mass of 208 g (71 g standard deviation). This also included a run of sample collections of gravel, which is a mixture of sand and rock chips. TERPS was able to collect both a bulk sample of the gravel as well as sift out sand particles, thus collecting only rock fragments. The tests also showed TERPS capable of grasping and holding, with the power off, a 9 cm wide, 160 g rock; a 1.3 kg, 15 cm wide rock; a hammer; a core tube; and a tool box.

The only requirement TERPS was unable to meet entirely was the rock cutting requirement. As discussed, the drill bit used was unable to penetrate past the rock's surface, so TERPS was unable to at least simulate collecting a sample of a large rock. TERPS was able to collect a soil core, but not to the length defined in the requirements. It collected two cores each less than 10 cm deep, but it did so in dense, wet, highly resistive clay. This was the only medium deep enough for that particular test; other available soils ranged in depth from 7.5 – 20 cm. In these soils, TERPS could reach the maximum depth, but there was not enough compaction or friction to keep the soil in the tube as it was extracted.

Table 7-4: Sampling Requirements Verification

No.	Requirement	Met?	Notes
S-1	Collect 200 g of regolith fines	YES	Avg sample size – 210 g Max sample size – 356 g
S-2	Collect multiple rock chips	YES	Avg bulk gravel sample – 167 g Chips range from 5 mm to 4 cm

S-3	Sifting rocks > 1 cm from fines	YES*	Successfully sifted sand, but 0.5 cm fragments remained
S-4	Collect single rock up to 10 cm in diameter	YES	Grasped 9 cm rock
S-5	Grasp and manipulate rocks larger than 10 cm, up to 20 cm in diameter and up to 2 kg of mass	YES	Grasped 15 cm rock
S-6	Expose rock interior	YES	Abraded 5 cm ² area of rock surface
S-7	Collect a sample of up to 5 g from large rocks and/or boulders	NO	Drill unable to penetrate rock
S-8	Collect a soil core of at least 30 cm	YES*	Collected 4 cm and 7 cm core of dense clay, no other soil type deep enough available
S-9	Grasp and manipulate ordinary hand tools	YES	Grasped hammer, core pipe, tool box, ½ in bolt, soda can

* - Requirement met with caveat

7.3.2 Mechanical Error/Issues

Mechanically, the TERPS prototype performed well, but was not without issues. The biggest area of concern is backlash. Backlash in a gear train is small gaps between the teeth of two meshed gears. This gap allows for motion in one gear/shaft without motion in the other. Each of the scoops has 5-10° in free motion, which is more a result of error in fabrication than in the gears themselves. A slight error in the position of the scoop axels with respect to the worm shafts resulted in extra space between the gear and worm. This was a problem for grasping some larger objects, but for the most part, once the worm tightened against the gear, the scoop remained still and the grip.

The overriding problem with the mechanism is the fact that it was designed and fabricated to be easily modified. This work was intended to establish design requirements and verify and validate concepts. As such, the prototype was designed and machined such that as a problem or issue arose it could be quickly addressed. As

previously discussed, this meant higher tolerances and errors were acceptable, as were less than optimal design choices (i.e. the bearings). With the concept now demonstrated, more effort can be placed in the specifics of the mechanical design, including machining and fabricating more precisely, using the appropriate bearings, and attaching gears to prevent slipping (no set screws).

7.3.3 Sampling

Aside from rock cutting, TERPS's sampling ability is quite good. Obviously, work needs to be done to better integrate a drilling system into the overall tool, but the drill did function well as an abrader and as a soil corer. In terms of sampling, the scoops performed excellently. Soil samples were easy and intuitive to collect and it performed adequately as a gripper. A specific area for improvement is the scoop sides. As mentioned, the sides were originally meant to overlap, but the available materials prevented that. Since the scoop sides were cut from a single aluminum channel, they did not close tightly together – the width of the saw blade caused a small gap. This resulted in openings where soil could escape. It also allowed small particles to get stuck in the top of the side, preventing closure, something avoidable with overlapping scoop sides.

Chapter 8

Conclusion & Future Work

This thesis presented a concept for a sampling tool with applications for research into human/robotic planetary surface exploration. Previous sampling activities, by both human and robot explorers were analyzed to define a set of requirements for this tool. A concept for this tool, TERPS, was developed and a prototype constructed and evaluated against the defined requirements as well as soil cutting theory. The result is a tool that shows great promise for future development and use in research human/robot cooperation.

8.1 Conclusions

The task of developing a sampling tool is a very broad one. The last broad survey of a region of a planetary surface was Apollo 17 in 1972. Since then, with the exception of a hand full of task specific robots, few people have put much thought into the details of the tools needed to conduct extraterrestrial planetary research – there has been no need. The result is that this design problem is very much open-ended, so a large portion of this research was reviewing previous sampling strategies and tools, and establishing a baseline set of requirements for future tools. These requirements, outlined in section 3.3, are a first cut of the attributes required in a tool in order to conduct a sound geologic analysis of a region of a planetary surface.

The Tool for EVA or Robotic Planetary Sampling was developed to both to meet and to evaluate those requirements. The TERPS concept showed in a lab setting that it could meet most of the defined requirements. In “field” testing, it showed that it has potential for being a useful crew aid tool and that the derived requirements do encompass all of the tasks one would reasonably assume are required for planetary sampling.

TERPS has two components that allow it to meet its sampling requirements, the scoops and the drill. The scoops worked extremely well in collecting soil/regolith fines and small rocks. They also proved to be capable as grippers, grasping both large rocks and other tools. The drill was more problematic, mostly because it was added and tested late in the process. It works well as an abrader as well as a soil corer, but more work is needed before it will be able cut and collect rock samples as originally intended.

In terms of actuation, both the drill and scoop motors were chosen based on cost and it was assumed that once the system was evaluated decisions could be made on higher quality motors. These motors, however, have proven quite capable and there is no need, at this time, to consider replacing them. The worm-gear actuation drive performed well. Problems and issues that arose during testing were more a result of errors in fabrication and the nature of the prototype than anything else. Future prototypes, machined with precision and functionality in mind, as opposed to just functionality, should avoid many of these complications.

The soil model used to compare TERPS’s performance to known soil behavior also proved quite useful. The model accurately predicts TERPS’s performance early in the scooping motion. When it diverges, it diverges in such a way that the predictive model is the worse case. The cause of this divergence needs to be investigated further,

but the consistency in the tests means that the soil model is useful in defining requirements for a given soil or estimating performance for a given motor and a given soil. The model may also be useful in directly measuring the properties of an unknown soil, though some properties of the soil need to be known.

Chapter 3 also defined four initial functional requirements. The first of these stated that nothing should preclude TERPS from being either a crew aid or an end-effector. At this stage, the only thing preventing TERPS's use as an end effector is its interface, which is entirely dependent on the manipulator. The requirement that differing designs for robotic and human use is not verifiable until the design diverges. In the testing conducted thus far, very little dust has made its way into the interior, however, as will be discussed, this is an area of future study. Finally, all parts are accessible as evidenced by the number of times TERPS was disassembled and reassembled.

In general, this work has demonstrated the validity of a multi-purpose geologic sampling tool. The developed prototype was intentionally low fidelity, but there was not much it could not do. The fact that it performed so well indicates that future development will only increase its performance and value as a tool.

8.2 Future Work

While TERPS has shown itself to be a capable sampling tool, there is room for improvement. There are mechanical design and hardware issues that need to be addressed. Once these items are dealt with, there is a wealth of study to be done using TERPS.

8.2.1 Design/Hardware Upgrades

As mentioned throughout this paper, most design choices were made in the interest of easily and inexpensively modifying the prototype(s) as issues and problems arose. With the concept now demonstrated, more emphasis should be placed on the mechanical details of the mechanism. Two areas of interest are the bearings and the support structure. The use of worm gears necessitates the use of axial load bearing bearings. Using thrust bearings requires a structure to support those loads and keep the worm and gear in place. A possible configuration is sketched in Figure 8-1.

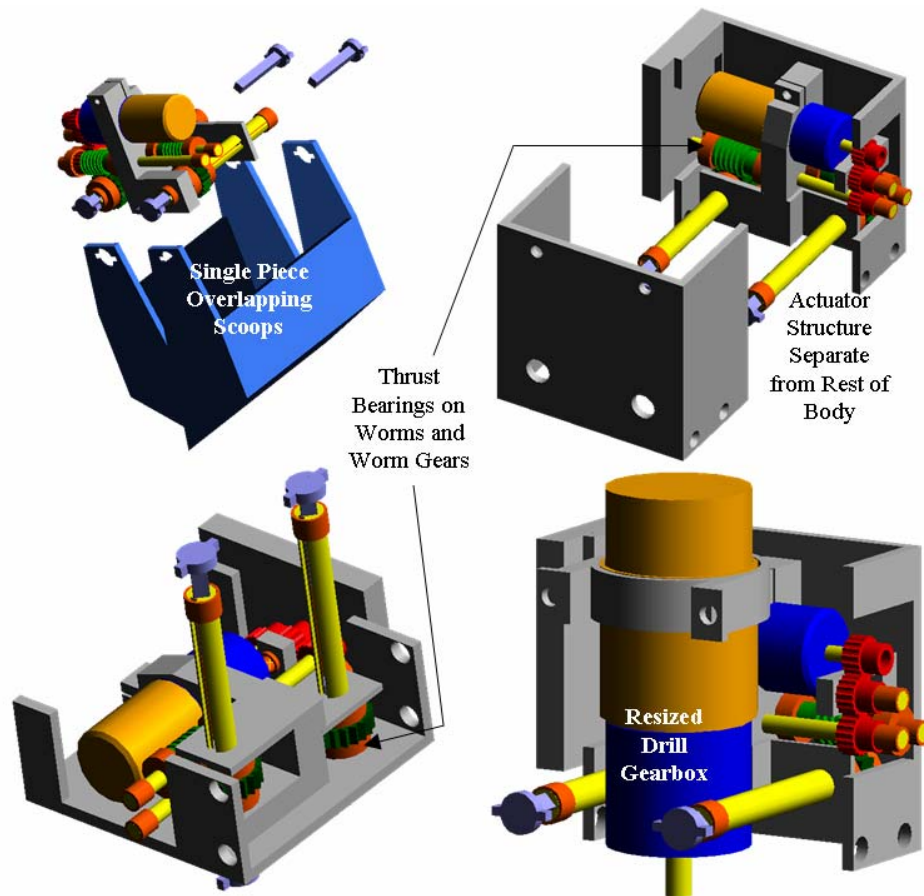


Figure 8-1: Sketch of Next TERPS Prototype

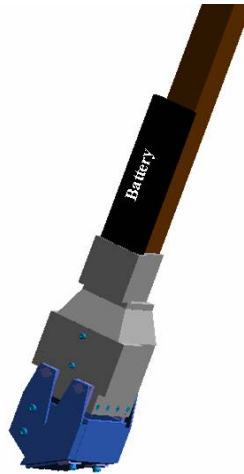


Figure 8-2: TERPS as Crew Aid

The scoops used for this work were designed and constructed using available materials. The next version of the scoops should be more inline with the original concept put forth in section 4.4, with the scoop sides overlapping. This should prevent losses out of the side, stop particles from getting stuck in the sides preventing closure, and give TERPS better gripping ability with large objects.

Another area for improvement is the drill. The limited testing of the drill in this work suggests that the current drill motor gear train is adequate for the work it has to do, but the gear casing is too large and awkward for the tool structure, as configured. Additionally, new bits (for both soil and rock cores) and a mechanism for attaching them to the drill need to be developed.

Without a robotic sampling system to work with, the immediate course of action would be to pursue the application as TERPS as a crew aid tool. As such, the interface between the tool and the staff needs to be refined and an interface between the tool and the user (the “astronaut”) needs to be developed. Longer term work on TERPS would include adapting it to a robotic manipulator.

8.2.2 Proposed Research & Experiments

In the near term, the current TERPS system, or its successor, could easily be used to further analyze human planetary sampling as well as the durability of the sampling system. With TERPS attached to a staff and used as a crew aid tool, research can be conducted into the human factors of planetary sampling. This includes operation in a suited glove, conducting a balance and stability analysis of using the tool while carrying the weight of the suit and backpack, and/or sampling strategies of a suited astronaut. Studying TERPS on its own can yield information about sampling tool durability. Dust is a major concern for any and all surface systems, and TERPS provides an excellent test bed for studying the effects of prolonged use in a dirty environment on a mechanical system.

As mentioned, TERPS is meant to be a research tool for developing future planetary surface systems and activities. It could be used for countless experiments in human, robotic, or human/robotic planetary surface sampling. These experiments could be useful in analyzing or optimizing human-robot interaction and roles, EVA task allocation, and EVA sampling strategies.

Appendix A

Apollo Sampling Tools

A.1 Apollo Tools Information

The table below summarizes the mass and sample volume capacity for each of the Apollo sampling tools. The capacities are based on dimensions given in [9].

Tool	Page	Tool Mass (g)	Sample Capacity	Mission Used						
				11	12	14	15	16	17	
Contact sampler	6	500	9.5x10.6 cm					•		1
Contingency Sampler	9	1200	~1200 cm ³	•	•	•	•			2
2cm Core Tube	10	327	400 cm ³	•	•	•				
4cm Core Tube	12	300	1759 cm ³				•	•	•	
Drill	15	13400	4200 cm ³				•	•	•	
Hammer	22	860	N/A	•	•	•	•	•	•	
LRV Soil Sampler	24	140	5200 cm ³						•	3
Rake	25	1500	9000 cm ³				•	•	•	4
Large Scoop	27	400	2025 cm ³	•	•	•				
Small Scoop	28	163	130 cm ³		•	•				
Small Adjustable Scoop	29	516	455 cm ³				•			
Large Adjustable Scoop	30	590	825 cm ³					•	•	
Short Tongs	31	140	6-10 cm	•	•	•				
32" Tongs	31	230	6-10 cm				•	•	•	
Trenching Tool	33	1315	1125 cm ³			•				5

1 – Adhesive sampler designed to collect upper most layer of regolith.
2 – Used to quickly collect sample immediately after egress in case of an emergency.
3 – Similar to Contingency Sampler. Used to collect a sample w/o getting out of the lunar rover.
4 – Typically collected up to 1 kg of small (~5 g) chips.
5 – Simple spade for trenching.

Appendix B

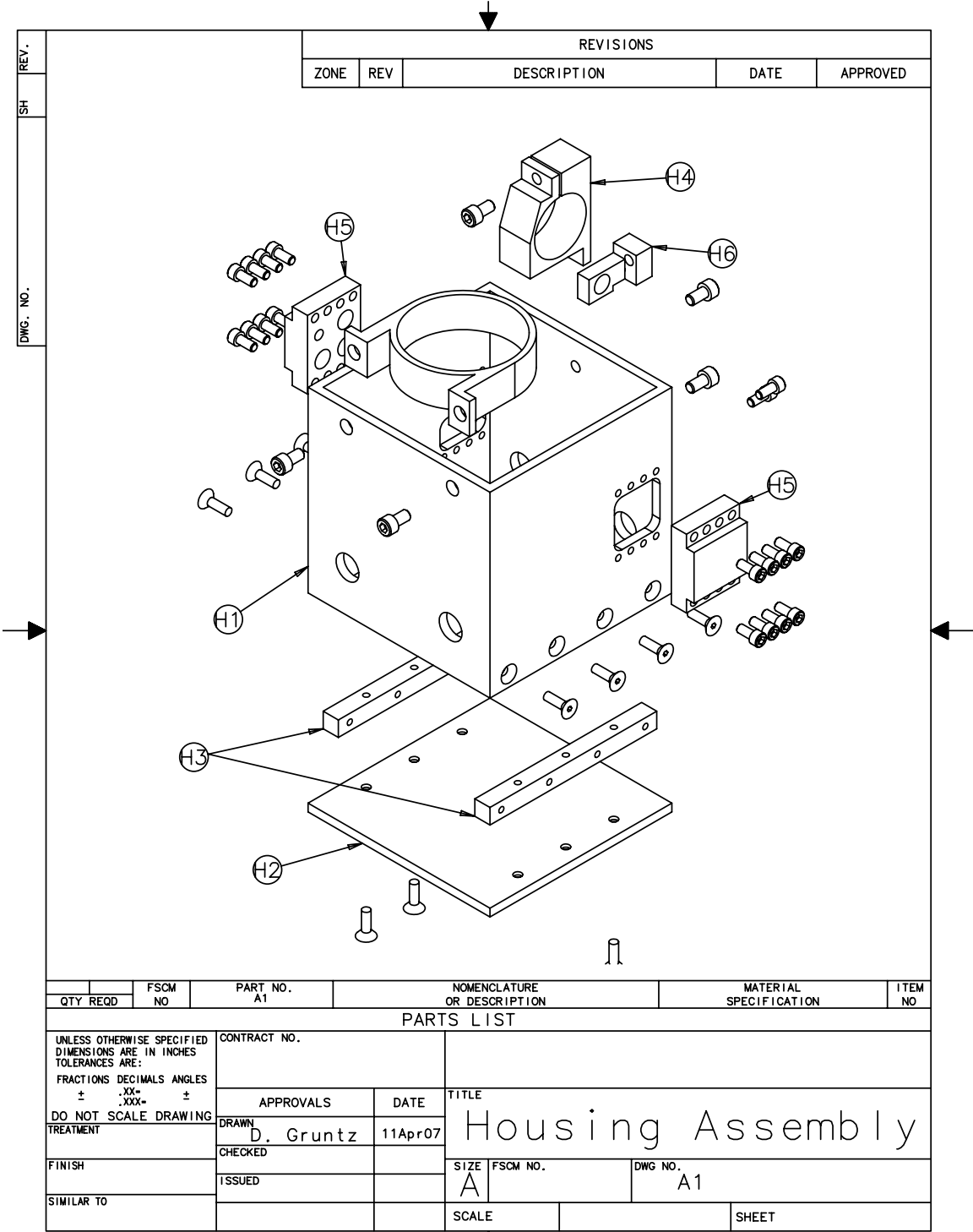
TERPS Hardware

B.1 Materials List

Provider	Part No.	Item
McMaster-Carr	88875K731	Alloy 6063 Aluminum Square Tube 3" X 3", .125" Wall, 1' Length (Same as 88875K73)
McMaster-Carr	1327K52	Miniature Precision 12L14 Steel Shaft 3/16" OD, 6" Length
McMaster-Carr	9041K13	Alloy 6061 Aluminum Strip 1/8" Thick, 3" Width X 24" Length
McMaster-Carr	1497K111	Fully Keyed 1045 Steel Drive Shaft 5/16" Od, 3/32" Keyway Width, 12" Length
McMaster-Carr	98535A125	Heat-Treatable Steel Standard Key Stock 3/32" X 3/32", 12" Length
McMaster-Carr	1327K54	Miniature Precision 12L14 Drive Steel Shaft 3/16" Od, 18" Length
McMaster-Carr	6391K403	SAE 841 Bronze Sleeve Bearing for 5/16" Shaft Diameter, 3/8" Od, 1/4" Length
McMaster-Carr	6391K122	SAE 841 Bronze Sleeve Bearing for 3/16" Shaft Diameter, 1/4" Od, 1/4" Length
Stock Drive Products	S1063Z-048S022	48 D.P., 22 Teeth, 20° Pressure. Angle, 303 Stainless Steel Gear
Stock Drive Products	A 1B 6-N32020A	20:1 GEAR RATIO, 20 TEETH WORM GEAR
Stock Drive Products	A 1C55-N32	32DP / 1 Lead / 0.438P.D, 4.08° Right Hand Worm
Stock Drive Products	S1084Z-048S018	48 D.P., 18 Teeth, 20° Pressure. Angle, 303 Stainless Steel Gear
Stock Drive Products	S1063Z-048A018	48 D.P., 18 Teeth, 20° Pressure. Angle, 2024 Aluminum Gear

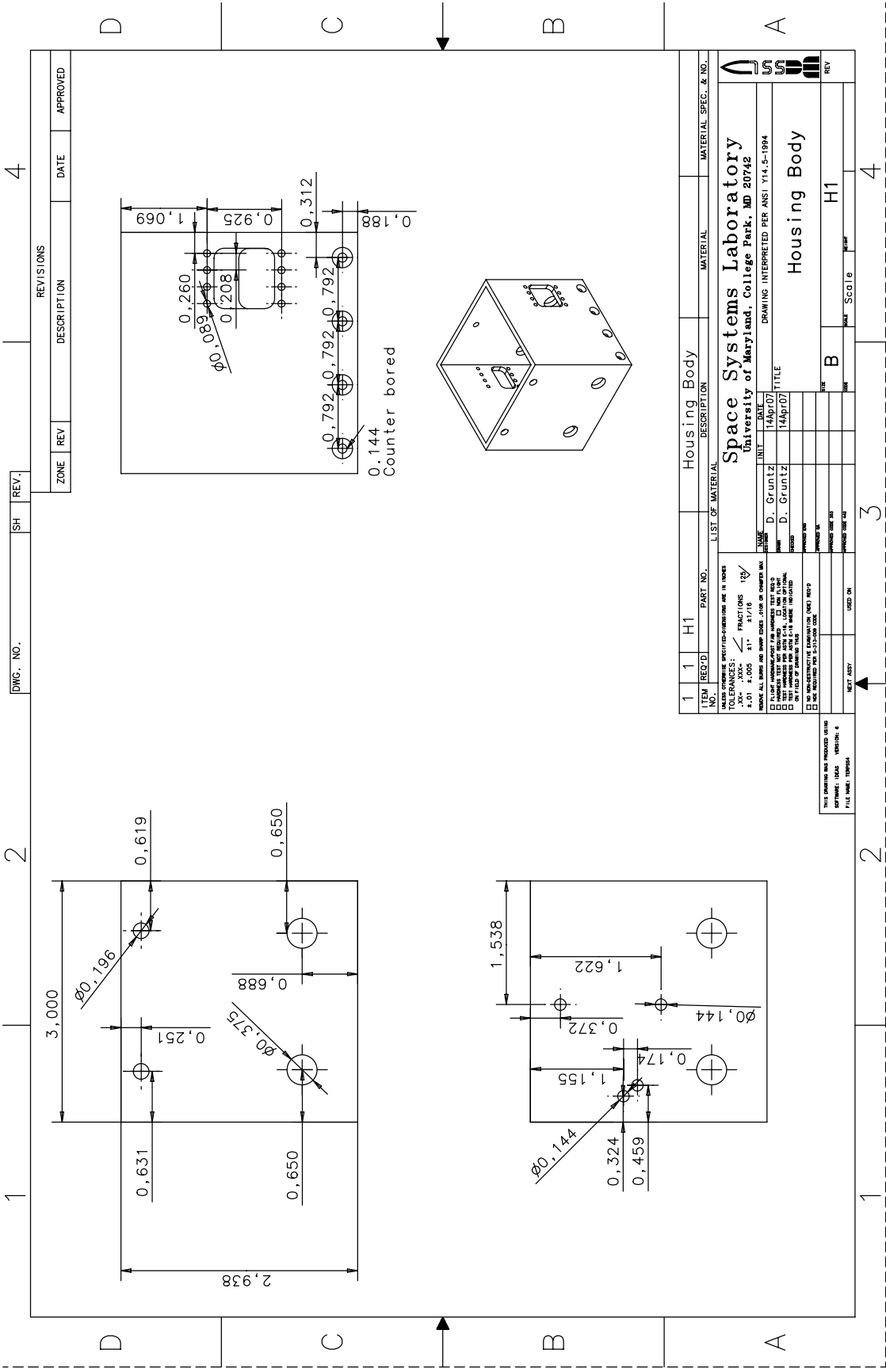
B.2 CAD Drawings

Drawing No.	Drawing Type	Title
A1	Assembly	Housing Assembly
H1	Part	Housing Body
H2	Part	Housing Palm
H3	Part	Palm Brace
H4	Part	Motor Mount
H5	Part	Side Bearing Support
H6	Part	Transfer Shaft Support
A2	Assembly	Scoop Actuation Drive
SA1	Part/Assembly	Transfer Shaft
SA2	Part/Assembly	Left Worm Shaft
SA3	Part/Assembly	Right Worm Shaft
SA4	Part/Assembly	Left worm Gear Shaft
SA5	Part/Assembly	Right Worm Gear Shaft
A3	Assembly	Right Side Scoop
A4	Assembly	Left Side Scoop
S1	Part	Scoop Side
S2	Part	Scoop Arm
S3	Part	Blade, Smooth
S4	Part	Blade, Serrated



REVISIONS				
ZONE	REV	DESCRIPTION	DATE	APPROVED

QTY REQD	FSCM NO	PART NO. A1	NOMENCLATURE OR DESCRIPTION	MATERIAL SPECIFICATION	ITEM NO	
PARTS LIST						
UNLESS OTHERWISE SPECIFIED DIMENSIONS ARE IN INCHES TOLERANCES ARE: FRACTIONS DECIMALS ANGLES ± .XX- ± ± .XXX- ± DO NOT SCALE DRAWING	CONTRACT NO.		TITLE Housing Assembly			
	APPROVALS	DATE				
	TREATMENT	DRAWN D. Gruntz	11Apr07	SIZE A	FSCM NO.	DWG NO. A1
	FINISH	CHECKED	ISSUED	SCALE	SHEET	
SIMILAR TO						



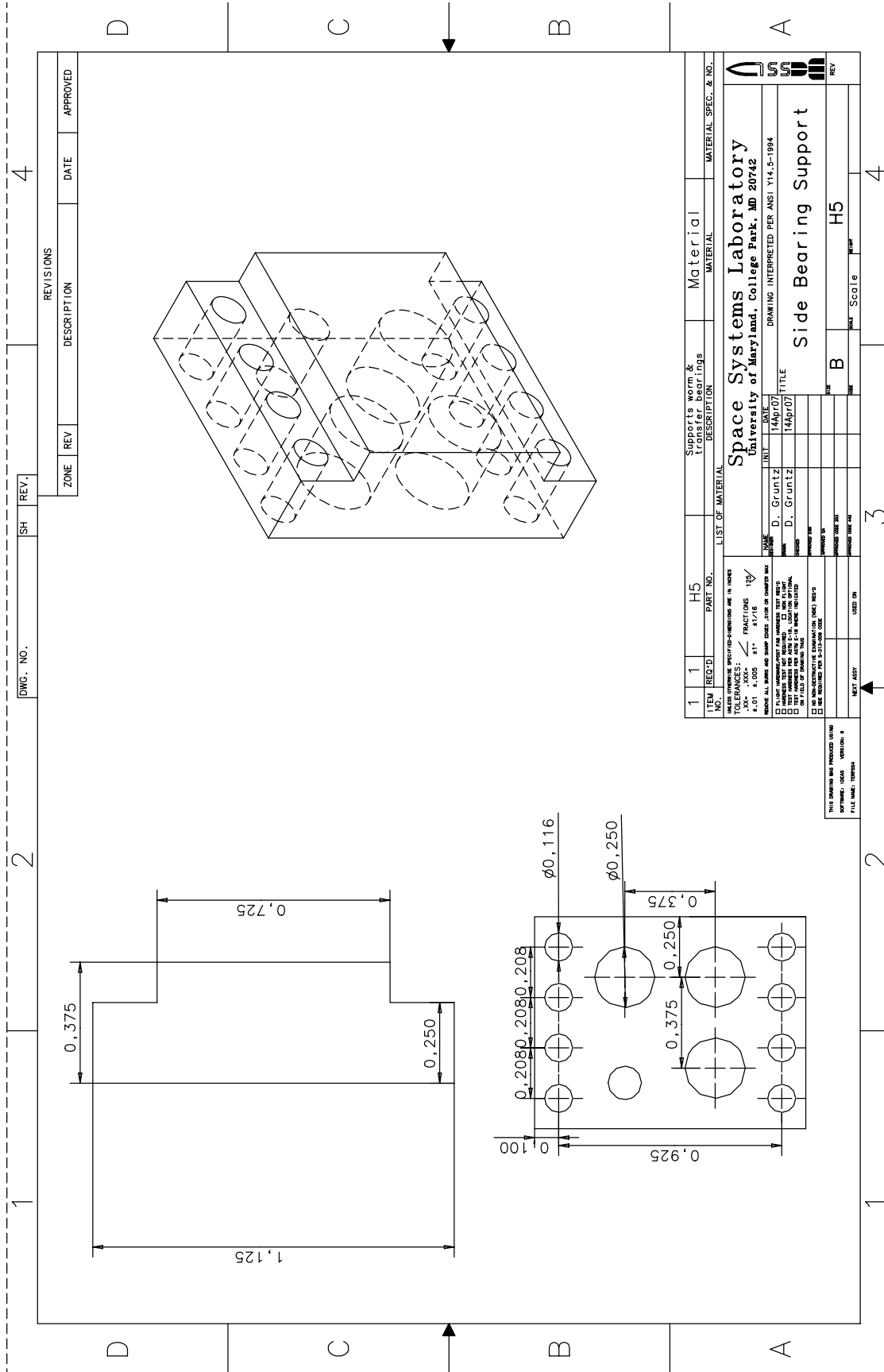
ZONE	REV	DESCRIPTION	DATE	APPROVED

DWG. NO.	SH	REV.
		4

ITEM	REQ'D	PART NO.	DESCRIPTION	MATERIAL	MATERIAL SPEC. & NO.
1	1	H1	Housing Body		

NAME	DATE	TITLE
D. Gruntz	14Apr07	Housing Body

REV	DATE	DESCRIPTION
H1		



DWG. NO.		SH		REV.	
1		2		4	

REVISIONS			
ZONE	REV	DESCRIPTION	DATE

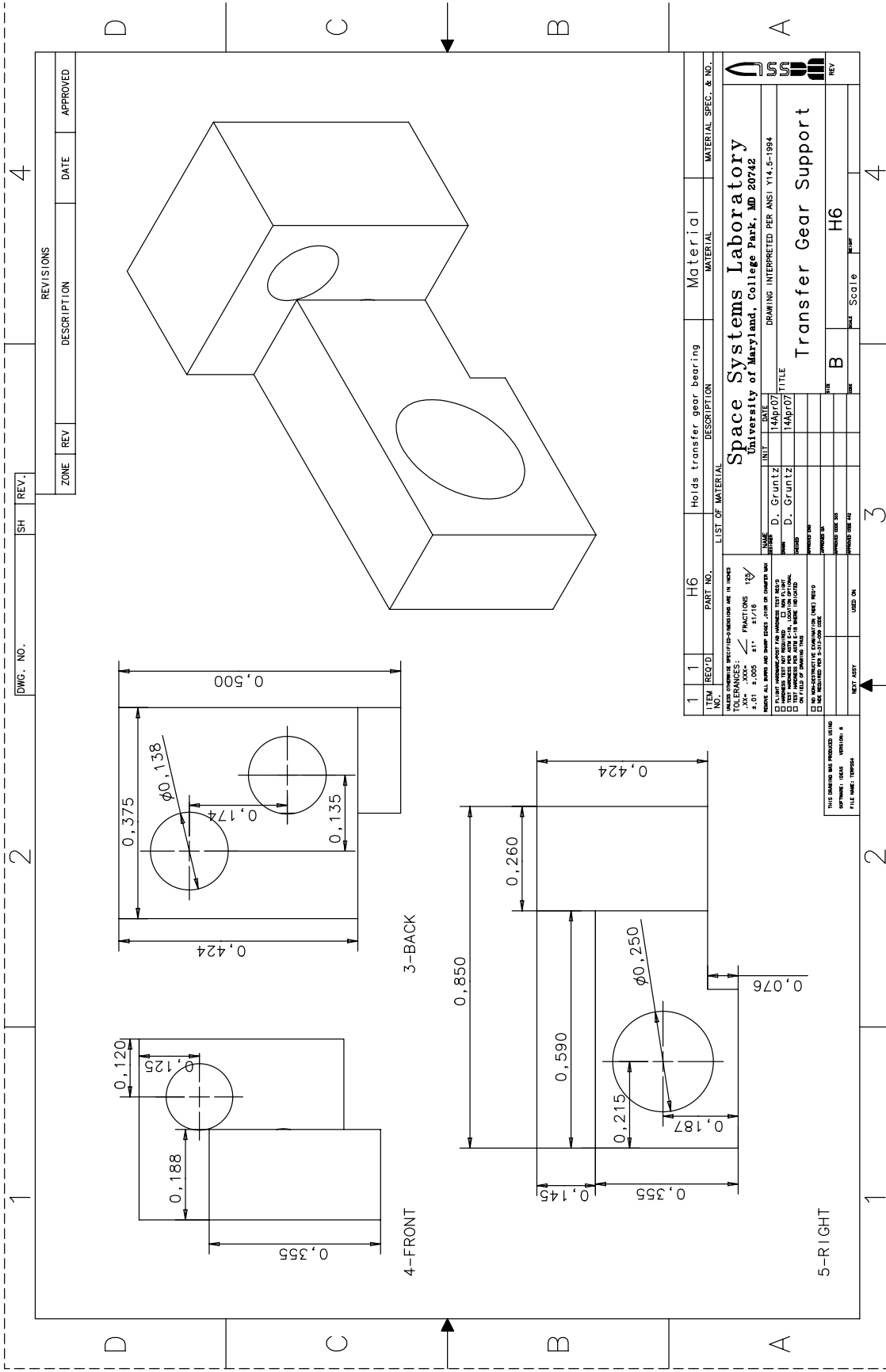
APPROVED	

ITEM	REQ'D	H5	PART NO.	Supports worm & transfer bearings	Material	MATERIAL SPEC. & NO.
1	1					

LIST OF MATERIAL	
DATE	14Apr/07
BY	D. Gruntz
CHECKED	D. Gruntz
DATE	14Apr/07
BY	D. Gruntz
CHECKED	D. Gruntz

Space Systems Laboratory
 University of Maryland, College Park, MD 20742
 DRAWING INTERPRETED PER ANST Y14.5-1984
 Side Bearing Support

REV	DATE	DESCRIPTION



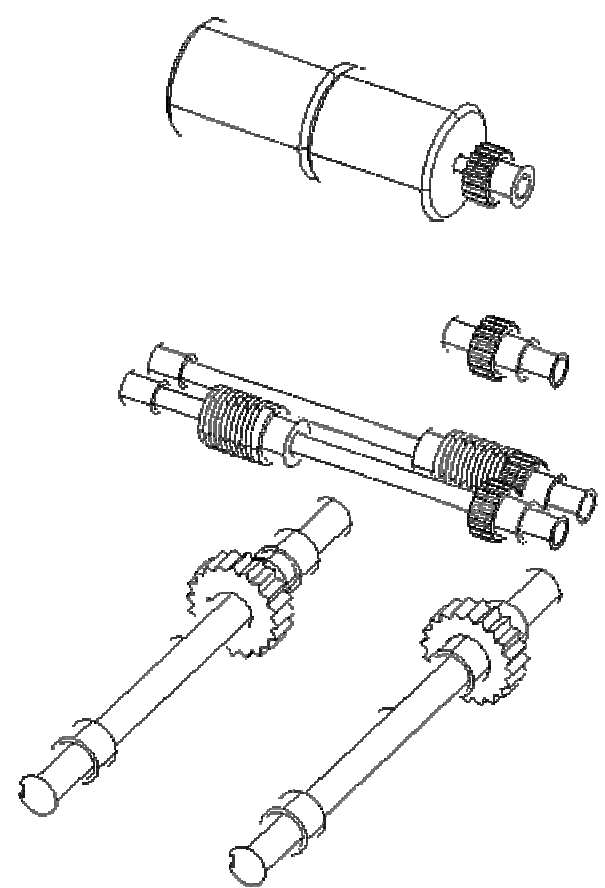
REVISIONS		DATE	APPROVED
ZONE	REV		

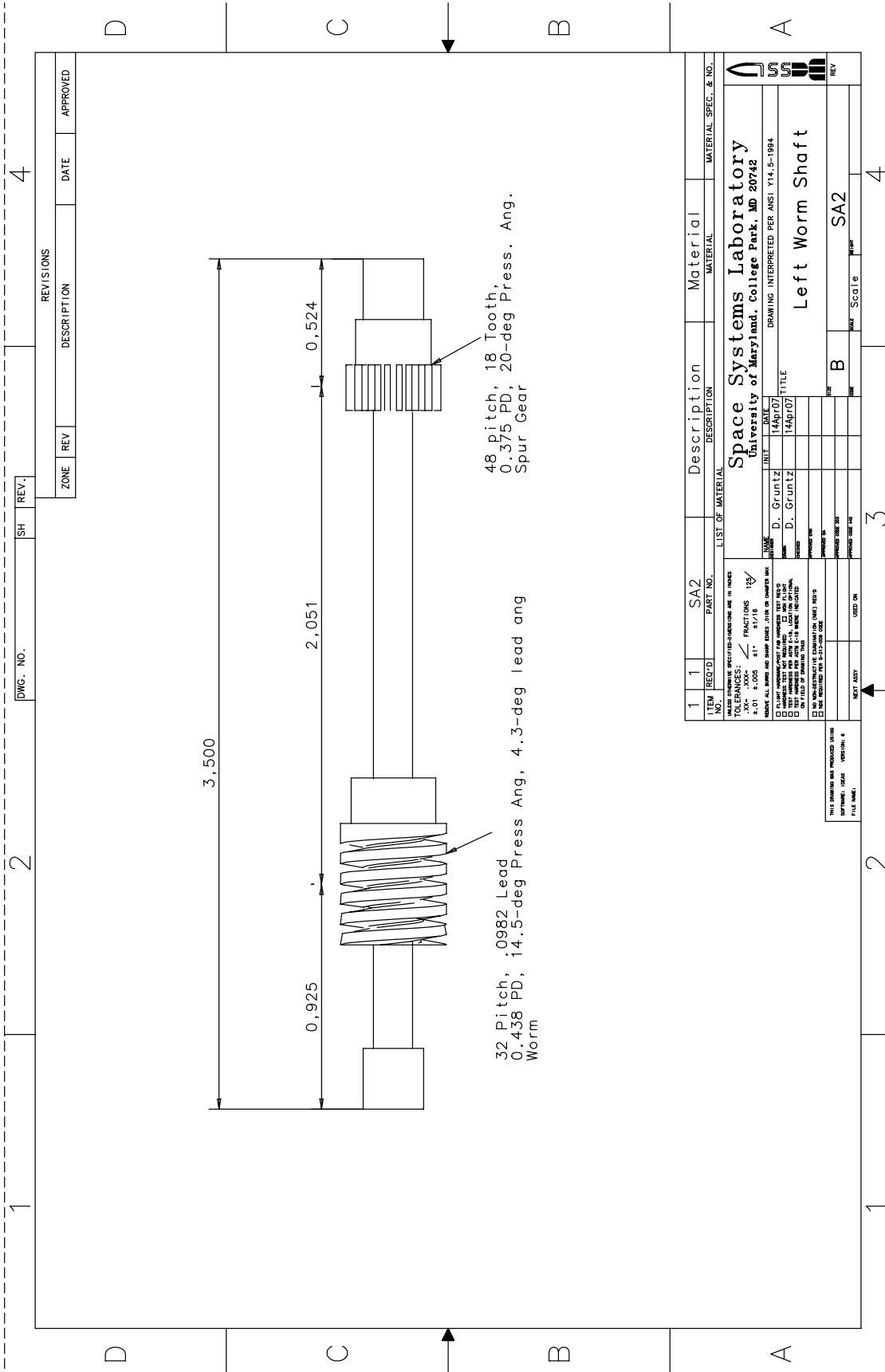
DWG. NO.	SH	REV.
2		4

ITEM NO.	REQ'D	PART NO.	H6	DESCRIPTION	MATERIAL	MATERIAL SPEC. & NO.
1				Holds transfer gear bearing	Material	

LIST OF MATERIAL		TITLE	
DATE	DRAWN BY	DATE	TITLE
14.07.07	D. G. UTI2	14.07.07	Transfer Gear Support
14.07.07	D. G. UTI2		
THIS DRAWING WAS PRODUCED USING AUTOMATIC DATA VERIFICATION & FILE NAME VERIFICATION			

REV	DATE	BY	SCALE
B			H6

REV.	REVISIONS								
SH	ZONE	REV	DESCRIPTION	DATE	APPROVED				
DWG. NO.									
	QTY REQD	FSCM NO	PART OR IDENTIFYING NO	NOMENCLATURE OR DESCRIPTION	MATERIAL SPECIFICATION	ITEM NO			
PARTS LIST									
UNLESS OTHERWISE SPECIFIED DIMENSIONS ARE IN INCHES TOLERANCES ARE: FRACTIONS DECIMALS ANGLES \pm .XX- \pm \pm .XXX- \pm DO NOT SCALE DRAWING TREATMENT		CONTRACT NO.		TITLE Scoop Actuation Drive					
		APPROVALS	DATE						
		DRAWN	D. Gruntz		14Apr07		SIZE	FSCM NO.	DWG NO.
		FINISH	CHECKED		ISSUED		A		A2
SIMILAR TO				SCALE		SHEET			

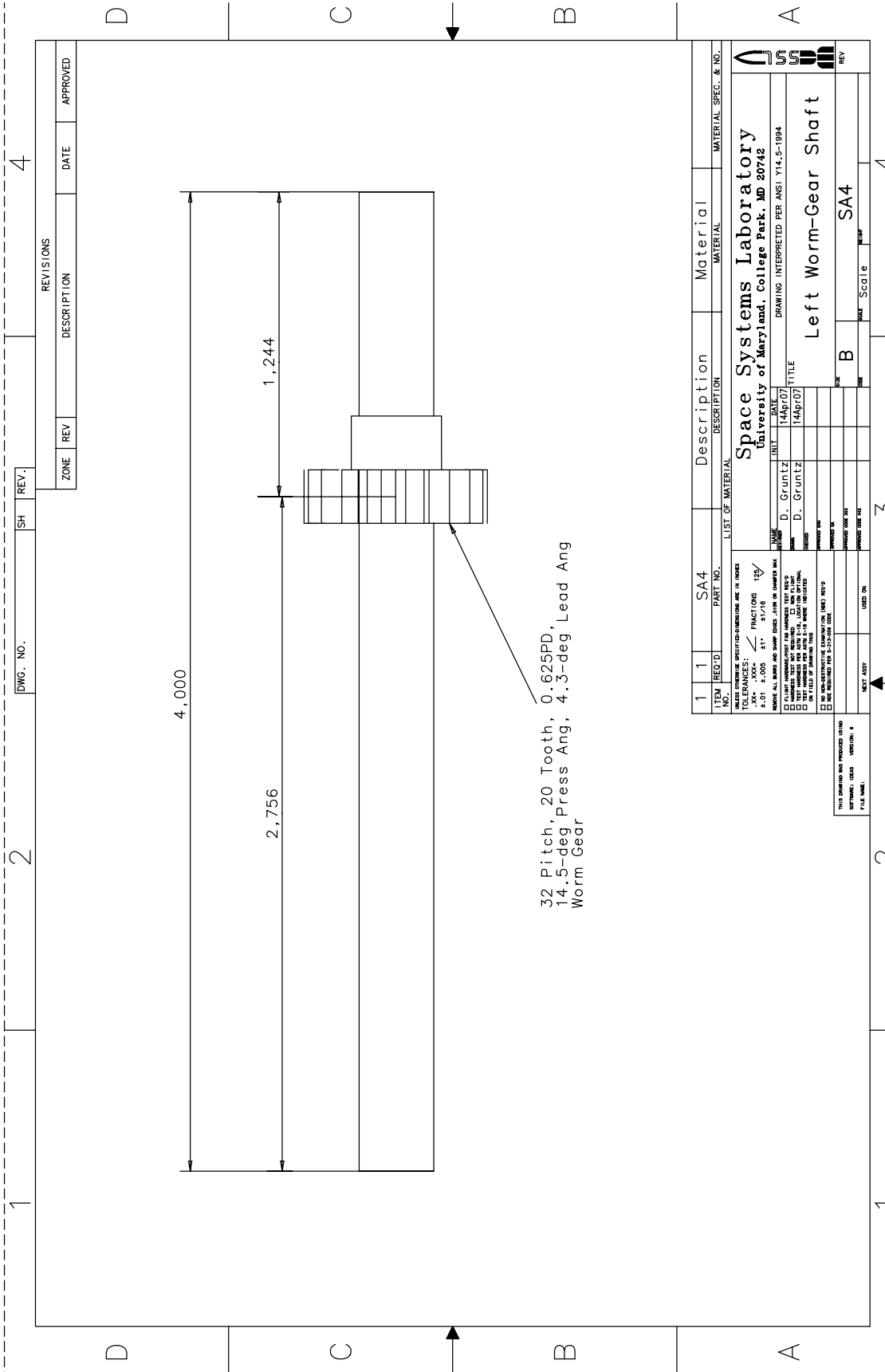


32 Pitch, .0982 Lead
0.438 PD, 14.5-deg Press Ang, 4.3-deg lead ang
Worm

48 pitch, 18 Tooth,
0.375 PD, 20-deg Press. Ang.
Spur Gear

ITEM	REQ'D	SA2	DESCRIPTION	MATERIAL	MATERIAL SPEC. & NO.
1	1		Left Worm Shaft	SA2	

ZONE	REV	DESCRIPTION	DATE	APPROVED
	1	Scale	14Apr/07	

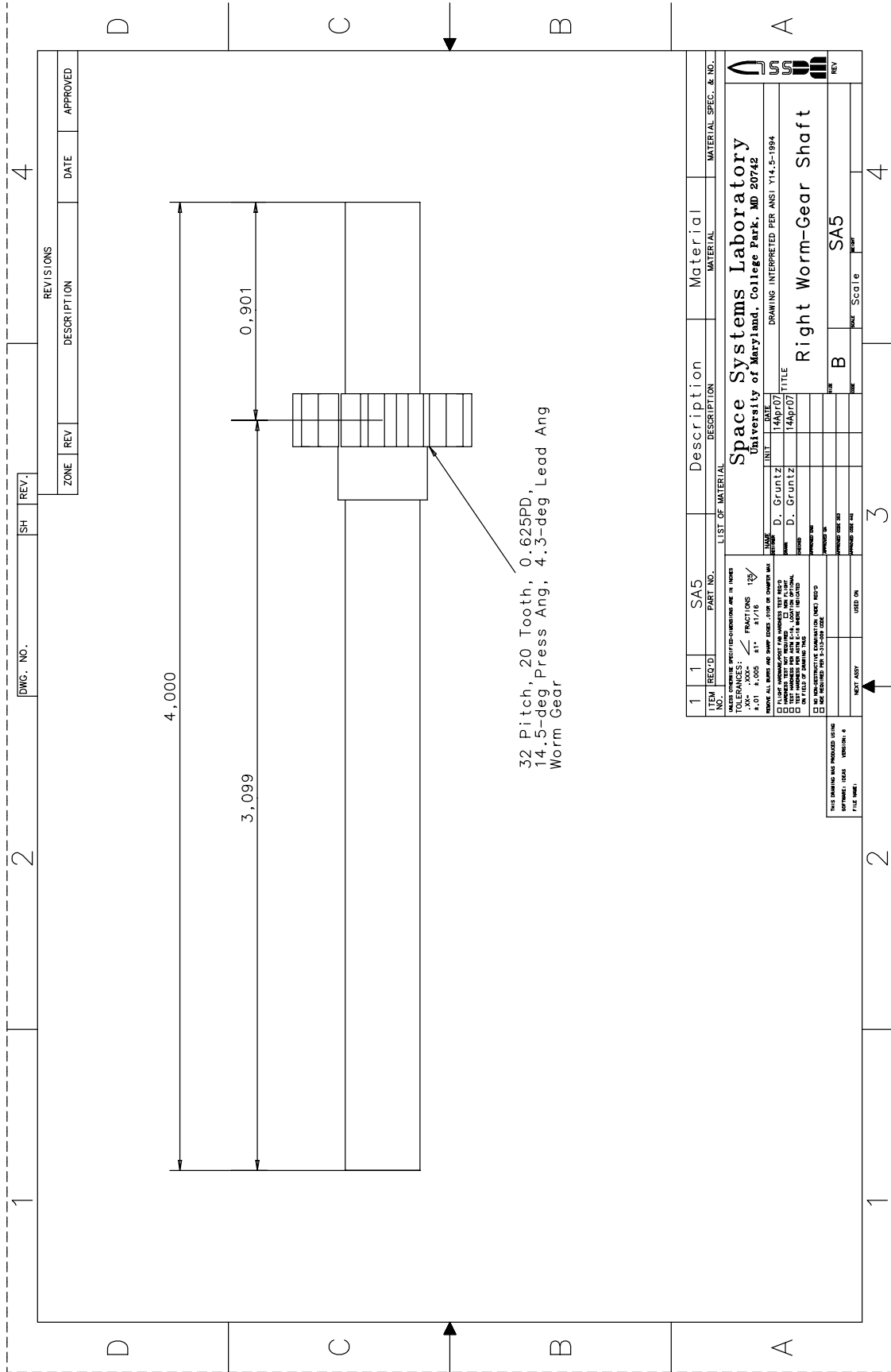


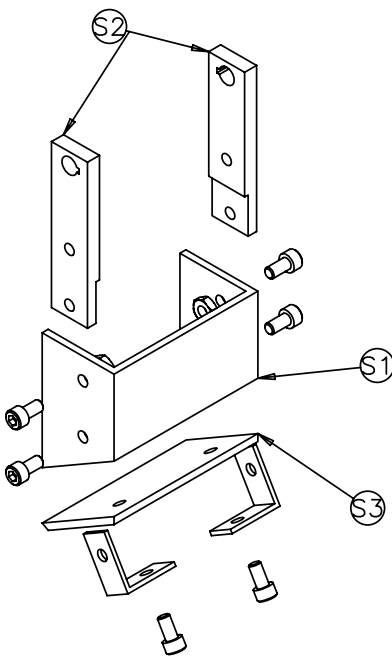
32 Pitch, 20 Tooth, 0.625PD,
 14.5-deg Press Ang, 4.3-deg Lead Ang
 Worm Gear

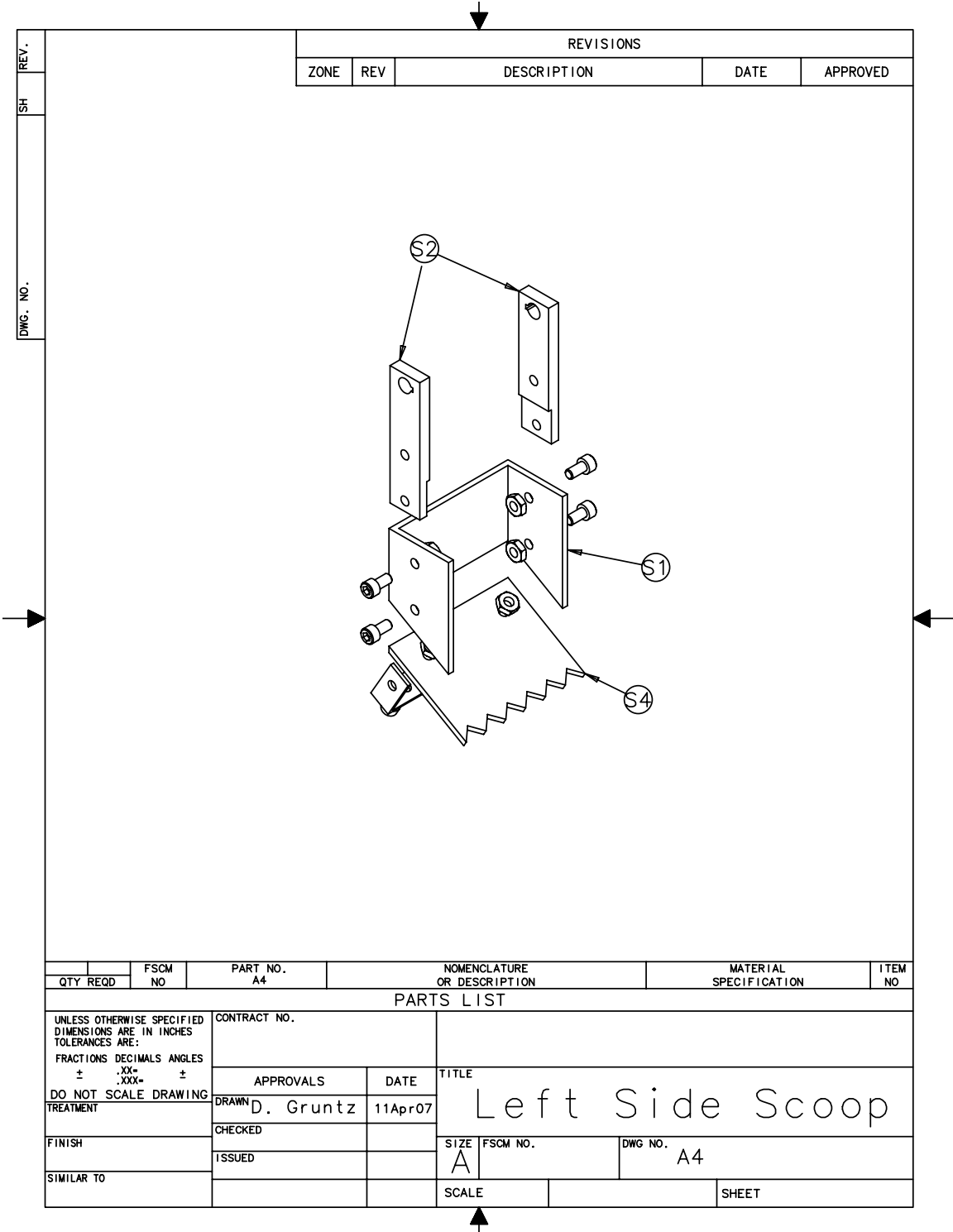
DWG. NO.		SH	REV.
2			4

REVISIONS		DATE	APPROVED
ZONE	REV	DESCRIPTION	

ITEM NO.	QUANTITY	DESCRIPTION	MATERIAL	MATERIAL SPEC. & NO.
1	1	SA4	Material	
<small>UNLESS OTHERWISE SPECIFIED DIMENSIONS ARE IN INCHES</small> <small>TOLERANCES: / FRACTIONS 1/8</small> <small>+ .01 ± .005 ±17 ±1/16</small> <small>REMOVE ALL BARRIERS AND SWAMP DICES - 10% OR CHEAPER MAX</small> <input type="checkbox"/> PLANT NUMBER/PART OR NUMBERED PART AIDS <input type="checkbox"/> TEST NUMBER AND DATE C-14, 1400 FOR OPTIONAL <input type="checkbox"/> ON FIELD OF DRAWING THIS <input type="checkbox"/> BY PRODUCTION (14.0000) (14.0000) (14.0000) (14.0000) <input type="checkbox"/> BY PRODUCTION (14.0000) (14.0000) (14.0000) (14.0000)				
Space Systems Laboratory University of Maryland, College Park, MD 20742 DRAWING INTERPRETED PER ANSI Y14.5-1994 D. Gruntz 14Apr07 D. Gruntz 14Apr07 Left Worm-Gear Shaft SA4 Scale 1:1				



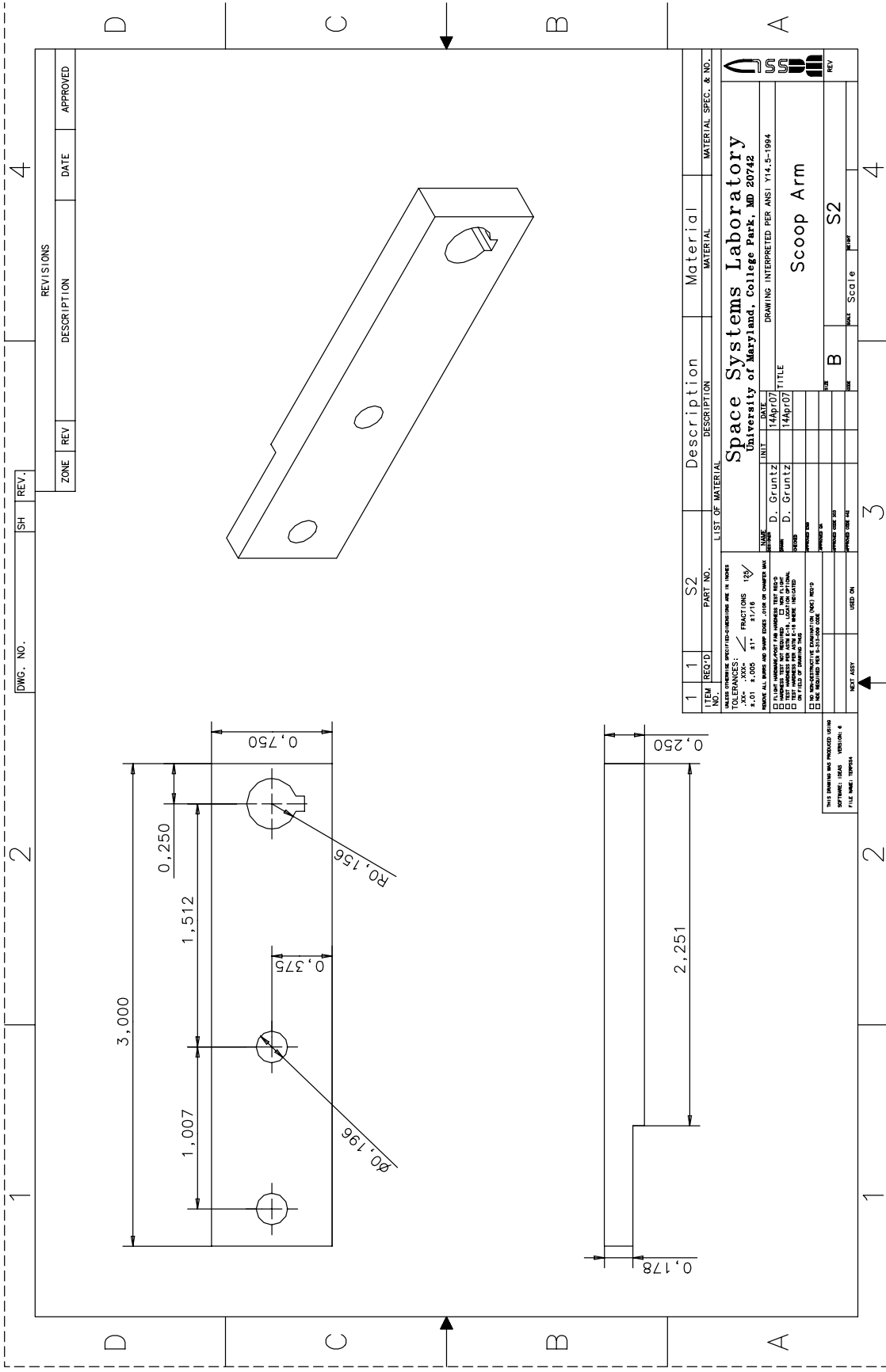
REV. SH DWG. NO.	REVISIONS				
	ZONE	REV	DESCRIPTION	DATE	APPROVED
					
	FSCM NO	PART NO. A3	NOMENCLATURE OR DESCRIPTION	MATERIAL SPECIFICATION	ITEM NO
PARTS LIST					
UNLESS OTHERWISE SPECIFIED DIMENSIONS ARE IN INCHES TOLERANCES ARE: FRACTIONS DECIMALS ANGLES ± .XX* ± ± .XXX* ± DO NOT SCALE DRAWING TREATMENT	CONTRACT NO.		TITLE		
	APPROVALS	DATE	Right Side Scoop		
FINISH	DRAWN D. Gruntz	11Apr07	SIZE A	FSCM NO.	DWG NO. A3
SIMILAR TO	CHECKED	ISSUED	SCALE	SHEET	



REVISIONS				
ZONE	REV	DESCRIPTION	DATE	APPROVED

REV. _____
SH _____
DWG. NO. _____

QTY REQD	FSCM NO	PART NO. A4	NOMENCLATURE OR DESCRIPTION	MATERIAL SPECIFICATION	ITEM NO	
PARTS LIST						
UNLESS OTHERWISE SPECIFIED DIMENSIONS ARE IN INCHES TOLERANCES ARE: FRACTIONS DECIMALS ANGLES ± .XX* ± .XXX- ± DO NOT SCALE DRAWING TREATMENT	CONTRACT NO.		TITLE Left Side Scoop			
	APPROVALS	DATE				
	DRAWN	D. Gruntz	11Apr07	SIZE	FSCM NO.	DWG NO.
	FINISH	CHECKED	ISSUED	A		A4
SIMILAR TO			SCALE		SHEET	



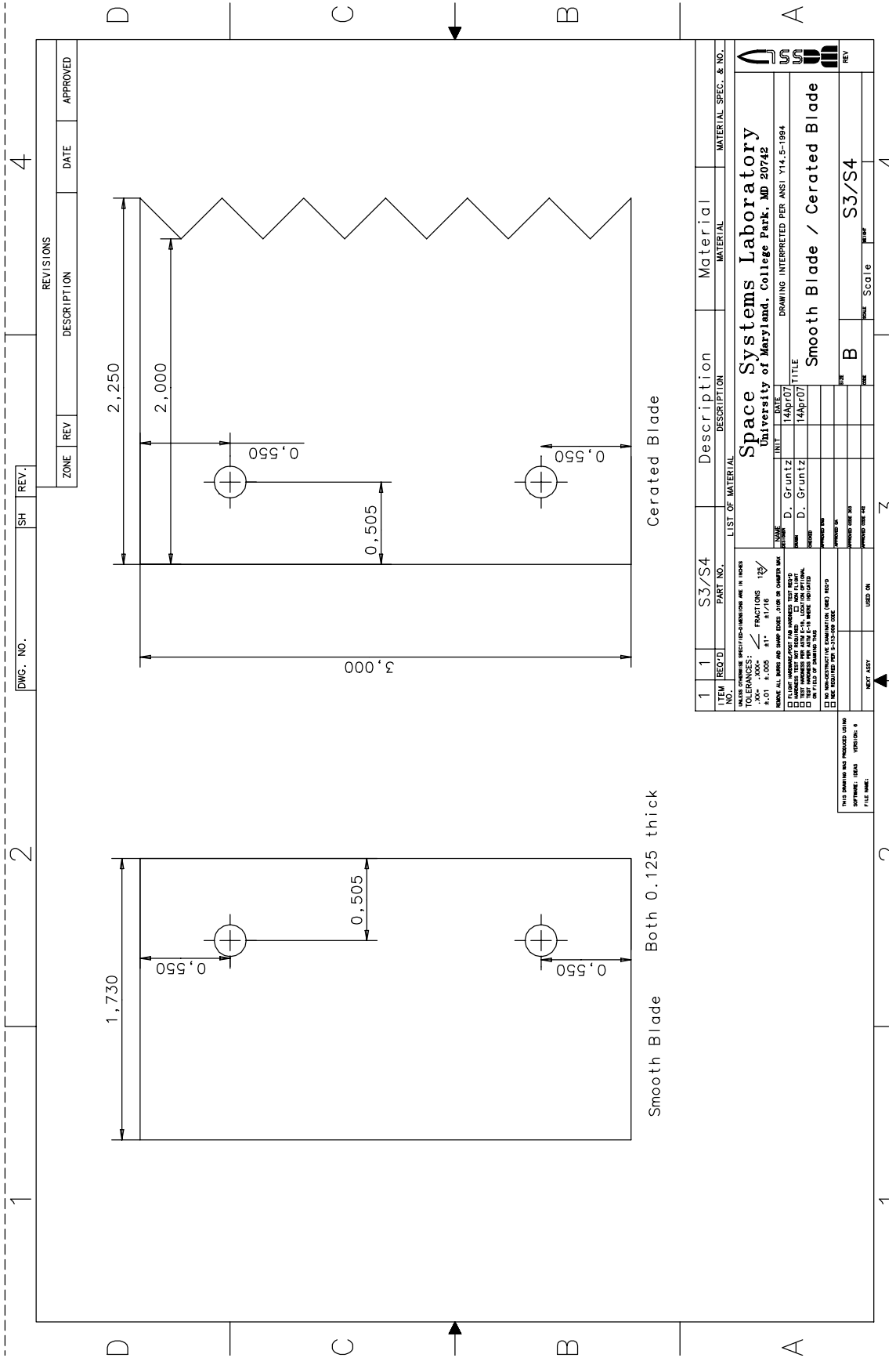
DWG. NO.		SH	REV.	REVISIONS		
ZONE	REV	DESCRIPTION	DATE	APPROVED		

ITEM NO.	REQ'D	S2	Part No.	Description	Material	MATERIAL SPEC. & NO.
1	1					

UNITS: DIMENSIONS ARE IN INCHES
 TOLERANCES: FRACTIONS 13/
 .XX+ .XX- 21/16
 +.01 +.005 - .01
 ALL DIMENSIONS UNLESS OTHERWISE SPECIFIED ARE TO BE HOLE OR MAX
 DIMENSIONS UNLESS OTHERWISE SPECIFIED
 DIMENSIONS TO CENTER UNLESS OTHERWISE SPECIFIED
 DIMENSIONS TO SURFACE UNLESS OTHERWISE SPECIFIED
 DIMENSIONS TO EDGE UNLESS OTHERWISE SPECIFIED
 DIMENSIONS TO CENTER UNLESS OTHERWISE SPECIFIED
 DIMENSIONS TO SURFACE UNLESS OTHERWISE SPECIFIED
 DIMENSIONS TO EDGE UNLESS OTHERWISE SPECIFIED
 DIMENSIONS TO CENTER UNLESS OTHERWISE SPECIFIED
 DIMENSIONS TO SURFACE UNLESS OTHERWISE SPECIFIED
 DIMENSIONS TO EDGE UNLESS OTHERWISE SPECIFIED

DATE	BY	CHKD	APP'D	TITLE
14Apr07	D. GRUNTZ			Scoop Arm
14Apr07	D. GRUNTZ			

DRAWING INTERPRETED PER ANSI Y14.5-1984
 SPACE SYSTEMS LABORATORY
 UNIVERSITY OF MARYLAND, COLLEGE PARK, MD 20742
 DRAWING NO. SC016
 REV. S2



ZONE	REV	DESCRIPTION	DATE	APPROVED

SH	REV.
	4

DWG. NO.

1	2

1	2

1	2

1	2

1	2

1	2

1	2

1	2

1	2

1	2

1	2

1	2

1	2

1	2

1	2

1	2

1	2

1	2

1	2

ITEM	REP'D	S3/S4	DESCRIPTION	Material	MATERIAL SPEC. & NO.
1					

LIST OF MATERIAL	DATE	TITLE
	14Apr07	Smooth Blade / Cerated Blade

NAME	DATE	TITLE
D. GRUNTZ	14Apr07	Smooth Blade / Cerated Blade

DESIGNER	CHECKED	DATE
D. GRUNTZ		

APPROVED BY	DATE

SCALE	UNIT
S3/S4	INCH

THIS DRAWING WAS PRODUCED USING	VERSION
PTC PROE	4

1	2

1	2

1	2

1	2

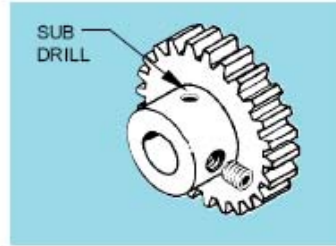
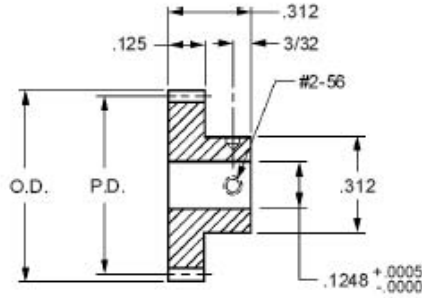
1	2

1	2

B.3 Gear Specifications



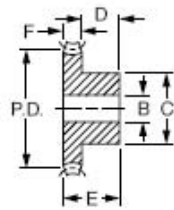
■ AGMA Q10 ■ 20° PRESSURE ANGLE ■ 1/8 FACE ■ 1/8 BORE



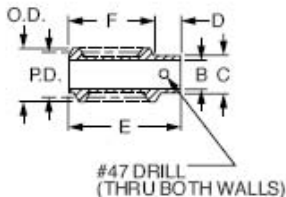
Catalog Number		No. of Teeth	P.D.	O.D.
303 Stainless Steel	2024 Aluminum * Anodized			
S1063Z-048S014	S1063Z-048A014	14	0.2917	0.333
S1063Z-048S018	S1063Z-048A018	18	0.3750	0.417
S1063Z-048S020	S1063Z-048A020	20	0.4167	0.458
S1063Z-048S022	S1063Z-048A022	22	0.4583	0.500
S1063Z-048S024	S1063Z-048A024	24	0.5000	0.542
S1063Z-048S028	S1063Z-048A028	28	0.5833	0.625
S1063Z-048S030	S1063Z-048A030	30	0.6250	0.667
S1063Z-048S032	S1063Z-048A032	32	0.6667	0.708
S1063Z-048S034	S1063Z-048A034	34	0.7083	0.750
S1063Z-048S036	S1063Z-048A036	36	0.7500	0.792
S1063Z-048S038	S1063Z-048A038	38	0.7917	0.833
S1063Z-048S040	S1063Z-048A040	40	0.8333	0.875
S1063Z-048S042	S1063Z-048A042	42	0.8750	0.917
S1063Z-048S046	S1063Z-048A046	46	0.9583	1.000
S1063Z-048S048	S1063Z-048A048	48	1.0000	1.042
S1063Z-048S050	S1063Z-048A050	50	1.0417	1.083
S1063Z-048S056	S1063Z-048A056	56	1.1667	1.208
S1063Z-048S060	S1063Z-048A060	60	1.2500	1.292
S1063Z-048S064	S1063Z-048A064	64	1.3333	1.375
S1063Z-048S065	S1063Z-048A065	65	1.3542	1.396
S1063Z-048S070	S1063Z-048A070	70	1.4583	1.500
S1063Z-048S072	S1063Z-048A072	72	1.5000	1.542
S1063Z-048S080	S1063Z-048A080	80	1.6667	1.708
S1063Z-048S084	S1063Z-048A084	84	1.7500	1.792
S1063Z-048S085	S1063Z-048A085	85	1.7708	1.813
S1063Z-048S090	S1063Z-048A090	90	1.8750	1.917
S1063Z-048S096	S1063Z-048A096	96	2.0000	2.042
S1063Z-048S100	S1063Z-048A100	100	2.0833	2.125
S1063Z-048S102	S1063Z-048A102	102	2.1250	2.167
S1063Z-048S105	S1063Z-048A105	105	2.1875	2.229

* T4 or T351 Aluminum Alloy, anodized before cutting.
Available on special order: 14-1/2° P.A., teeth not listed, different bore size and/or material, passivation for stainless steel.

■ 14-1/2° PRESSURE ANGLE ■ RIGHT-HAND ■ SINGLE THREAD



WORM GEAR



WORM



MATERIAL: Bronze

WORM GEARS							
Catalog Number	No. of Teeth	P.D.	B Bore	F Face Width	E Length	C Hub Dia.	D Hub Proj.
A 1B 6-N32020	20	.625		3/16	7/16		
A 1B 6-N32020A	20	.625		7/32	15/32	1/2	
A 1B 6-N32024	24	.750		3/16	7/16		1/4
A 1B 6-N32030	30	.938	3/16	3/16	7/16	5/8	
A 1B 6-N32030A	30	.938		7/32	15/32	5/8	
A 1B 6-N32036	36	1.125		3/16	7/16	1/2	
A 1B 6-N32040	40	1.250		3/16	1/2		5/16
A 1B 6-N32040A	40	1.250		7/32	15/32	5/8	1/4
A 1B 6-N32050	50	1.562		3/16	1/2		5/16
A 1B 6-N32050A	50	1.562	1/4	7/32	17/32	5/8	
A 1B 6-N32060	60	1.875		3/16	1/2	11/16	5/16
A 1B 6-N32060A	60	1.875		7/32	17/32	11/16	
A 1B 6-N32072	72	2.250		3/16	1/2	5/8	
A 1B 6-N32080	80	2.500		3/16	1/2	11/16	5/16
A 1B 6-N32080A	80	2.500		7/32	17/32	11/16	
A 1B 6-N32096	96	3.000		3/16	1/2		
A 1B 6-N32096A	96	3.000	5/16	7/32	17/32	11/16	5/16
A 1B 6-N32100	100	3.125		3/16	1/2		
A 1B 6-N32100A	100	3.125		7/32	17/32	3/4	5/16
A 1B 6-N32120	120	3.750		3/16	1/2		

MATERIAL: Steel

LEAD: .0982
LEAD ANGLE: 4° 5'

WORMS								
Catalog Number	P.D.	O.D.	B Bore	F Face Width	E Length	C Hub Dia.	D Hub Proj.	Finish
A 1C 5-N32				11/16	7/8			
A 1C55-N32	.438	.500	3/16	1/2	11/16	.320	3/16	Soft
A 1C55-5N32				1/2	1/2	Hubless		
A 1C55-55N32			1/4	1/2	11/16	.350	3/16	
ΔA 1Q55-N32				7/32	11/16	7/8	.320	Hardened & Polished
A 1Q55-5N32	.438	.500	1/4	11/16	7/8	.340	3/16	Hardened & Ground
A 1Q55-55N32			1/4	1/2	11/16	.340		Hardened & Polished

*This worm has no cross-drilled holes.

ΔTo be discontinued when present stock is depleted.

For engineering assistance for all SDP components, call on our applications engineers.

B.4 Motor Specifications

Scoop Motor

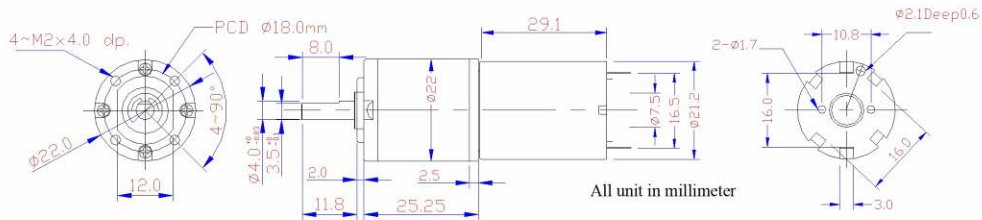


Hennkwell Ind. Co., Ltd.

Issued Date: February. 05, 2005

Model : PK22G2150-104(12VDC,144rpm) Micro DC Planetary Gear Motor

(A). Dimensional Figures:



(B). Gearbox Specifications :

Reduction Ratio	Rated Tolerance Torque	Max. momentary tolerance Torque	Efficiency	Radial play of shaft	Thrust play of shaft
1/104	2.5 kgf-cm Max.	7.5 kgf-cm	55%	Ø05mm	Ø2mm

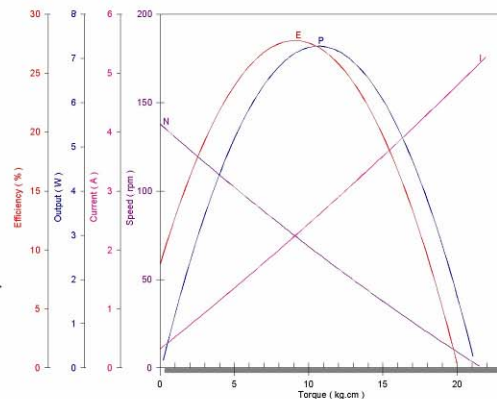
(C). Electrical Specifications :

Model	Voltage		No-Load		AT Maximum Efficiency					Stall Torque
	Operating Range	Nominal	Speed	Current	Speed	Current	Torque	Output	Eff	
			r.p.m.	mA	r.p.m.	mA	Kg-cm	Watt	%	
PK22G2150-104	6V~18V	12V CONSTANT	144	200	124	880	2.0	3.2	34	10.2

(E). Characteristic Curves:

(D). Mechanical Specifications:

Reduction Ratio : 1: 104
 Rated tolerance torque: Max. 2.5 kg-cm
 Max. momentary to tolerance torque : 7.5 kg-cm
 Radial play of shaft : 0.05mm
 Thrust play of shaft : 0.2mm
 Operating temperature Range : -10 to + 60
 Expectant life: approx.400 hours on normal operation.
 Weight: Approx. 140 grams.
 The specifications are subject to change without notice.
 The graphs are shown for reference only.



HENNKWELL IND. CO., LTD.

Dynamic Test Report

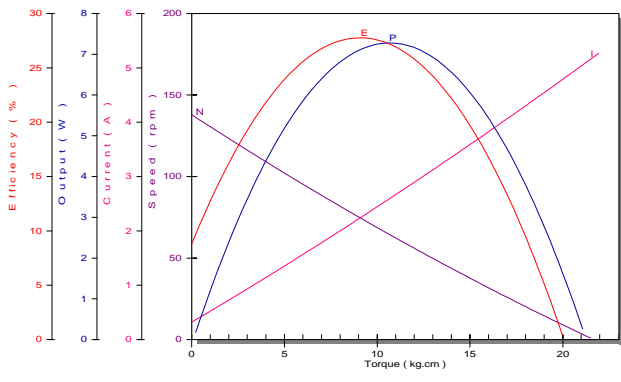
Product: DC Gear Motor
 Customer: PK22-950324-0-10
 Mode NO.: PK22G2150-104
 Test Date: 2006/3/24

Rated Voltage: 12 VDC
 No Load Speed: 144 RPM
 No Load Current: 0.246 A
 Gear Ratio: 1:104

(A) Dimensional Figures:



(B) MOTOR PERFORMANCE CURVES AND CHARACTERISTICS:



Supply Voltage = 12 VDC

AT NO LOAD
 SPEED = 137.9 RPM
 CURRENT = 0.32 AMP

AT STALL EXTRAPOLATION
 TORQUE = 21.72 kg-cm
 CURRENT = 5.21 AMP

AT MAXIMUM EFFICIENCY
 EFFICIENCY = 27.76 %
 SPEED = 74.4 RPM
 TORQUE = 9.12 kg-cm
 CURRENT = 2.25 AMP
 OUTPUT = 7.12 WATTS

AT MAXIMUM OUTPUT
 SPEED = 64.6 RPM
 TORQUE = 10.64 kg-cm
 CURRENT = 2.59 AMP
 OUTPUT = 7.28 WATTS
 EFFICIENCY = 27.20 %

Torque Conversions:
 1.0 kgf-cm = 0.098 Nm = 98 mNm
 = 13.887 oz-in = 0.867 lb-in

PREPARED BY: _____ APPROVED BY: _____

HENNKWELL IND. CO., LTD.

Dynamic Test Report

Product: DC Gear Motor
 Customer: PK22-950324-0-10
 Mode NO.: PK22G2150-104
 Test Date: 2006/3/24 PM 04:44:59

Rated Voltage: 12 VDC
 No Load Speed: 140 RPM
 No Load Current: 0.246 A
 Gear Ratio: 1:104

	Voltage (V)	Current (A)	Input (W)	Torque (kg-cm)	Speed (RPM)	Output (W)	Efficiency (%)
1	12	0.265	3.18	0.01	141.3	0.014	0.44
2	11.98	0.913	10.94	2.58	116.2	3.076	28.12
3	11.95	1.66	19.84	6.28	91.3	5.883	29.65
4	11.94	1.965	23.46	7.92	81.2	6.598	28.12
5	11.92	2.702	32.21	11.1	61.3	6.981	21.67
6	11.89	3.579	42.55	15.25	40.5	6.337	14.89
7	11.86	4.436	52.61	18.54	20.6	3.919	7.449
8	11.85	4.95	58.66	20.54	1.5	0.316	0.539

Drill Motor



LS-550PX/555PX

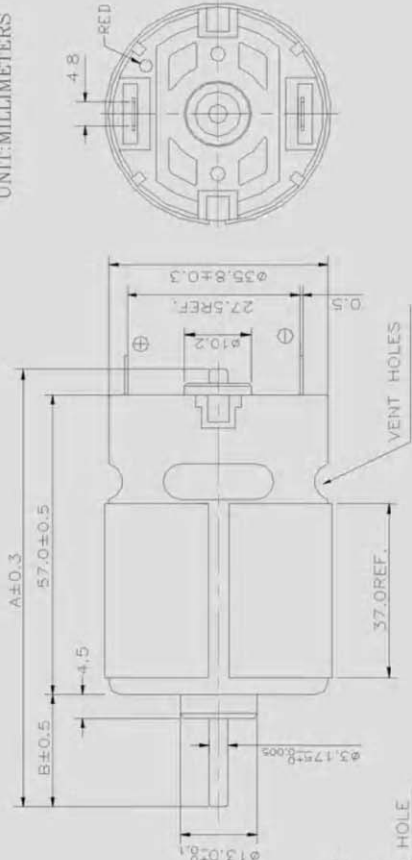


MODEL	VOLTAGE		NO LOAD		AT MAXIMUM EFFICIENCY				STALL			
	OPERATING RANGE	NOMINAL	SPEED RPM	CURRENT A	SPEED RPM	CURRENT A	TORQUE g.cm	TORQUE mNm	OUTPUT W	TORQUE g.cm	CURRENT A	
LS-550PX-60659	4.0-9.6	7.20V	14500	1.50	12570	9.77	380.0	37.24	48.99	2855	279.8	63.6
LS-550PX-60728	6.0-12.0	9.6V	16800	1.60	14266	9.78	450.0	44.10	65.84	3200	313.6	59.8
LS-550PX-62814	6.0-12.0	12.0V	24000	2.00	20886	13.40	545.0	53.41	116.75	4200	411.6	89.9
LS-550PX-60923	12.0-14.4	14.4V	22500	1.55	19753	11.13	586.0	57.43	118.72	4600	470.4	80.0
LS-555PX-60901	10.0-24.0	12.0V	3300	0.18	2730	0.86	226.0	22.34	6.38	1320	129.4	4.1
LS-555PX-61170	12.0-20.0	18.0V	21000	1.30	18221	8.25	602.0	59.00	112.50	4549	445.8	55.9

DIRECTION OF ROTATION



UNIT: MILLIMETERS



Appendix C

Bearing Calculations

Section 4.5.3 briefly discussed the loading conditions on the bearings in the transmission. These loads were calculated based on the torque applied by the motor using a static force and moment balance. The loads and dimensions are illustrated on the next page.

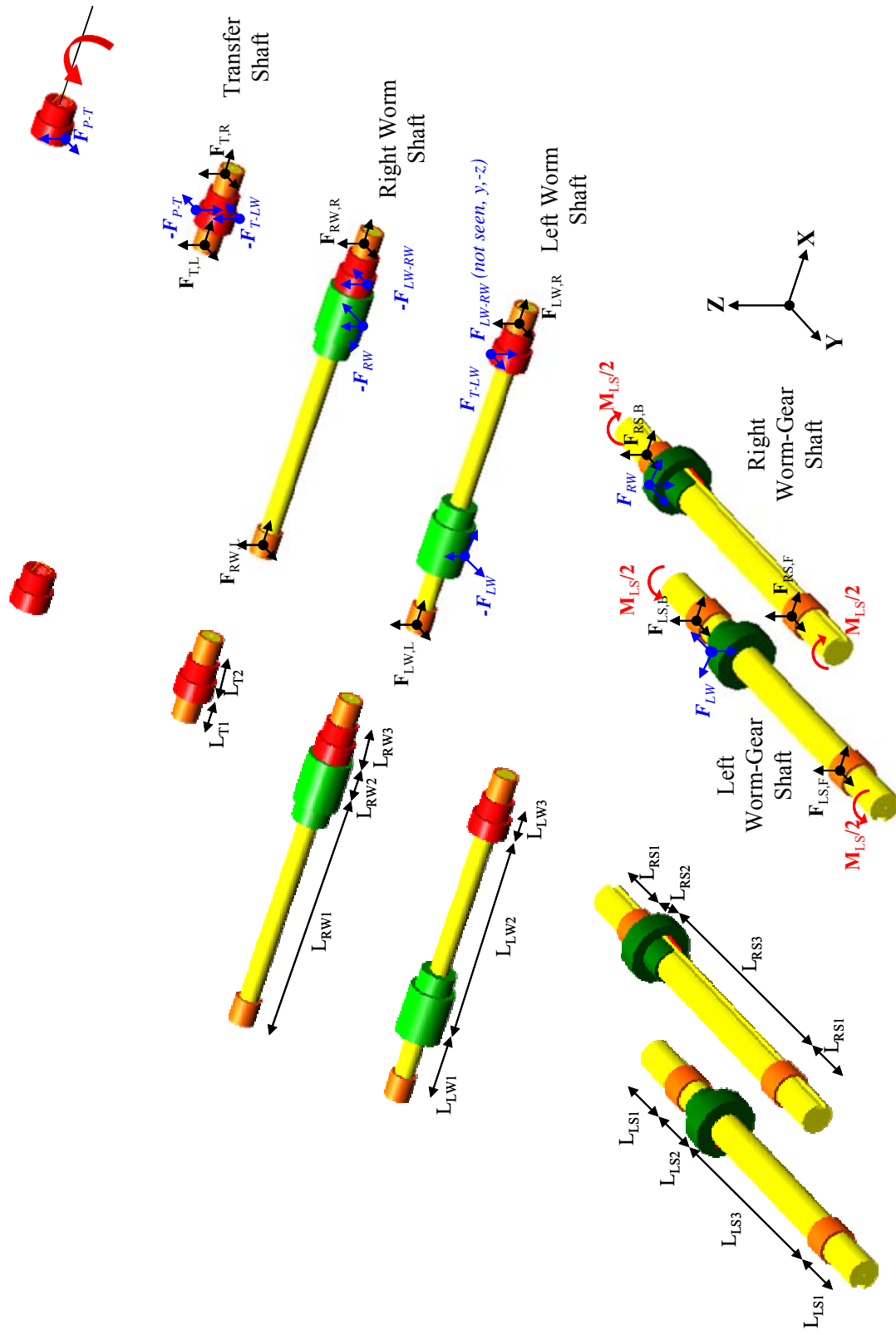
Forces on Gears

Gears transmit torque through their teeth, which are shaped to allow meshing, so the forces do not act completely tangentially, there is also a small radial force. In spur gears, this is based on the pressure angle (ϕ_g), which is based on the geometry of the teeth as well as on the pitch radius of the gear (PR). The force components are given by:

$$F_{\text{tangential}} = \left(\frac{T}{\text{PR}} \right) \cos(\phi_g)$$
$$F_{\text{radial}} = \left(\frac{T}{\text{PR}} \right) \sin(\phi_g)$$

Worm gears change the direction rotation vector by 90° . As a result, the forces transmitted by the teeth are in three dimensions. This is based on both the pressure angle as well as the lead angle (λ) of the worm. The force at the worm/gear mesh and the relationship to shaft torque are given by [48]:

$$\bar{F} = \begin{bmatrix} F_{\text{axial, worm/tangential, gear}} \\ F_{\text{axial, gear/tangential, worm}} \\ F_{\text{radial}} \end{bmatrix} = F \begin{bmatrix} \cos(\phi_g) \cos(\lambda) \\ \cos(\phi_g) \sin(\lambda) \\ \sin(\phi) \end{bmatrix} = \begin{bmatrix} T_{\text{gearshaft}} / \text{PR}_{\text{gear}} \\ T_{\text{wormshaft}} / \text{PR}_{\text{worm}} \end{bmatrix}$$



Transfer Shaft

The summation of forces and moments is given below. Refer to the figure for notation. PD refers to the pitch diameter of the gear.

$$\Sigma F_x = 0 = F_{TR,x} + F_{TL,x}$$

$$\Sigma F_y = 0 = F_{TR,y} + F_{TL,y} - F_{P-T,y} - F_{T-LW,y}$$

$$\Sigma F_z = 0 = F_{TR,z} + F_{TL,z} - F_{P-T,z} + F_{T-LW,z}$$

$$\Sigma M_{x,TR} = 0 = -F_{P-T,y} \left(\frac{PD_{spur}}{2} \right) + F_{T-LW,y} \left(\frac{PD_{spurs}}{2} \right)$$

$$\Sigma M_{y,TR} = 0 = -F_{P-T,z} (L_{T2}) + F_{T-LW,y} (L_{T2}) - F_{TL,z} (L_{T1} + L_{T2})$$

$$\Sigma M_{z,TR} = 0 = -F_{P-T,y} (L_{T2}) + F_{T-LW,y} (L_{T2}) + F_{TL,y} (L_{T1} + L_{T2})$$

F_{P-T} is found using the gear equations above with θ being the angle between the line connecting the pinion and transfer gear centers and vertical. Solving the above equation yields:

$$\bar{F}_{P-T} = \bar{F}_{T-L} = \left(\frac{2T_{motor}}{PD_{pinion}} \right) \begin{bmatrix} 0 \\ \cos(\theta - \phi) \\ \sin(\theta - \phi) \end{bmatrix}$$

$$F_{TL,z} = (F_{P-T,z} - F_{L-W,z}) \left(\frac{L_{T2}}{L_{T1} + L_{T2}} \right)$$

$$F_{TR,z} = F_{TL,z} + F_{PT,z} - F_{T-LW,z}$$

$$F_{TL,y} = (F_{P-T,y} - F_{L-W,y}) \left(\frac{L_{T2}}{L_{T1} + L_{T2}} \right)$$

$$F_{TR,y} = F_{TL,y} + F_{PT,y} - F_{T-LW,y}$$

$$F_{TR,x} = F_{TL,x} = 0 \quad (\text{no applied axial load})$$

Left Worm Shaft

$$\Sigma F_x = 0 = F_{LWR,x} + F_{LWL,x} + F_{LW,x}$$

$$\Sigma F_y = 0 = F_{LWR,y} + F_{LWL,y} + F_{LW,y} + F_{T-LW,y} + F_{LW-RW,y}$$

$$\Sigma F_z = 0 = F_{LWR,z} + F_{LWL,z} + F_{LW,z} - F_{T-LW,z} - F_{LW-RW,z}$$

$$\Sigma M_{x,\text{right bearing}} = 0 = -F_{LW,y} \left(\frac{PD_{\text{worm}}}{2} \right) + F_{T-LW,y} \left(\frac{PD_{\text{spur}}}{2} \right) - F_{LW-RW,z} \left(\frac{PD_{\text{spur}}}{2} \right)$$

$$\Sigma M_{y,\text{right bearing}} = 0 = F_{T-LW,z} (L_{LW3}) + F_{LW-RW,z} (L_{LW3}) - F_{LW,z} (L_{LW2} + L_{LW3}) + F_{LW,x} \left(\frac{PD_{\text{worm}}}{2} \right) - F_{LWL,z} (L_{LW1} + L_{LW2} + L_{LW3})$$

$$\Sigma M_{z,\text{right bearing}} = 0 = F_{T-LW,y} (L_{LW3}) + F_{LW-RW,y} (L_{LW3}) - F_{LW,y} (L_{LW2} + L_{LW3}) + F_{LWL,y} (L_{LW1} + L_{LW2} + L_{LW3})$$

Assuming the torque applied from the transfer gear is split equally between the two worm shafts:

$$F_{LW-RW,z} \left(\frac{PD_{\text{spur}}}{2} \right) = F_{LW,y} \left(\frac{PD_{\text{spur}}}{2} \right) = \frac{1}{2} F_{T-LW,y} \left(\frac{PD_{\text{spur}}}{2} \right)$$

From the gear equations:

$$F_{LW-RW,y} = F_{LW-RW,z} \tan(\varphi_{\text{spur}})$$

$$F_{LW,y} = F_{LW-RW,z} \left(\frac{PD_{\text{spur}}}{PD_{\text{worm}}} \right)$$

$$F_{LW,x} = F_{LW,y} \cot(\lambda)$$

$$F_{LW,z} = F_{LW,y} \tan(\varphi_{\text{worm}}) \csc(\lambda)$$

So at the bearings:

$$F_{LWL,z} = [L_{LW3} (F_{T-LW,z} + F_{LW-RW,z}) - F_{LW,z} (L_{LW2} + L_{LW3})] / (L_{LW1} + L_{LW2} + L_{LW3})$$

$$F_{LWR,z} = F_{T-LW,z} + F_{LW-RW,z} - F_{LW,z} - F_{LWL,z}$$

$$F_{LWL,y} = -[L_{LW3} (F_{T-LW,y} + F_{LW-RW,y}) - F_{LW,y} (L_{LW2} + L_{LW3})] / (L_{LW1} + L_{LW2} + L_{LW3})$$

$$F_{LWR,y} = -(F_{T-LW,y} + F_{LW-RW,y} + F_{LW,y} + F_{LWL,y})$$

$$F_{LWR,x} = F_{LWL,x} = \frac{1}{2} F_{LW,x}$$

Right Worm Shaft

$$\Sigma F_x = 0 = F_{RWR,x} + F_{RWL,x} - F_{RW,x}$$

$$\Sigma F_y = 0 = F_{RWR,y} + F_{RWL,y} - F_{RW,y} - F_{LW-RW,y}$$

$$\Sigma F_z = 0 = F_{RWR,z} + F_{RWL,z} + F_{RW,z} + F_{LW-RW,z}$$

$$\Sigma M_{x,\text{right bearing}} = 0 = F_{RW,y} \left(\frac{PD_{\text{worm}}}{2} \right) - F_{LW-RW,z} \left(\frac{PD_{\text{spur}}}{2} \right)$$

$$\Sigma M_{y,\text{right bearing}} = 0 = -F_{LW-RW,z} (L_{RW3}) - F_{RW,z} (L_{RW2} + L_{RW3}) - F_{RW,x} \left(\frac{PD_{\text{worm}}}{2} \right) - F_{RWL,z} (L_{RW1} + L_{RW2} + L_{RW3})$$

$$\Sigma M_{z,\text{right bearing}} = 0 = -F_{LW-RW,y} (L_{RW3}) - F_{RW,y} (L_{RW2} + L_{RW3}) + F_{RWL,y} (L_{RW1} + L_{RW2} + L_{RW3})$$

As before:

$$F_{RW,y} = F_{LW-RW,z} \left(\frac{PD_{\text{spur}}}{PD_{\text{worm}}} \right)$$

$$F_{RW,x} = F_{RW,y} \cot(\lambda), \quad F_{RW,z} = F_{RW,y} \tan(\phi_{\text{worm}}) \csc(\lambda)$$

$$F_{RWL,z} = -[F_{LW-RW,z} (L_{RW3}) + F_{RW,z} (L_{RW2} + L_{RW3})] / (L_{RW1} + L_{RW2} + L_{RW3})$$

$$F_{RWR,z} = -F_{LW-RW,z} - F_{RW,z} - F_{RWL,z}$$

$$F_{RWL,y} = [F_{LW-RW,y} (L_{RW3}) + F_{RW,y} (L_{RW2} + L_{RW3})] / (L_{RW1} + L_{RW2} + L_{RW3})$$

$$F_{RWR,y} = F_{LW-RW,y} + F_{RW,y} - F_{RWL,y}$$

$$F_{RWR,x} = F_{RWL,x} = \frac{1}{2} F_{RW,x}$$

Left Scoop Shaft

$$\Sigma F_x = 0 = F_{LSB,x} + F_{LSF,x} - F_{LW,x}$$

$$\Sigma F_y = 0 = F_{LSB,y} + F_{LSF,y} - F_{LW,y}$$

$$\Sigma F_z = 0 = F_{LSB,z} + F_{LSF,z} - F_{LW,z}$$

$$\Sigma M_{x,B} = 0 = -F_{LW,z} (L_{LS2}) + F_{LW,y} \left(\frac{PD_{\text{gear}}}{2} \right) - F_{LSF,z} (L_{LS2} + L_{LS3})$$

$$\Sigma M_{z,B} = 0 = 2 \frac{M_{LS}}{2} + F_{LW,x} \left(\frac{PD_{\text{gear}}}{2} \right)$$

$$\Sigma M_{z,B} = 0 = -F_{LW,x} (L_{LS2}) + F_{LSF,x} (L_{LS2} + L_{LS3})$$

$$\begin{aligned}
M_{LS} &= F_{LW,x} (PD_{gear}) \\
F_{LSF,x} &= F_{LW,y} \left(\frac{L_{LS2}}{L_{LS2} + L_{LS3}} \right) \\
F_{LSB,x} &= -(F_{LSF,x} - F_{LW,x}) \\
F_{LSF,z} &= \frac{F_{LW,y} \left(\frac{PD_{gear}}{2} \right) - F_{LW,z} (L_{LS2})}{L_{LS2} + L_{LS3}} \\
F_{LSB,z} &= F_{LW,z} - F_{LSF,z}
\end{aligned}$$

Right Scoop Shaft

$$\begin{aligned}
\Sigma F_x = 0 &= F_{RSB,x} + F_{RSF,x} + F_{RW,x} \\
\Sigma F_y = 0 &= F_{RSB,y} + F_{RSF,y} + F_{RW,y} \\
\Sigma F_z = 0 &= F_{RSB,z} + F_{RSF,z} - F_{RW,z} \\
\Sigma M_{x,B} = 0 &= F_{RW,z} (L_{RS2}) + F_{RW,y} \left(\frac{PD_{gear}}{2} \right) - F_{RSF,z} (L_{RS2} + L_{RS3}) \\
\Sigma M_{z,B} = 0 &= -2 \frac{M_{RS}}{2} - F_{RW,x} \left(\frac{PD_{gear}}{2} \right) \\
\Sigma M_{z,B} = 0 &= F_{RW,x} (L_{RS2}) + F_{RSF,x} (L_{RS2} + L_{RS3}) \\
M_{RS} &= F_{RW,x} (PD_{gear}) \\
F_{RSF,x} &= -F_{RW,y} \left(\frac{L_{RS2}}{L_{RS2} + L_{RS3}} \right) \\
F_{RSB,x} &= -(F_{RSF,x} + F_{RW,x}) \\
F_{RSF,z} &= \frac{F_{RW,z} (L_{RS2}) + F_{RW,y} \left(\frac{PD_{gear}}{2} \right)}{L_{RS2} + L_{RS3}} \\
F_{RSB,z} &= F_{RW,z} - F_{RSF,z}
\end{aligned}$$

Appendix D

McKyes/Ali Soil Model

D.1 Soil Model

The model used to predict the forces on the TERPS scoops is based heavily on the soil model proposed by McKyes and Ali in [44]. The model they present is intended to find the horizontal force on a blade moving linearly parallel to the surface with a constant depth and rake angle. Their derivation is shown here.

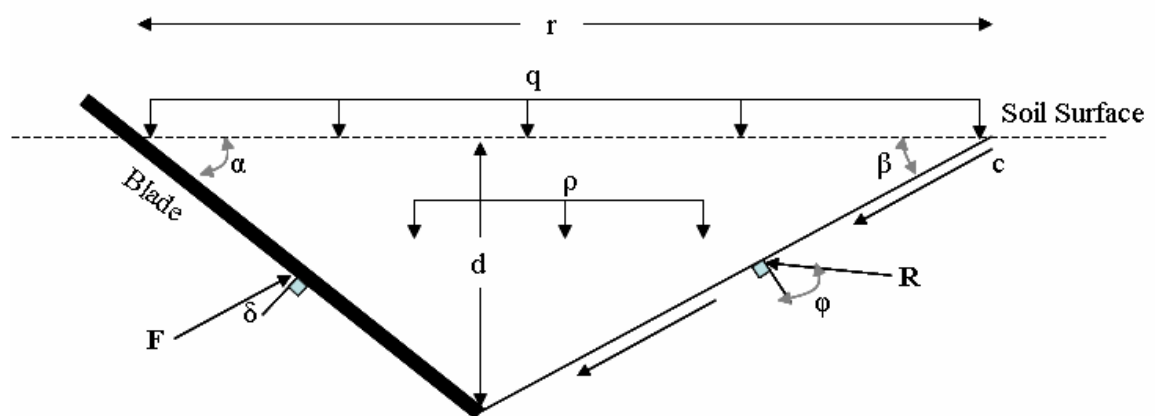


Figure 6-2: Side View of McKyes/Ali Soil Failure Region

Horizontal and Vertical Forces in front of blade:

$$F_1 \sin(\alpha + \delta) - R_1 \sin(\beta + \varphi) = \frac{c w d \cos(\beta)}{\sin(\beta)}$$

$$F_1 \cos(\alpha + \delta) + R_1 \cos(\beta + \varphi) = \frac{\rho d r w}{2} + \frac{c w d \sin(\beta)}{\sin(\beta)} + q r w$$

Eliminating R_1 and solving for F_1

$$F_1 = \frac{\left(\rho d^2 \frac{r}{2d} + c d [1 + \cot(\beta) \cot(\beta + \varphi)] + q d \frac{r}{d} \right) w}{\cos(\alpha + \delta) + \sin(\alpha + \delta) \cot(\beta + \varphi)} \quad (6-3)$$

Horizontal component:

$$H_1 = F_1 \sin(\alpha + \delta) = \frac{\left(\rho d^2 \frac{r}{2d} + c d [1 + \cot(\beta) \cot(\beta + \varphi)] + q d \frac{r}{d} \right) w}{\cot(\alpha + \delta) + \cot(\beta + \varphi)}$$

Horizontal and Vertical Forces next to blade:

$$dF_1 \sin(\alpha + \delta) - dR_2 \sin(\beta + \varphi) = \frac{cr d dv \cos(\beta)}{2 \sin(\beta)}$$

$$dF_1 \cos(\alpha + \delta) + dR_2 \cos(\beta + \varphi) = \frac{1}{6} \rho dr^2 dv + \frac{cr d dv \sin(\beta)}{2 \sin(\beta)} + \frac{1}{2} dr^2 dv$$

$$dF_2 = \frac{\left(\frac{1}{6} \rho dr^2 + \frac{1}{2} cr d [1 + \cot(\beta) \cot(\beta + \varphi)] + \frac{1}{2} qr^2 \right) d\rho}{\cos(\alpha + \delta) + \sin(\alpha + \delta) \cot(\beta + \varphi)}$$

Taking the horizontal component and integrating:

$$dH_2 = dP_2 \sin(\alpha + \delta) \cos(dv)$$

$$H_2 = \int_0^v dP_2 \sin(\alpha + \delta) \cos(dv)$$

$$H_2 = \frac{\left(\frac{1}{6} \rho dr^2 + \frac{1}{2} cr d [1 + \cot(\beta) \cot(\beta + \varphi)] + \frac{1}{2} qr^2 \right) \sin(v)}{\cot(\alpha + \delta) + \cot(\beta + \varphi)}$$

Summing the two Sections:

$$F_H = H_1 + 2H_2$$

$$F_H = \frac{\left(\rho d^2 \frac{rw}{2d} \left[1 + \frac{2rd}{3dw} \sin(v) \right] + cdw [1 + \cot(\beta) \cot(\beta + \varphi)] \left[1 + \frac{rd}{dw} \sin(v) \right] + qwd \left[1 + \frac{rd}{dw} \sin(v) \right] \right)}{\cot(\alpha + \delta) + \cot(\beta + \varphi)}$$

This is in the same form as the fundamental earth moving equation:

$$F = \left(\rho d^2 N_p + c d N_c + q d N_q \right) w \quad (6-2)$$

The blade force, F is found as before. With R1 being found with equation 6-2 evaluated

for $\alpha = 90^\circ - \varphi$, $\delta = \varphi$, $d' = d$:

$$R_1 = \left[\rho d'^2 N_p^* + cd' N_c^* + qd' N_q^* \right] w$$

$$N_p^* = \frac{\frac{r}{2d'} \left[1 + \frac{2rd'}{3d'w} \sin(v) \right]}{\cot((90^\circ - \varphi) + (\varphi)) + \cot(\beta + \varphi)}$$

$$N_c^* = \frac{[1 + \cot(\beta)\cot(\beta + \varphi)] \left[1 + \frac{rd'}{d'w} \sin(v) \right]}{\cot((90^\circ - \varphi) + (\varphi)) + \cot(\beta + \varphi)}$$

$$N_q^* = \frac{\left[1 + \frac{rd'}{d'w} \sin(v) \right]}{\cot((90^\circ - \varphi) + (\varphi)) + \cot(\beta + \varphi)}$$

The N-terms for equation 6-2 can be found to be:

$$N_p = \frac{\frac{d'}{2d} \left(\tan(\varphi) - \cot(\alpha) + \frac{2d'}{d} N_p^* \cot(\theta + \varphi) \right)}{\cot(\alpha + \delta) + \cot(\theta + \varphi)}$$

$$N_c = \frac{1 - \frac{2d'}{d} - \left[\frac{2d'}{d} \tan(\varphi) - \cot(\alpha) \right] \cot(\theta + \varphi) + \frac{d'}{d} N_c^* \cot(\theta + \varphi)}{\cot(\alpha + \delta) + \cot(\theta + \varphi)}$$

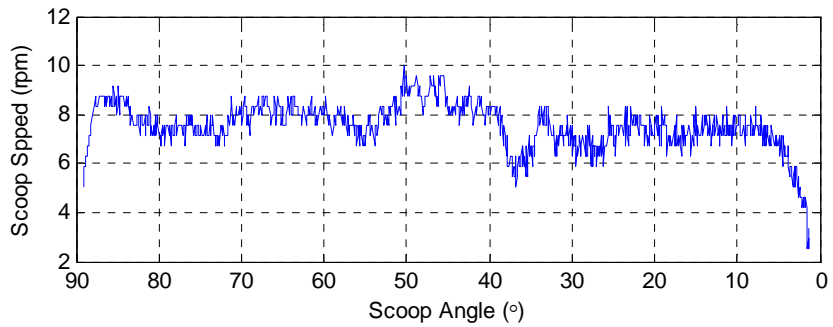
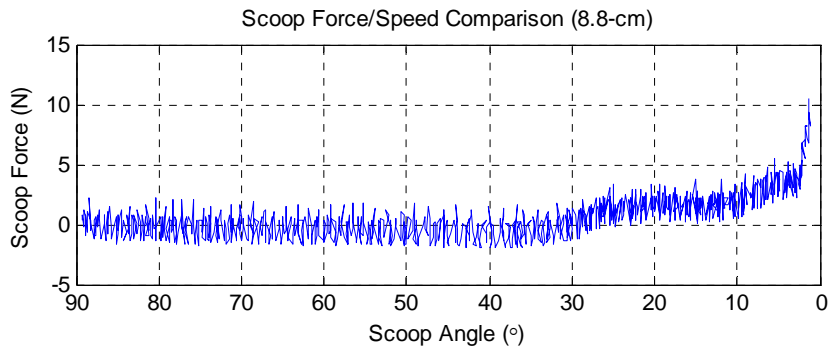
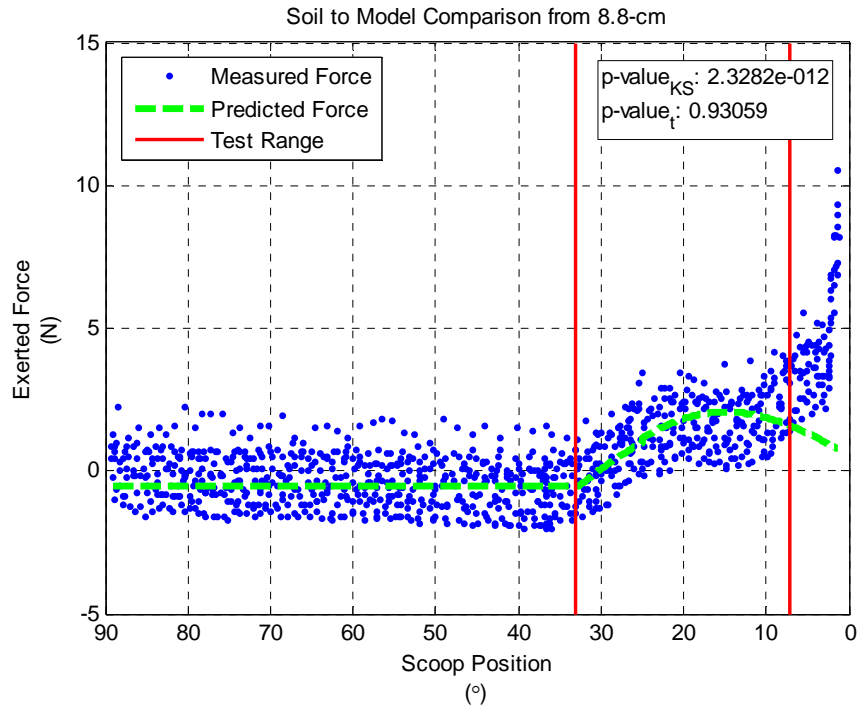
$$N_q = \frac{\frac{d'}{d} N_q^* \cot(\theta + \varphi)}{\cot(\alpha + \delta) + \cot(\theta + \varphi)}$$

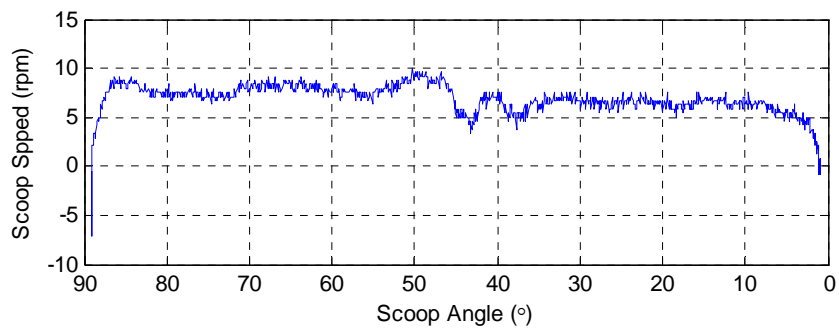
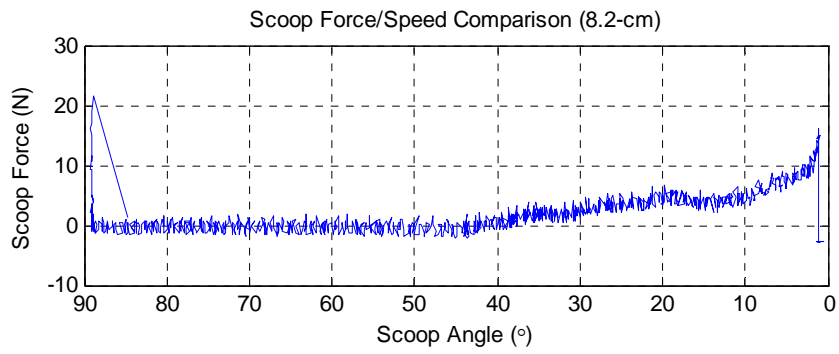
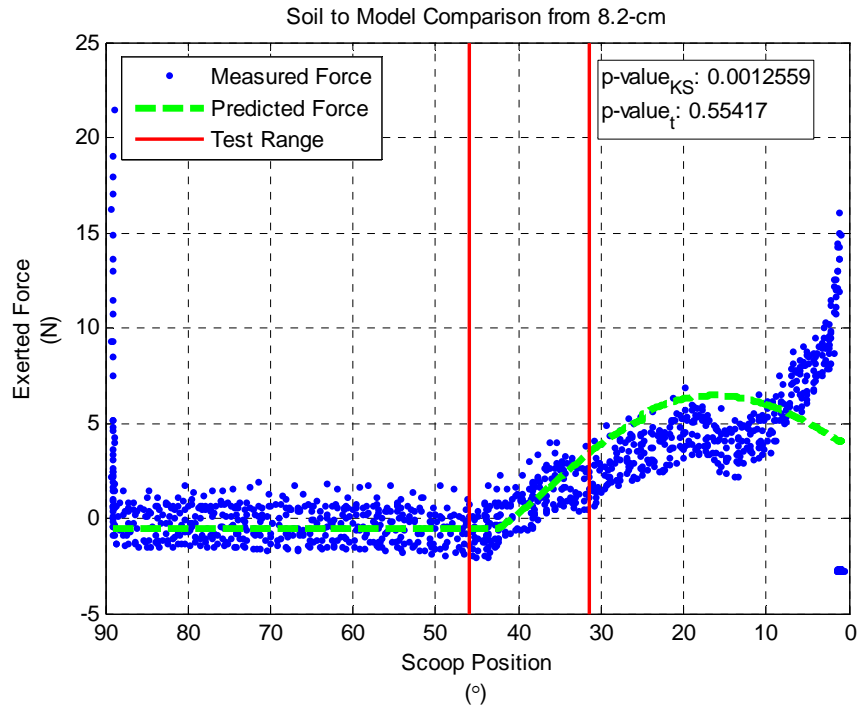
Unknowns:

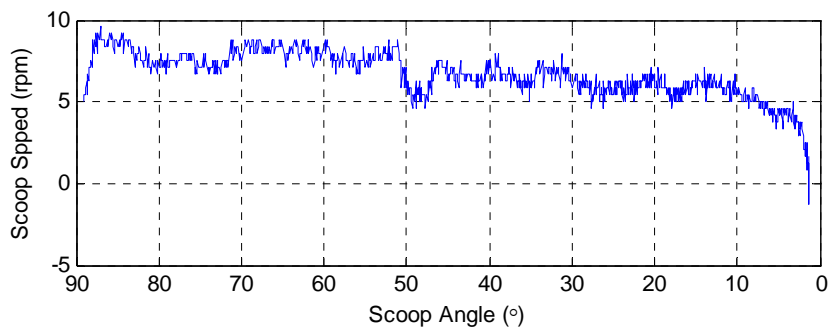
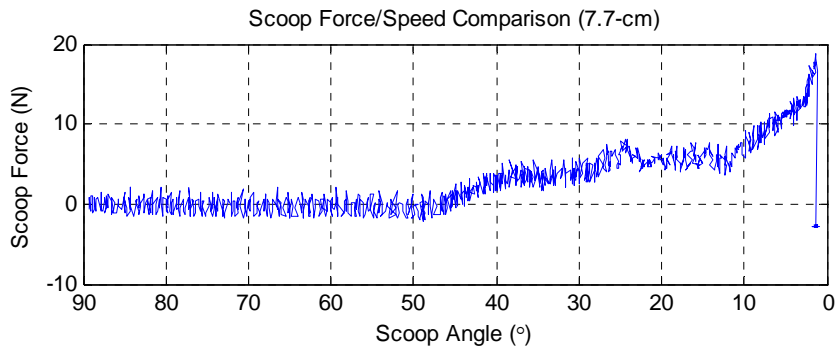
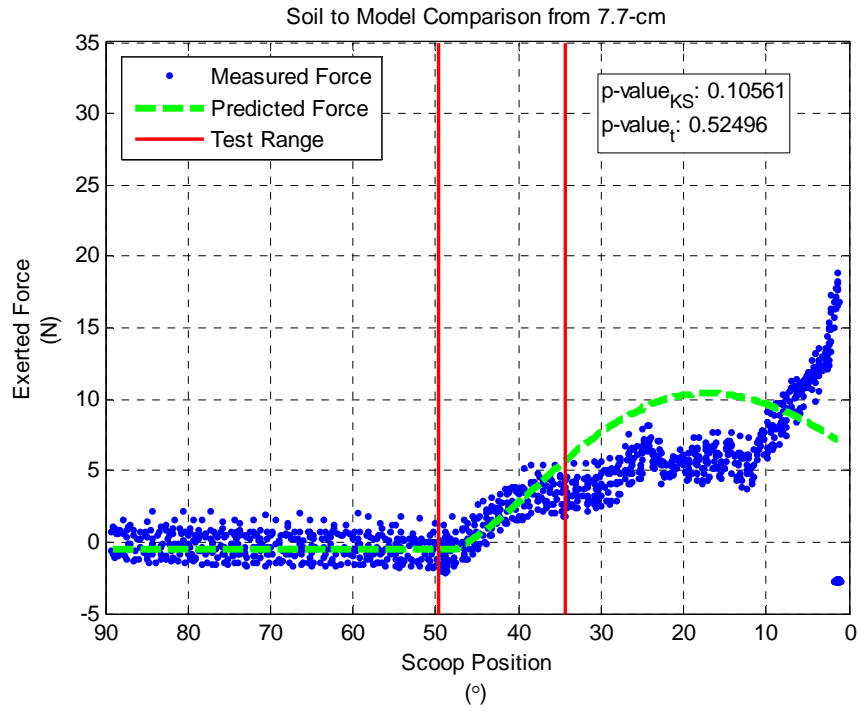
$$\frac{d'}{d} = \frac{\cos(\varphi)}{\sin(\alpha)} \left[\sin(\alpha + \delta) + \cos(\alpha + \delta) \tan(135^\circ) - \frac{5}{2} \varphi - \alpha \right]$$

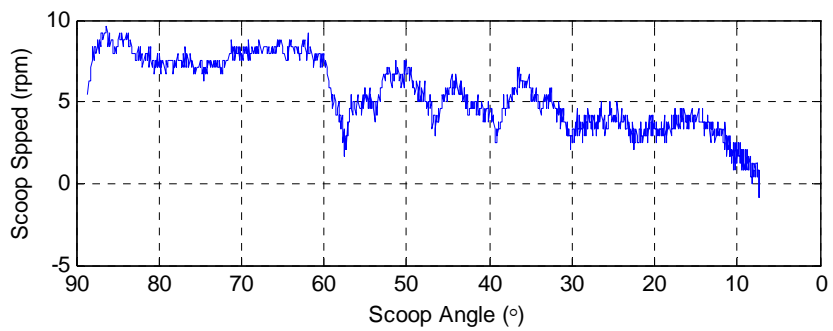
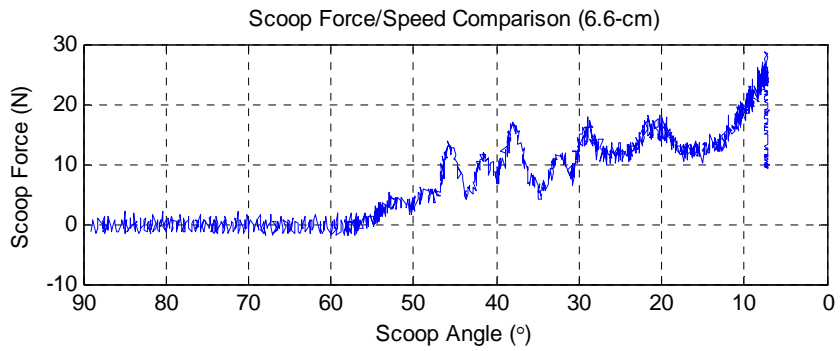
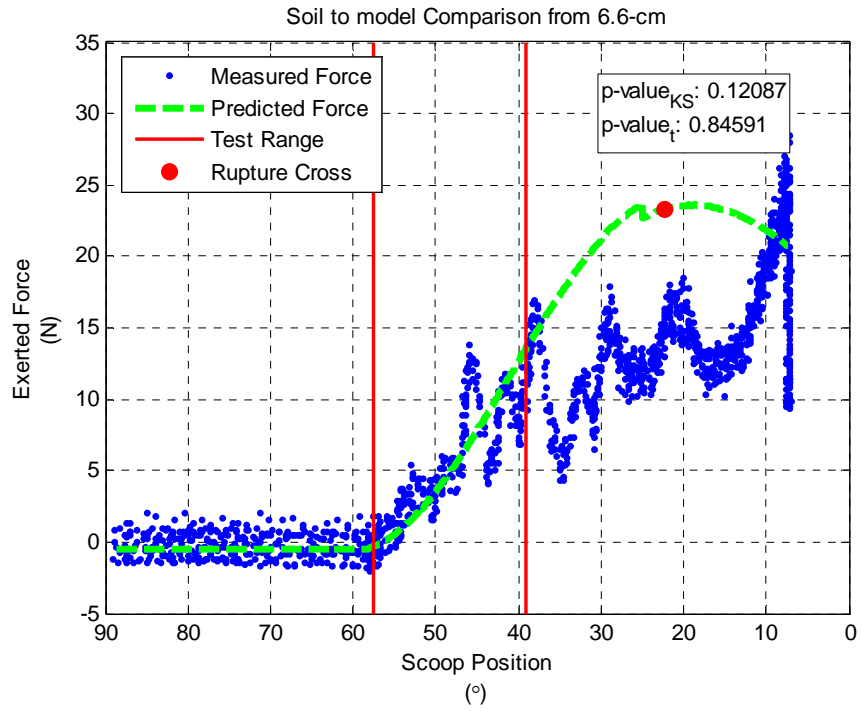
$$\theta = 135^\circ - \frac{3}{2} \varphi - \alpha$$

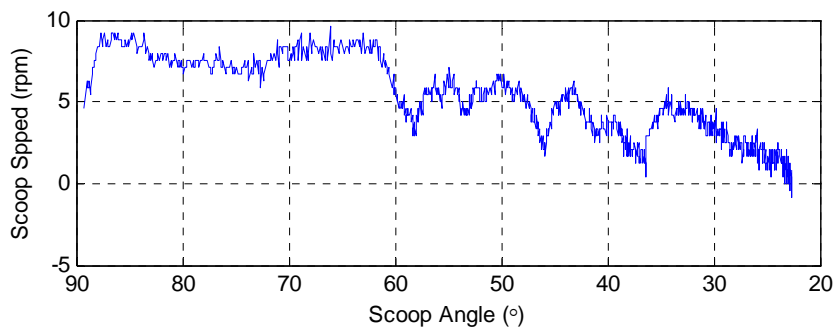
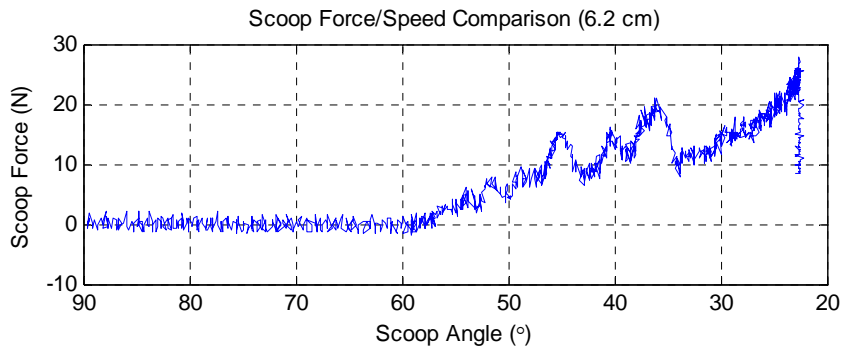
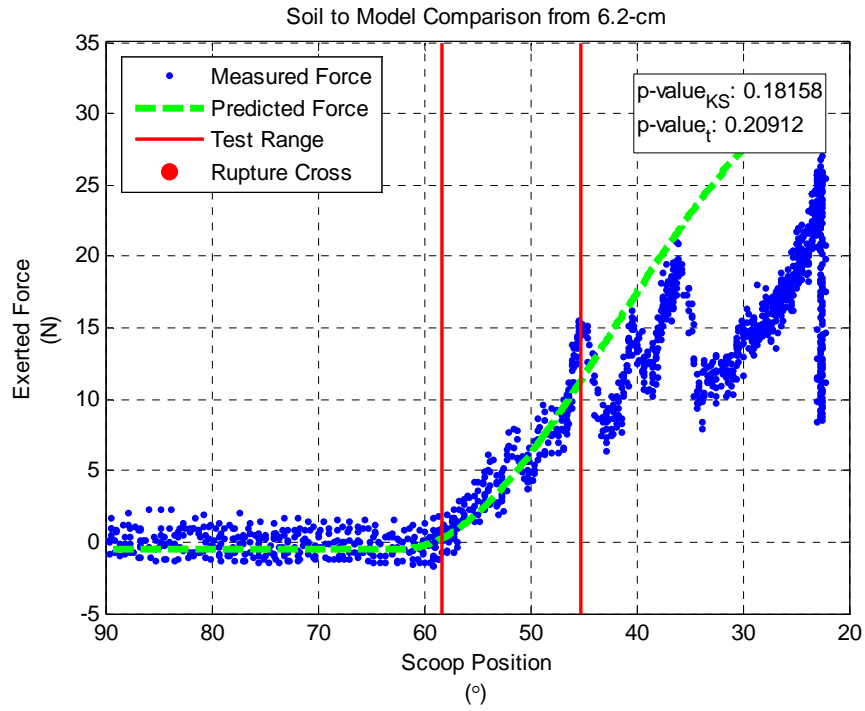
D.2 Soil Test Results

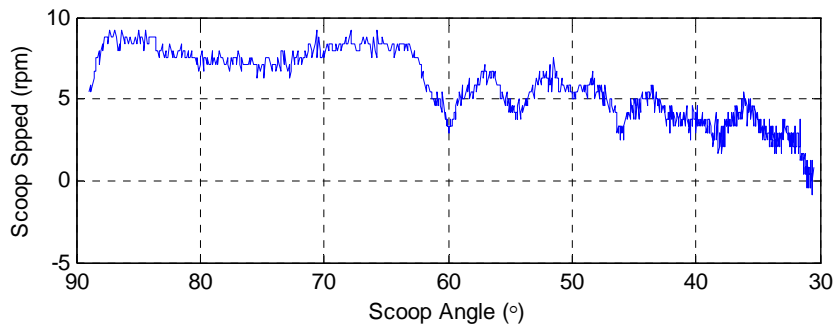
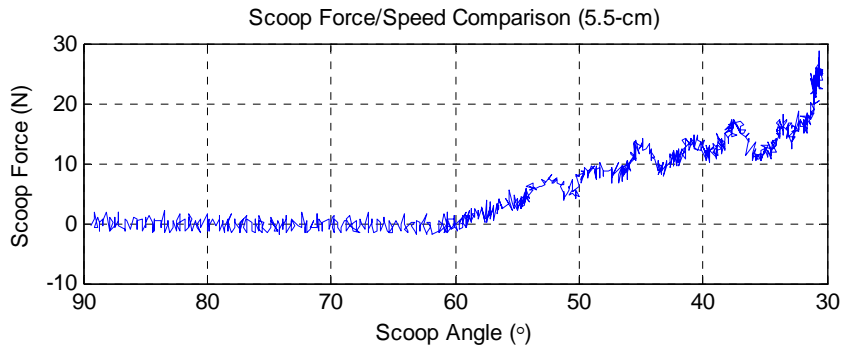
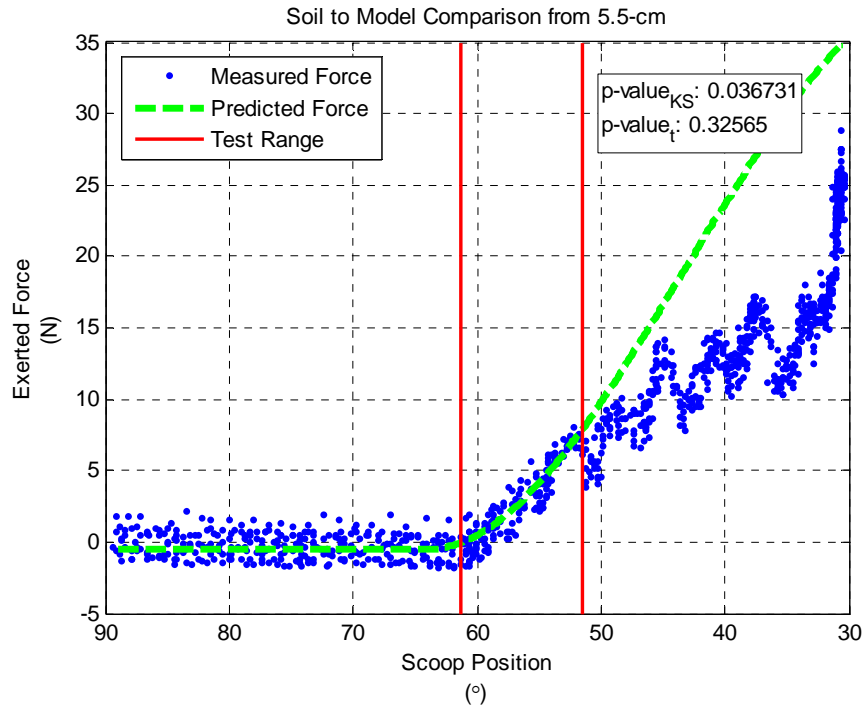






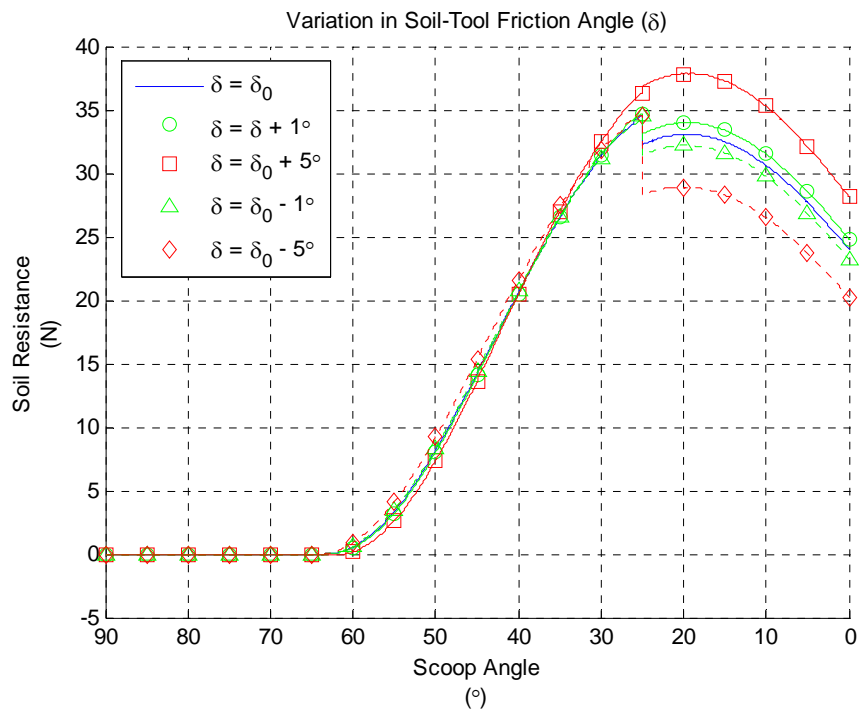
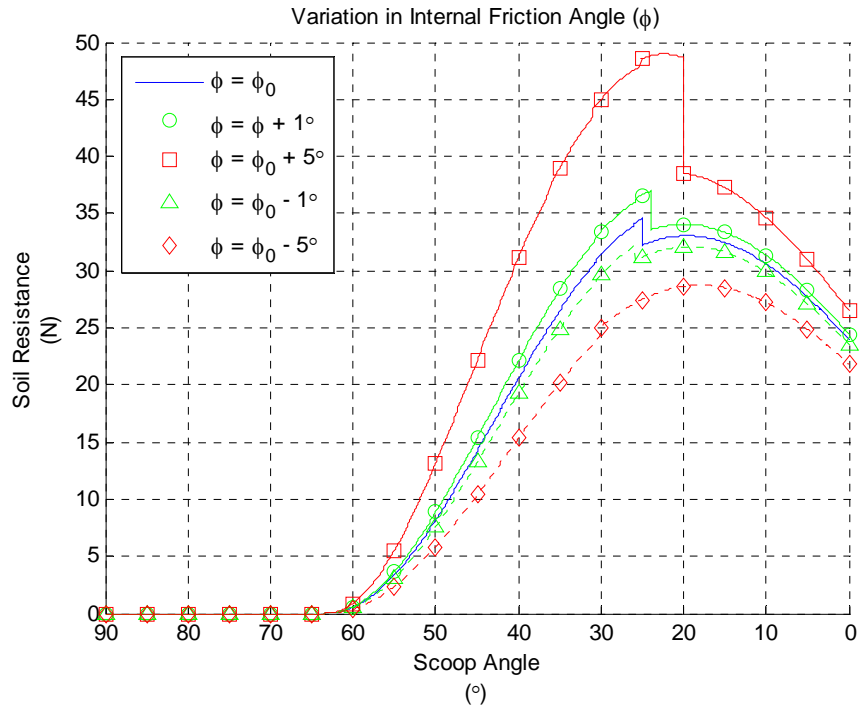


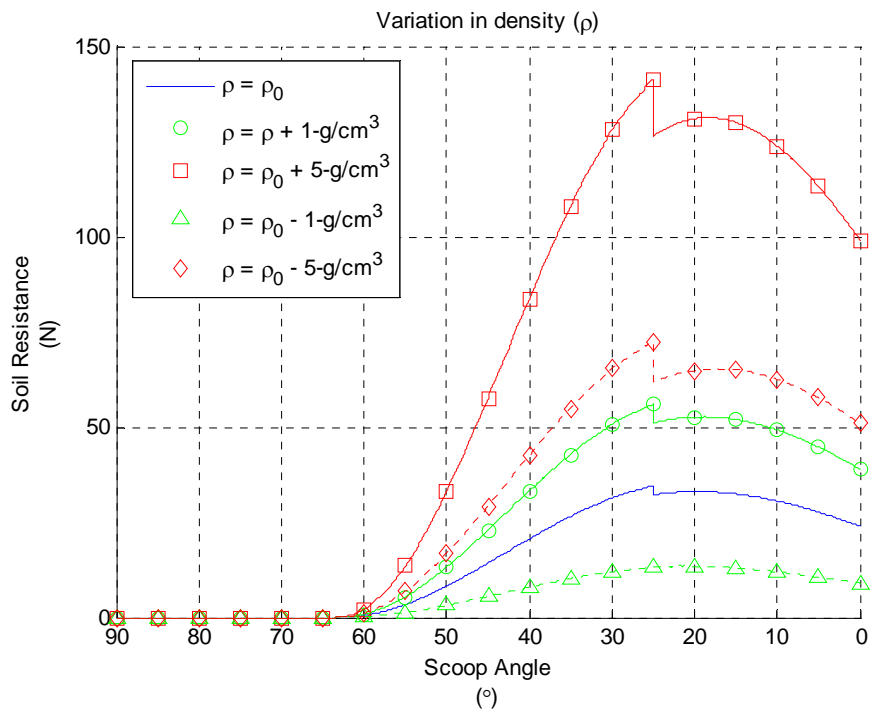
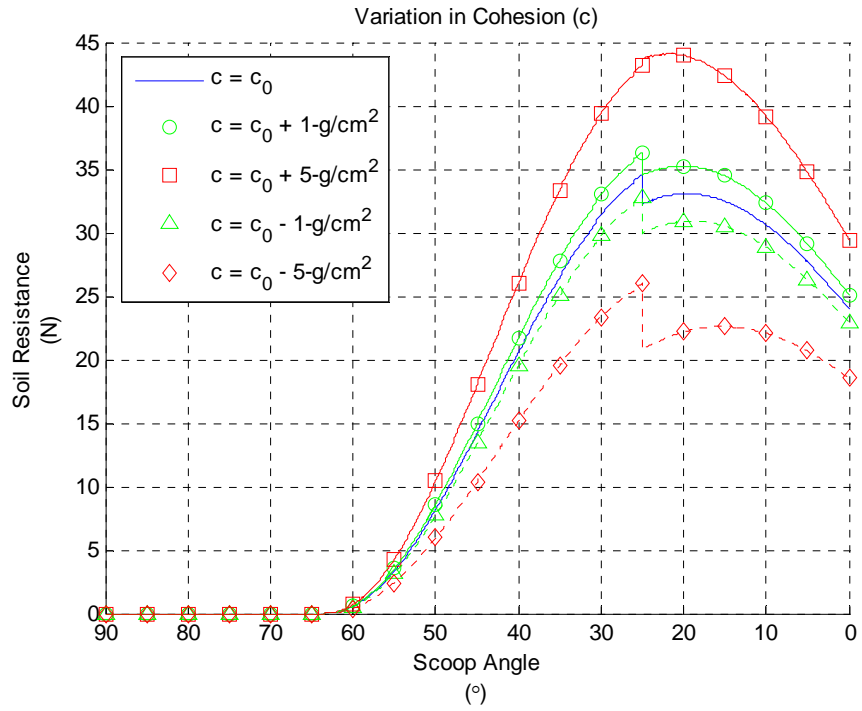




D.3 Sensitivity Analysis

$\Delta\phi$ (°)	$\Delta\delta$ (°)	Δc (g/cm ²)	$\Delta\rho$ (g/cm ³)	ΔF_{avg} (%)	$\Delta\phi$ (°)	$\Delta\delta$ (°)	Δc (g/cm ²)	$\Delta\rho$ (g/cm ³)	ΔF_{avg} (%)	$\Delta\phi$ (°)	$\Delta\delta$ (°)	Δc (g/cm ²)	$\Delta\rho$ (g/cm ³)	ΔF_{avg} (%)		
0	0	0	0	5	-1	0	0	0	4	-1	0	0	0	4		
			1	69				1	54							
			-1	59				-1	62							
		1	0	11			0	1								
			1	75			1	59								
			-1	53			-1	57								
	-1	-1	0	1		0	10									
			1	63		1	48									
			-1	65		-1	68									
		0	0	6		0	3									
			1	71		1	56									
			-1	59		-1	62									
0	1	1	0	12	-1	1	1	0	3	-1	1	1	0	3		
			1	77				1	62							
			-1	53				-1	56							
		-1	0	0			0	8								
			1	65			1	51								
			-1	64			-1	67								
	0	0	0	0		4	-1	0	0	0	6	-1	0	0	0	6
				1		67				1	52					
				-1		60				-1	63					
		1	0	9		0		0								
			1	73		1		57								
			-1	54		-1		58								
-1	-1	-1	0	2	-1	-1	-1	0	11	-1	-1	-1	0	11		
			1	61				1	46							
			-1	65				-1	68							
	0	0	7	0		7										
		1	69	1		53										
		-1	55	-1		56										
-1	-1	-1	0	4	-1	-1	-1	0	8	-1	-1	-1	0	8		
			1	57				1	51							
			-1	66				-1	67							
		0	0	1			0	1								
			1	59			1	52								
			-1	61			-1	63								
	1	0	4	0		4										
		1	64	1		57										
		-1	56	-1		58										
	-1	-1	-1	0		7	-1	-1	-1	0	7	-1	-1	-1	0	7
				1		53				1	46					
				-1		67				-1	68					





Appendix E

MATLAB Code

E.1 Scoop Soil Force Function

```
% SoilForceScoop
% This function calculates the resistive soil force on the blade given:
% % scoop_ang = Scoop Angle [degrees]
% % h = Scoop Height [cm]
% % phi = Angle of Internal Friction [rad]
% % delta = Soil-Tool Friction Angle [rad]
% % c = Cohesion [kg/cm^2]
% % rho = Density [kg/cm^3]
% % w = Blade Width [cm]
%
% Sub-Functions:
% % BladePos
% % SoilForce
function [F rupcrs Fx Fy T F2] = SoilForceScoop(scoop_ang, h, phi, delta, c, rho, w)

gamma = scoop_ang*pi/180;

d = zeros(length(gamma),1);
alpha = zeros(length(gamma),1);
F = zeros(length(gamma),1);
rupcrs = zeros(length(gamma),1);

for J = 1:length(gamma)
    [alpha(J), d(J),x(J),y(J)] = BladePos(gamma(J), h);
end

j = find(d>=0);
j = j(1);

for m = j:length(gamma)
    alpha1 = alpha(m);
    atest=abs(gamma(m)-gamma(j))*180/pi;
    if atest > 15
        D=1;
    else
        D=1;
    end

    [f1 f2 r]= SoilForce(alpha(m), phi, delta, d(m), w, c, rho, alpha1,D);
    Fx(m) = f1;
    Fy(m) = f2;
    f = [Fx(m) Fy(m) 0];
```

```

Fsoil(m) = 2*9.81*norm(f);
F(m) = Fsoil(m)*cos(alpha(m)+delta+gamma(m)-pi/2); %puts force perp to scoop moment arm

X = d(m)/tan(alpha(m))+abs(x(m))+2.159;
if r>X
    rupcrs(m)=1;
end

end

for h=1:length(F)
    if F(h)==NaN
        F(h)=0;
    end
end
end

```

Blade Position Sub-function

```

% BladePos
% This function calculates the x-y postion of the blade tip given:
% % gamma = Scoop Angle [rad]
% % h = Scoop Height [cm]
function [alpha, d,x,y] = BladePos(gamma, h)

a = 30;

alphas = a*pi/180;
alpha = alphas + gamma;

x0 = 2.12;
y0 = 3.6*2.54;
X0 = [x0; y0];

for m = 1:length(gamma)
    c = cos(gamma(m));
    s = sin(gamma(m));
    R = [c -s; s c];
    X = R*X0;
    x(m) = X(1);
    y(m) = X(2);
end

d = y - h;

```

Soil Force Sub-function

```

% SoilForce
% This function calculates the soil force based on the McKyes model given:
% % alpha = Blade Rake Angle [rad]
% % phi = Angle of Internal Friction [rad]
% % delta = Soil-Tool Friction Angle [rad]
% % d = Blade Depth [cm]
% % w = Blade Width [cm]
% % c = Cohesion [kg/cm^2]

```

```

%% rho = Density [kg/cm^3]
%% alpha1 = Critical Angle [rad]
%% D = Coeficient
%
% Sub-functions
%% BetaMin
function [F1 F2 r] = SoilForce(alpha, phi, delta, d, w, c, rho, alpha1,D)

rad = pi/180;
g = 9.81;
if d<0
    beta = 0;
    dd = 0;
else
    beta = BetaMin(alpha, delta, phi, w, d);
    dd = d*cos(phi)/sin(alpha)*(sin(alpha+phi) + cos(alpha+phi)*tan(135*rad-5/2*phi-alpha));
    if min(size(beta))==0
        beta=eps;
    end
end
end
q = rho*d*4.5;

% Test for angle
ang_crit = pi/2 - phi;
betaphi = beta+phi;
if beta+phi < eps
    betaphi = eps;
end
if alpha1 < ang_crit
    rd = cot(alpha) + cot(beta);
    dw = d/w;
    r = rd*d;
    bot = cot(alpha+delta) + cot(betaphi);

    cosomega = 1./rd.*cot(alpha);
    sinomega = (1-cosomega.^2).^5;

    Nyh = (.5*rd*(1 + 2/3*rd*dw*sinomega))/bot;
    Nch = ((1+cot(beta)*cot(betaphi))*(1 + rd*dw*sinomega))/bot;
    Nqh = (rd*(1 + rd*dw*sinomega))/bot;

    F1 = D*w*(rho*d^2*Nyh + c*d*Nch + q*Nqh);
    F2 = F1*(bot/(1+tan(alpha+delta)*cot(betaphi)));
else
    del = phi;
    alp = ang_crit;
    bots = cot(alp+del) + cot(betaphi);
    rdd = cot(alp) + cot(beta);
    ddw = dd/w;
    r = rdd*dd;

    cosomega = 1./rdd.*cot(alp);
    sinomega = (1-cosomega.^2).^5;

    Nyhs = (.5*rdd*(1 + 2/3*rdd*ddw*sinomega))/bots;
    Nchs = ((1+cot(beta)*cot(betaphi))*(1 + rdd*ddw*sinomega))/bots;

```

```

Nqhs = (rdd*(1 + rdd*ddw*sinomega))/bots;

theta = 135*rad - 3/2*phi - alpha;
bot = cot(alpha+delta) + cot(theta+phi);
ddd = dd/d;

Nyh = (.5*ddd*(tan(phi) - cot(alpha) + 2*ddd*Nyhs*cot(theta+phi)))/bot;
Nch = (1 - 2*ddd - (2*ddd*tan(phi) - cot(alpha))*cot(theta+phi) + ddd*Nchs*cot(theta+phi))/bot;
Nqh = (ddd*Nqhs*cot(theta+phi))/bot;

F1 = D*w*(rho*dd^2*Nyh + c*dd*Nch + q*Nqh);
F2 = F1*((cot(alpha+delta) + cot(theta+phi))/(1+tan(alpha+delta)*cot(theta+phi)));
end

```

Minimum Beta Sub-sub-function

```

% BetaMin
% This function finds the minimum value of Beta given:
% % alpha = Blade Rake Angle [rad]
% % delta = Soil-Tool Friction Angle [rad]
% % phi = Internal Friction Angle [rad]
% % w = Blade Width [cm]
% % d = Blade Depth [cm]
function [beta_min] = BetaMin(alpha, delta, phi, w, d)
a = [alpha, pi/2-phi];
ang = min(a);
if ang == a(2)
    d = d*cos(phi)/sin(alpha)*(sin(alpha+phi) + cos(alpha+phi)*tan(135*pi/180-5/2*phi-alpha));
else
    d = d;
end

beta = [.01:pi/500:pi/2];
rd = cot(ang)+cot(beta);
rw = rd*d/w;
cosomega = 1./rd.*cot(ang);
sinomega = (1-cosomega.^2).^5;

Ntop = .5.*rd.*(1+2/3.*rw.*sinomega);
Nbot = cot(ang+delta) + cot(beta+phi);
N = Ntop./Nbot;
for j = 1:length(N)
    if N(j)<=0
        J = j-1;
        break
    else
        J = (length(N));
    end
end

NN = N(1:J);
BETA = beta(1:J);

m = find(NN==min(NN));
beta_min = BETA(m);

```

E.2 Parsing Function

```
% Parse
% % This function parses the test data given:
% % fname = File Name of Test Run ['string']
% % fcal = File Name of Calibration Run ['string']
% % res = Measured Resistance of Resistor [Ohm]
% % span = Number of Data Point in Moving Average
% % th_op = Angle of Scoops when Fully Open
%
% Sub Functions
% % readColData
% % PotCal
function [raw, raw_smooth, act, act_smooth] = Parse(fname, fcal, res, span, th_op)

addpath('C:\Documents and Settings\David\My Documents\School\Grad Classes\Test
Runs\MATLAB\Test_Data');

fldr = 'Test_Data\';
file = [fldr fname];
filecal = [fldr fcal];

[labels,x,y] = readColData(file,5,5,1);

%Collect Raw Data
motorV = y(:,1);
potV = y(:,2);
sysV = y(:,3);
swtchV = y(:,4);

lgth = length(y);

% Median of pot values at open/closed position - from calibration run
potavg1 = mean(potV(1:100));
potavg2 = mean(potV(lgth-100:lgth));

motorC = motorV/res;

%potR = potV/maxpot;
[a b]=PotCal(filecal, th_op);
scoopang = th_op - a*(potV-b);

raw = [potV, scoopang, motorC, swtchV, sysV];

scoopang_smooth = MovAvg(scoopang,span);
motorC_smooth = MovAvg(motorC,span);
swtchV_smooth = MovAvg(swtchV,span);
sysV_smooth = MovAvg(sysV,span);
raw_smooth = [scoopang_smooth, motorC_smooth, swtchV_smooth, sysV_smooth];

for m = lgth:-1:1
    if potV(m) < .99*potavg2
        M=m+250;
        break
    end
end
```

```

else
    M=lgth;
end
end

for k = 2:lgth
    if potV(k) > 1.01*potavg1
        K = k;
        break
    else
        end
    end
end

act = [scoopang(K:M), motorC(K:M), swtchV(K:M), sysV(K:M)];
act_smooth = [scoopang_smooth(K:M), motorC_smooth(K:M), swtchV_smooth(K:M),
sysV_smooth(K:M)];

```

Data Reading Sub-function

```

% Accessed at:
% http://web.cecs.pdx.edu/~gerry/MATLAB/plotting/examples/readColData.m
% Accessed on: Feb 5, 2007

```

```

function [labels,x,y] = readColData(fname,ncols,nhead,nlrows)
% readColData reads data from a file containing data in columns
% that have text titles, and possibly other header text
%
% Synopsis:
% [labels,x,y] = readColData(fname)
% [labels,x,y] = readColData(fname,ncols)
% [labels,x,y] = readColData(fname,ncols,nhead)
% [labels,x,y] = readColData(fname,ncols,nhead,nlrows)
%
% Input:
% fname = name of the file containing the data (required)
% ncols = number of columns in the data file. Default = 2. A value
% of ncols is required only if nlrows is also specified.
% nhead = number of lines of header information at the very top of
% the file. Header text is read and discarded. Default = 0.
% A value of nhead is required only if nlrows is also specified.
% nlrows = number of rows of labels. Default = 1
%
% Output:
% labels = matrix of labels. Each row of labels is a different
% label from the columns of data. The number of columns
% in the labels matrix equals the length of the longest
% column heading in the data file. More than one row of
% labels is allowed. In this case the second row of column
% headings begins in row ncol+1 of labels. The third row
% column headings begins in row 2*ncol+1 of labels, etc.
%
% NOTE: Individual column headings must not contain blanks
%
% x = column vector of x values
% y = matrix of y values. y has length(x) rows and ncols columns

```

```

%
% Author:
% Gerald Recktenwald, gerry@me.pdx.edu
% Portland State University, Mechanical Engineering Department
% 24 August 1995

% process optional arguments
if nargin < 4
    nlrws = 1; % default
    if nargin < 3
        nhead = 0; % default
        if nargin < 2
            ncols = 2; % default
        end
    end
end

% open file for input, include error handling
fin = fopen(fname,'r');
if fin < 0
    error(['Could not open ',fname,' for input!']);
end

% Preliminary reading of titles to determine number of columns
% needed in the labels matrix. This allows for an arbitrary number
% of column titles with unequal (string) lengths. We cannot simply
% append to the labels matrix as new labels are read because the first
% label might not be the longest. The number of columns in the labels
% matrix (= maxlen) needs to be set properly from the start.

% Read and discard header text on line at a time
for i=1:nhead, buffer = fgetl(fin); end

maxlen = 0;
for i=1:nlrws
    buffer = fgetl(fin); % get next line as a string
    for j=1:ncols
        [next,buffer] = strtok(buffer); % parse next column label
        maxlen = max(maxlen,length(next)); % find the longest so far
    end
end

end

% Set the number of columns in the labels matrix equal to the length
% of the longest column title. A complete preallocation (including
% rows) of the label matrix is not possible since there is no string
% equivalent of the ones() or zeros() command. The blank() command
% only creates a string row vector not a matrix.
labels = blanks(maxlen);
frewind(fin); % rewind in preparation for actual reading of labels and data
% Read and discard header text on line at a time
for i=1:nhead, buffer = fgetl(fin); end
% Read titles for keeps this time
for i=1:nlrws

    buffer = fgetl(fin); % get next line as a string

```

```

for j=1:ncols
    [next,buffer] = strtok(buffer); % parse next column label
    n = j + (i-1)*ncols; % pointer into the label array for next label
    labels(n,1:length(next)) = next; % append to the labels matrix
end
end
% Read in the x-y data. Use the vectorized fscanf function to load all
% numerical values into one vector. Then reshape this vector into a
% matrix before copying it into the x and y matrices for return.
data = fscanf(fin,'%f'); % Load the numerical values into one long vector
nd = length(data); % total number of data points
nr = nd/ncols; % number of rows; check (next statement) to make sure
if nr ~= round(nd/ncols)
    fprintf(1,'\ndata: nrow = %d\ncol = %d\n',nr,ncols);
    fprintf(1,'number of data points = %d does not equal nrow*ncol\n',nd);
    error('data is not rectangular')
end
data = reshape(data,ncols,nr)'; % notice the transpose operator
x = data(:,1);
y = data(:,2:ncols);
% end of readColData.m

```

Potentiometer Sub Function

```

% PotCal
% This function converts the potentiometer voltage into scoop angle given:
% % calfile = Calibration File Name ['string']
% % th_op = Angle of Scoop when Open [degrees]
function [a b]=PotCal(calfile, th_op)

[labels,x,y] = readColData(calfile,5,5,1);
pot = y(:,2);

% Closed
V2 = mean(pot(1:250));

% Open
op = find(pot<3);
mid = floor(median(op));

V1 = mean(pot(mid-125:mid+125));

a = th_op/(V2-V1);
b = V1;

```

Appendix F

Testing Supplemental

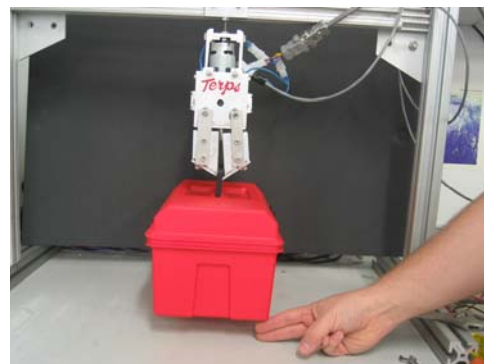
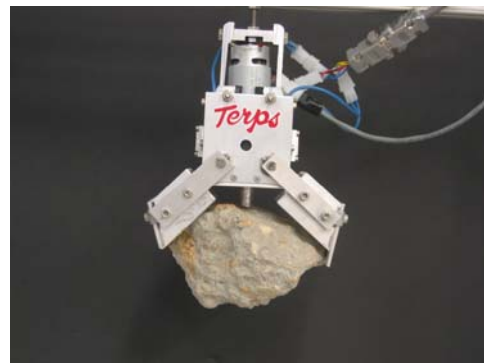
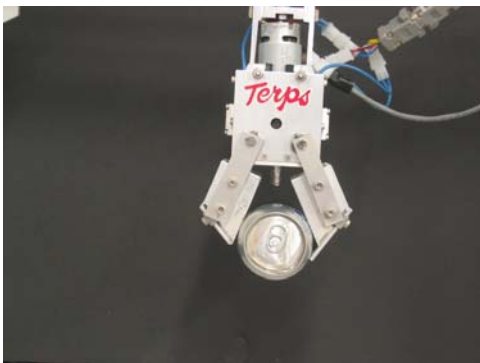
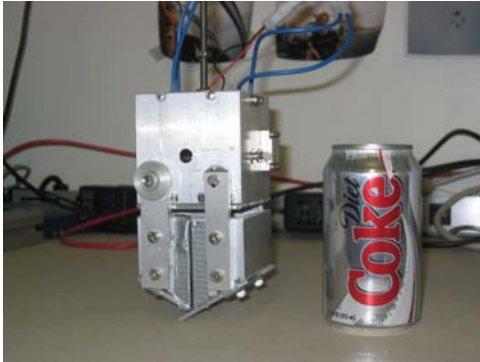
F.1 Test Log

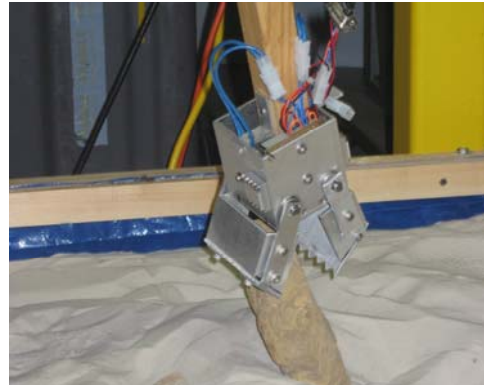
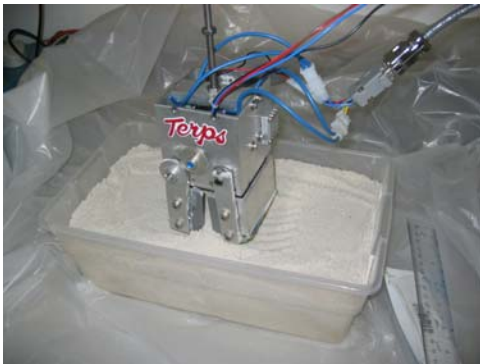
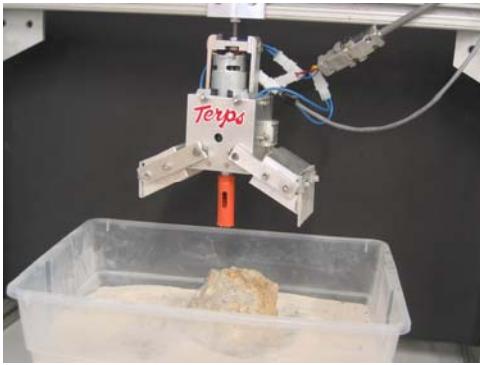
This is a log of all of the soil tests performed that recorded motor currents and scoop angle. The soils are: DS – Dry Sand, MS – Moist Sand, Cl – Clay loam, G Gravel, and Cal – No Soil/Calibration Run. The height is the vertical distance between the scoop axels and the soil surface.

File	Soil	Height (cm)	Notes
2_5_2007_3_08_24.806 PM.txt	DS	9.2	12V @1.5A
2_5_2007_3_12_36.381 PM.txt	DS	9.2	12V @ 2A
2_5_2007_3_19_11.088 PM.txt	DS	9.2	12V @ 2A
2_5_2007_3_20_40.791 PM.txt	DS	9.2	9V @ 2A
2_5_2007_3_22_35.572 PM.txt	DS	9.2	9V @ 2A
2_5_2007_3_23_58.494 PM.txt	DS	9.2	18V
2_5_2007_3_24_46.603 PM.txt	DS	9.2	18V
2_5_2007_3_27_09.135 PM.txt	DS	7.4	18V - failed to close
2_5_2007_3_28_56.666 PM.txt	DS	7.4	18V - failed to close
2_5_2007_3_33_38.119 PM.txt	DS	7.4	12V - failed to close
2_5_2007_3_34_51.306 PM.txt	DS	7.4	12V - failed to close
2_5_2007_3_37_23.181 PM.txt	DS	7.4	9V - failed to close
2_5_2007_3_38_31.291 PM.txt	DS	7.4	9V - failed to close
2_5_2007_3_40_17.291 PM.txt	DS	8.4	9V - failed to close
2_5_2007_3_41_22.697 PM.txt	DS	8.4	12V - failed to close fully (~2-5deg gap)
2_5_2007_3_42_52.056 PM.txt	DS	8.4	18V
2_5_2007_3_51_13.889 PM.txt	G	8.5	18V - stuck on rock
2_5_2007_3_52_33.369 PM.txt	G	8.5	18V - closed fully
2_5_2007_3_53_36.369 PM.txt	G	8.5	12V - briefly got stuck mid-closure but recovered and closed
2_5_2007_3_55_02.213 PM.txt	G	8.5	9V - barely closed
2_5_2007_3_59_58.510 PM.txt	G	7.3	18V - no closure, barely broke surface
2_5_2007_4_24_31.541 PM.txt	MS	na	open/close in air
2_7_2007_1_58_44.911 PM.txt	G	9	stuck and released a couple time, choppy motion
2_7_2007_11_03_13.515 AM.txt	Cal	na	open/close for pot
2_7_2007_11_10_05.437 AM.txt	MS	8.5	
2_7_2007_11_13_04.078 AM.txt	MS	8.5	
2_7_2007_11_17_19.203 AM.txt	MS	8.5	smooth blade stuck on surface
2_7_2007_11_19_17.078 AM.txt	MS	8.5	tried to "bump" it closed, no success
2_7_2007_11_22_51.437 AM.txt	G	8.5	failed
2_7_2007_11_24_06.625 AM.txt	G	8.5	failed
2_7_2007_11_28_07.937 AM.txt	DS	8.5	

File	Soil	Height (cm)	Notes
2_7_2007_11_30_16.437 AM.txt	DS	8.5	
2_7_2007_2_00_53.335 PM.txt	G	9	
2_7_2007_2_08_09.702 PM.txt	DS	9	
2_7_2007_2_09_07.942 PM.txt	DS	9	
2_7_2007_2_13_41.472 PM.txt	MS	9	
2_7_2007_2_14_20.539 PM.txt	MS	9	
2_12_2007_11_16_41.500 AM.txt	Cl	9.2	
2_12_2007_11_22_09.984 AM.txt	Cl	9.2	
2_12_2007_4_12_08.625 PM.txt	Cal		12V @ 2A - pot battery at 9.31V
2_12_2007_4_12_36.437 PM.txt	Cal		12V @ 2A - pot battery at 9.31V
2_12_2007_4_15_08.640 PM.txt	Cl	9	12V @ 2A - pot battery at 9.31V
2_12_2007_4_16_45.109 PM.txt	Cl	8	12V @ 2A - pot battery at 9.31V
2_12_2007_4_19_20.906 PM.txt	Cl	7	12V @ 2A - pot battery at 9.31V
2_12_2007_4_21_49.328 PM.txt	Cl	6	12V @ 2A - pot battery at 9.31V
2_12_2007_4_30_49.859 PM.txt	MS	9	12V @ 2A - pot battery at 9.31V
2_12_2007_4_32_05.781 PM.txt	MS	8	NC - 12V @ 2A - pot battery at 9.31V
2_12_2007_4_33_29.406 PM.txt	MS	7	NC - 12V @ 2A - pot battery at 9.31V
2_12_2007_4_35_19.093 PM.txt	MS	6	NC - 12V @ 2A - pot battery at 9.31V
2_12_2007_4_38_45.625 PM.txt	DS	9	Barely collected any sample - 12V @ 2A - pot battery at 9.31V
2_12_2007_4_40_06.156 PM.txt	DS	8	NC - 12V @ 2A - pot battery at 9.31V
2_12_2007_4_42_11.968 PM.txt	DS	7	NC - 12V @ 2A - pot battery at 9.31V
2_12_2007_4_43_25.625 PM.txt	DS	6	NC - 12V @ 2A - pot battery at 9.31V
2_24_2007_3_50_45.690 PM.txt	Cal		Closed-Opened-Closed, not pot V - 6V/.5A/8.37V/1.4Ohm
2_24_2007_3_51_34.406 PM.txt	Cal		Closed-Opened-Closed - 6V/.5A/8.37V/1.4Ohm
2_24_2007_3_54_24.406 PM.txt	Cal		Closed-Opened-Closed - 12V/2A/8.37V/1.4Ohm
2_24_2007_3_55_44.265 PM.txt	Cal		Closed-Opened-Closed - 12V/2A/8.37V/1.4Ohm
2_24_2007_3_58_09.750 PM.txt	Cal		just motor (open) - 12V/2A/8.37V/1.4Ohm
2_24_2007_3_58_55.218 PM.txt	Cal		just motor (close) - 12V/2A/8.37V/1.4Ohm
2_24_2007_4_00_11.109 PM.txt	Cal		just motor off-open-off-close-off - 12V/2A/8.37V/1.4Ohm
2_24_2007_4_01_02.046 PM.txt	Cal		just motor, off-open-close-off - 12V/2A/8.37V/1.4Ohm
2_24_2007_4_03_33.000 PM.txt	Cal		just motor - open, long - 12V/2A/8.37V/1.4Ohm
2_26_2007_3_59_44.89 PM.txt	Cal		pot calibration open-close - 12V/2A/8.37V/1.4Ohm
2_26_2007_4_01_10.390 PM.txt	Cal		pot calibration open-close - 12V/2A/8.37V/1.4Ohm
2_26_2007_4_02_32.765 PM.txt	Cal		strength test - 5.0N peak - 12V/2A/8.37V/1.4Ohm
2_26_2007_4_04_54.343 PM.txt	Cal		strength test - 5.3N peak - 12V/1.5A/9.53V/1.6Ohm
2_26_2007_4_06_49.148 PM.txt	Cal		strength test - 4.6N peak - 12V/1.5A/9.53V/1.6Ohm
2_26_2007_4_07_53.468 PM.txt	Cal		strength test - 4.2N peak - 12V/1.5A/9.53V/1.6Ohm

F.2 Photos





References

- [1] Williams, David (author/curator). "Chronology of Lunar and Planetary Exploration." National Space Science Data Center. Website. National Aeronautics and Space Administration. Updated June, 5, 2006 as of March 5, 2007. <<http://nssdc.gsfc.nasa.gov/planetary/chronology.html>>
- [2] "The Vision for Space Exploration." Website. Accessed on March 8, 2007. Updated February 23, 2007. <http://www.nasa.gov/mission_pages/exploration/main/index.html>
- [3] *NASA's Exploration Systems Architecture Study: Final Report*. NASA-TM-2005-214062. National Aeronautics and Space Administration. 2005.
- [4] Meyer, Charles; Treiman, Allan; and Kostiuk, Theodor (editors). *Planetary Surface Instruments Workshop*. LPI Technical Report Number 95-05. Lunar and Planetary Institute. 1995.
- [5] Eppler, Dean. "Conduct of Geologic Field Work During Planetary Exploration: Implications for EVA Suit Design." Proceedings of the International Conference on Environmental Systems. 2004.
- [6] Shearer, Charles; Papike, James; and Borg, Lars. "Planetary Sampling Strategies: Lessons Learned from the Analysis of Small Extraterrestrial Samples." AIP Conference Proceedings. 2004.
- [7] *Surveyor Program Results*. NASA Document SP-184. National Aeronautics and Space Administration. 1969.
- [8] "regolith." *The American Heritage® Science Dictionary*. Houghton Mifflin Company. 10 Mar. 2007. <<http://dictionary.reference.com/browse/regolith>>.
- [9] Allton, Judith. *Catalog of Apollo Lunar Surface Geological Sampling Tools and Containers*. NASA Document JSC-23454 / LESC-26676. National Aeronautics and Space Administration. 1989
- [10] McCleese, Dan (Chair, Mars Expeditions Strategy Group). "The Search for Evidence of Life on Mars." NASA JPL Whitepaper, 1996 Accessed at <[http://mepag.jpl.nasa.gov/reports/JPL_Pub_01-7_\(Part_1\).pdf](http://mepag.jpl.nasa.gov/reports/JPL_Pub_01-7_(Part_1).pdf)>, on February 23, 2007.
- [11] Johnson, Nicholas. *Handbook of Soviet Lunar and Planetary Exploration*. Science and Technology Series, American Astronautical Society, San Diego. 1979.
- [12] Antilla, Matti. *Concept Evaluation of Mars Drilling and Sampling Instrument*. Doctoral Dissertation, Laboratory of Space Technology, Helsinki University of Technology, Espoo, Finland. 2005.
- [13] Paulsen, G., et. al. "Robotic Drill Systems for Planetary Exploration." Proceedings of the AIAA Space 2006 Conference. 2006.
- [14] Marchesi, M., et. al. "Camoet Sample Acquisition for ROSETTA Lander Mission." Proceedings of the 9th European Space Mechanisms & Tribology Symposium. 2001.
- [15] Moore, H. J.; Hutton, R. E.; Clow, G. D.; and Spitzer, C. R. *Physical Properties of the Surface Materials at the Viking Landing Sites on Mars*. U. S. Geological Survey Professional Paper 1389. United States Government Printing Office. 1987.
- [16] Bonitz, Robert, et. al. "Mars Volatiles and Climate Surveyor Robotic Arm." *Journal of Geophysical Research*, Vol 106, No. E8. pp17,623-17,634. 2001.

- [17] Bonitz, Robert; Nguyen, Tam; and Kim, Won. "The Mars Surveyor '01 Rover and Robotic Arm." IEEE Aerospace Conference Proceedings. 2000.
- [18] Goldstein, Barry. "Phoenix – The First Mars Scout Mission (A Mid-Term Report)." *Proceedings of the 2006 IEEE Aerospace Conference*. 2006.
- [19] *The Phoenix Mars Mission*. Website. National Aeronautics and Space Administration. Accessed March 10, 2007. <<http://phoenix.lpl.arizona.edu/>>
- [20] Baumgartner, Eric; Bonitz, Robert; Melko, Joseph; Shiraishi, Lori; and Leger, Chris. "The Mars Exploration Rover Instrument Positioning System." *Proceedings of the 2005 IEEE Aerospace Conference*. 2005.
- [21] "Honeybee Robotics Space Craft Mechanisms Corporation." Website accessed March 11, 2007. <<http://www.honeybeerobotics.com/index.html>>
- [22] Udomkesmalee, S. Gabriel; and Hayati, Samad. "Mars Science Laboratory Focused Technology Program Overview." *Proceedings of the 2005 IEEE Aerospace Conference*. 2005.
- [23] Vasavada, Ashwin. "NASA's 2009 Mars Science Laboratory." PowerPoint presentation, 2006. Accessed on March 12, 2007. <http://marsoweb.nas.nasa.gov/landingsites/msl/memoranda/MSL_overview_LS.pdf>
- [24] Bar-Cohen, Y.; Bao, X.; Chang, Z.; and Sherrit, S. "An Ultrasonic Sampler and Sensor Platform for In-situ Astrobiological Exploration." *Proceedings of the SPIE Smart Structures Conference*. 2003.
- [25] Barnouin-Jha, Olivier, et. al. "Sampling a Planetary Surface With a Pyrotechnic Rock Chipper." IEEE Aerospace Conference Proceedings, pp. 351-362. 2004.
- [26] "Space Systems Lab: University of Maryland." Website. Accessed on April 29, 2007. <<http://www.ssl.umd.edu/index.php>>
- [27] Frantz, Carie Marie. "Potential End Effectors for the Autonomous Sample Collection of Hydrothermal Vent Sites." Internal SSL Document (DT20-0037). 2005. Unpublished.
- [28] *Apollo 17: Complete Downlink Edition*. Compilation of all audio/video transmissions from Apollo 17. DVD, Spacecraft Films. 2002.
- [29] Jones, Eric (editor). *Apollo Lunar Surface Journal*. Website. Updated August 10, 2006 as of March 14, 2007. <<http://history.nasa.gov/alsj/>>
- [30] Connors, Mary; Eppler, Dean; and Morrow, Daniel. *Interviews with the Apollo Lunar Surface Astronauts in Support of Planning for EVA Systems Design*. NASA Technical Memorandum 108846. National Aeronautics and Space Administration. 1994.
- [31] Williams, David (author/curator). "The Apollo Program (1963 – 1972)." National Space Science Data Center. Website. National Aeronautics and Space Administration. Updated December 8, 2006 as of March 14, 2007. <<http://nssdc.gsfc.nasa.gov/planetary/lunar/apollo.html>>
- [32] *Apollo 12 Crew Technical Debriefing*. NASA Document, prepared by mission Operations Branch, Flight Crew Support Division, Manned Spacecraft Center (now Lyndon B. Johnson Space Center), Houston. National Aeronautics and Space Administration. 1969.

- [33] Allton, J. H. and Darando, C. B. "How Successful Were the Lunar Sampling Tools?: Implications for Sampling Mars." Workshop on Mars Sample Return Science, pp. 30-31. Lunar and Planetary Institute. 1988.
- [34] *Apollo 15 Crew Technical Debriefing*. NASA Document, prepared by mission Operations Branch, Flight Crew Support Division, Manned Spacecraft Center (now Lyndon B. Johnson Space Center), Houston. National Aeronautics and Space Administration. 1971.
- [35] *Apollo 17 Crew Technical Debriefing*. NASA Document, prepared by mission Operations Branch, Flight Crew Support Division, Manned Spacecraft Center (now Lyndon B. Johnson Space Center), Houston. National Aeronautics and Space Administration. 1973.
- [36] Eckart, Peter (ed.). *The Lunar Base Handbook: An introduction to Lunar Base Design, Development, and Operations*. Space Technology Series, McGraw-Hill. 1999.
- [37] Cabrol, Natalie A., et. al. "Results of the First Astronaut-Rover (ASRO) Interaction Field Experiment and recommendations for Future Planetary Surface Exploration." 18th Digital Avionics Conference Proceedings. 1999.
- [38] Christian, Daniel, et. al. "Field Experiments with the Ames Marsokhod Rover." *Proceedings of the 1997 Field and Service Robotics Conference*. 1997.
- [39] Cabrol, Natalie. "Astronaut-Rover Exploration Strategy (ARES) for the Human Exploration of Mars." Abstract, Lunar and Planetary Science XXXI. 2000.
- [40] Burrige, Robert R. and Graham, Jeffery. "Providing Robotic Assistance During Extra-Vehicular Activity." Proceedings of Mobile Robots XVI: intelligent Systems and Advanced Manufacturing. 2001.
- [41] Burrige, Robert, et. al. "Experiments with an EVA Assistant Robot," in The 7th International Symposium on Artificial Intelligence, Robotics and Automation in Space (i-SAIRAS-03). 2003.
- [42] Culbert, Chris. "ERA Home Page." Website, source for Figure 3-7. Updated April 24, 2003 as of March 18, 2007. <http://www1.jsc.nasa.gov/er/era/ERA_Home_Page.html>
- [43] Shigley, Joseph; Mischke, Charles; and Budynas, Richard. *Mechanical Engineering Design (Seventh Edition)*. McGraw-Hill Higher Education, Boston. 2004.
- [44] McKyes, E. and Ali, O. S. "The Cutting of Soil by Narrow Blades." *Journal of Terramechanics*, Vol. 14, No. 2, pp. 43-58. 1977.
- [45] Willman, Brian and Boles, Walter. "Soil-Tool Interaction Theories as They Apply to Lunar Soil Simulant." *Journal of Aerospace Engineering*, Vol. 8, No. 2, pp. 88-99. 1995.
- [45] Perko, Howard; Nelson, John; and Green, Jacklyn. "Mars Soil Mechanical Properties and Suitability of Mars Soil Simulants." *Journal of Aerospace Engineering*, Vol. 19, No. 3. 2006.
- [46] Whitlow, Roy. *Basic Soil Mechanics, Fourth Edition*. Prentice Hall, Essex, England. 2001.
- [47] Lapin, Lawrence. *Probability and Statistics for Modern Engineering, Second Edition*. Waveland Press, Prospect heights, IL. 1993.
- [48] Spotts, M.F., and Shoup, T.E. *Design of Machine Elements, Seventh Edition*. Prentice Hall, Upper Saddle River, NJ. 1998.